NUCLEAR PHYSICS LABORATORY

UNIVERSITY OF
WASHINGTON

ANNUAL REPORT

JUNE 1965

U.S. ATOMIC ENERGY COMMISSION
CONTRACT A.T. (45-1)-1388

ANNUAL REPORT

UNIVERSITY OF WASHINGTON

Nuclear Physics Laboratory

June, 1965

PROGRAM "A"--EXPERIMENTAL NUCLEAR PHYSICS PROGRAM (CYCLOTRON)

UNDER

U.S. ATOMIC ENERGY COMMISSION CONTRACT A.T. (45-1)-1388

PREFACE

This report reviews the research and technical development conducted at the Nuclear Physics Laboratory of the University of Washington during the year ending June 15, 1965.

Research at this laboratory is performed by the faculty and graduate students of the Departments of Physics and Chemistry of the University of Washington. Support for this project is provided by the State of Washington, the U.S. Atomic Energy Commission, and the National Science Foundation.*

The arrangement of this report follows the pattern used in previous years. The sections are numbered consecutively through the report; each table and figure is assigned the number of the section to which it pertains. As has been our practice, the names of investigators listed at the end of each section are given in strict alphabetical order.

The investigations described in this report for the most part continue and extend experimental work described in several earlier reports. Continued emphasis has been placed on elastic and inelastic scattering, including alpha-gamma and proton-gamma angular correlations. Other studies include pickup reactions, particles and gamma rays emitted by compound nuclei, fluctuations in compound nuclear reactions, fission, and light-element capture and breakup reactions.

The two-stage tandem Van de Graaff has been delivered and installed. Work is in progress to develop a beam of usable intensity and stability.

---

* The National Science Foundation has provided funds for the purchase of the Van de Graaff accelerator and some of its associated equipment and, in part, for the building to house the new accelerator.

TABLE OF CONTENTS

I. BETA SPECTROSCOPY

1. 4.1 MeV Positron Spectrum of O^{14}

The determination of the shape of the positron spectrum for the 4.1 MeV Gamow-Teller transition in O^{14} has been completed. Various aspects of the experiment have been discussed in earlier reports.[1] Since the transition under investigation (see Figure 1-1) involves relatively high decay energy and a very small allowed matrix element, the spectrum shape factor is expected to have some energy dependence due to the non-negligible forbidden matrix elements.

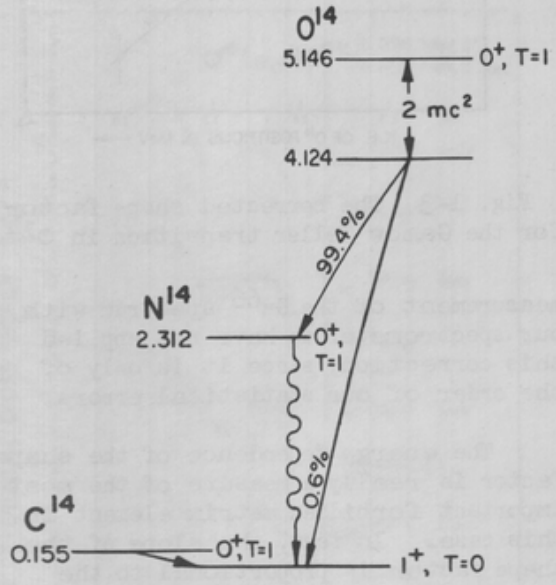

DECAY SCHEME FOR MASS-14 NUCLEI

Fig. 1-1 The decay scheme of the mass-14 nuclei.

We have been able to reduce the distortion of the spectrum due to back-scattering of source positrons by using, as source backing, a cooled beryllium tip instead of the copper rod used in earlier attempts. Furthermore the use of a 512 channel analyser to accumulate and display the positron and monitor pulses enabled us to apply corrections for gain shifts and thus compare results from various runs. Finally, a control experiment with a source of Ga^{66} positrons (which have nearly the same endpoint energy as the O^{14} transition) puts limits on the errors which might be instrumental in origin.

Some of the results of the measurements are presented in Figure 1-2. The observed shape factor (not Fermi-Kurie plot) for the O^{14} positrons between 2 MeV and 4 MeV is shown in Figure 1-2(d). This must be corrected for distortion due to backscattering from beryllium metal. The control experiment, with a Ga^{66} positron source mounted on the Be tip, provides an estimate of such distortion. This correction factor is shown in Figure 1-2(c). By dividing the observed O^{14} spectrum by the correction factor, we obtain the "true" shape factor of the O^{14} spectrum shown in Figure 1-3. Of course this is based on the assumption that our beta ray spectrometer reproduces the spectrum shape faithfully and that the Ga^{66} shape factor is energy independent. Actually a spectrum of a Ga^{66} positron source ($\approx 4 mg/cm^2$) mounted on 1/4 mil Al foil gave the shape factor shown in Figure 1-2(b). This should be compared with the results of Camp and Langer[2] for the Ga^{66} spectrum shape factor shown in Figure 1-2(a). The lack of complete agreement makes it difficult to decide about the amount of additional correction for instrumental distortion, the ratio of true Ga^{66} shape factor to 1 that should be applied. As Wu has pointed out,[3] the shape measurements by iron type and iron-free spectrometers have disagreed by small amounts in several other cases. Pending a more detailed

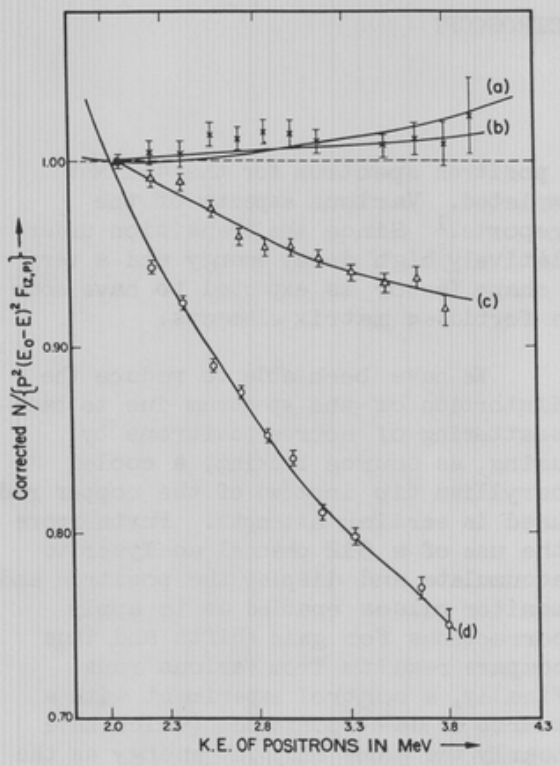

Fig. 1-2 The observed shape factor of the positron spectrum for: (a) Ga^{66} according to Camp and Langer.[2] (b) Ga^{66} using thin backing. (c) Ga^{66} using solid beryllium backing. (d) Gamow Teller transition in O^{14} using solid beryllium backing.

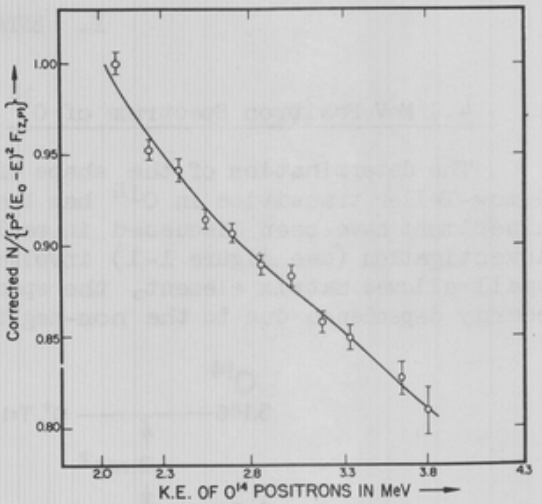

Fig. 1-3 The corrected shape factor for the Gamow Teller transition in O^{14}.

measurement of the Ga^{66} spectrum with our spectrometer we have not applied this correction, since it is only of the order of our statistical errors.

The energy dependence of the shape factor is really a measure of the most important forbidden matrix element in this case. In fact, the slope of the shape factor is proportional to the ratio of $<\vec{\alpha} \times \vec{r}>_{fi}$ to $<\vec{\sigma}>_{fi}$ where the latter is the allowed matrix element and the former is $(v_{nucleon}/c)$ part of the first forbidden Fermi matrix element (hence, twice forbidden). Except for coupling strength this is identical to the matrix element responsible for the M1 transition in N^{14*}.

According to the conserved vector current theory, we should be able to calculate the lifetime of the analogous gamma transition in N^{14*}, once $<\vec{\alpha} \times \vec{r}>_{fi}$ is known from the shape of the O^{14} spectrum. The lifetime of the 2.31 MeV gamma transition thus estimated is shorter than the measured value[4] by a factor of 3 or 4.

We find the ft value of this transition to be in good agreement with known values. (J. B. Gerhart and G. S. Sidhu)

---

1 Cyclotron Research, University of Washington (1964), p. 1; (1963), p. 1; (1962), p. 2; (1961), p. 2; (1959), p. 5.
2 D. C. Camp and L. M. Langer, Phys. Rev. 129, 1782 (1963).
3 C. S. Wu, Alpha, Beta and Gamma Ray Spectroscopy, Vol. II (Edited by K. Siegbahn), North-Holland Publishing Company, Amsterdam (1965), 1389.
4 C. P. Swann, V. K. Rasmussen, and F. R. Metzer, Phys. Rev. 121, 242 (1961).

II. ELASTIC AND INELASTIC SCATTERING

2. Inelastic Alpha-Particle Scattering from O^{16}

The $O^{16}(\alpha,\alpha')O^{16*}$ studies reported last year,[1] at incident energies of 41.0 MeV and 39.8 MeV, have been extended to three additional energies, namely 38.5 MeV, 37.1 MeV, and 35.4 MeV. Angular distributions of the inelastic scattering to the unresolved pair at 6.1 MeV, to the 2^-(8.875 MeV) state, and to the 4^+(10.363 MeV) state are shown in Figure 2-1, Figure 2-2, and Figure 2-3 respectively. The integral of the differential cross sections from 18° to 75° are

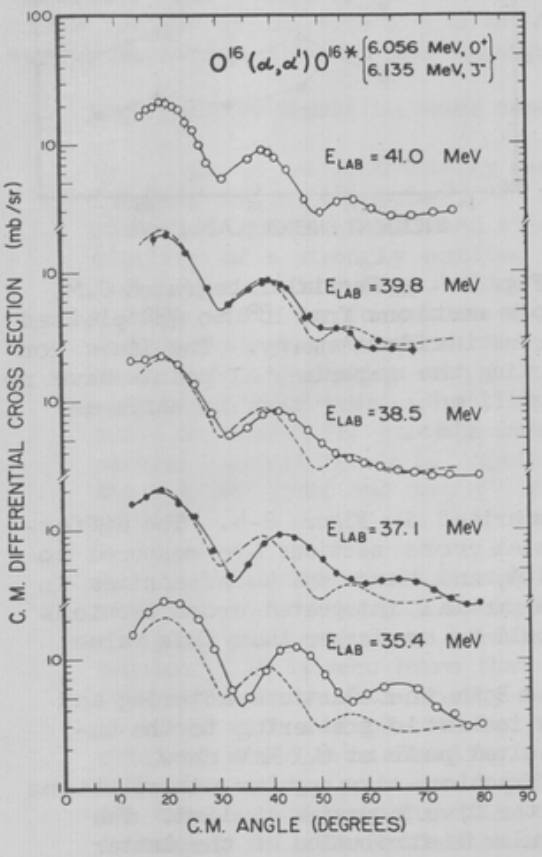

Fig. 2-1 C.M. differential cross sections of the $O^{16}(\alpha,\alpha')O^{16*}$ (0^+ -6.056 MeV and 3^- -6.135 MeV, unresolved) reaction at the five incident energies studied. An additional uncertainty of 15% in the magnitude is not folded in. The solid curves drawn through the experimental points have no significance other than to serve as visual aids.

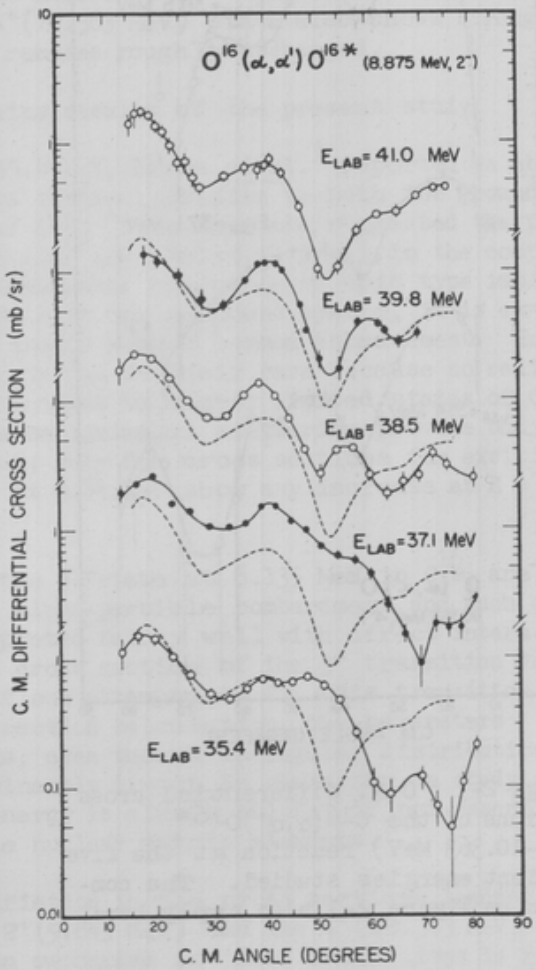

Fig. 2-2 C.M. differential cross sections of the $O^{16}(\alpha,\alpha')O^{16*}$ (2^- -8.875 MeV) reaction at the five incident energies studied. The comments on Figure 2-1 also apply here.

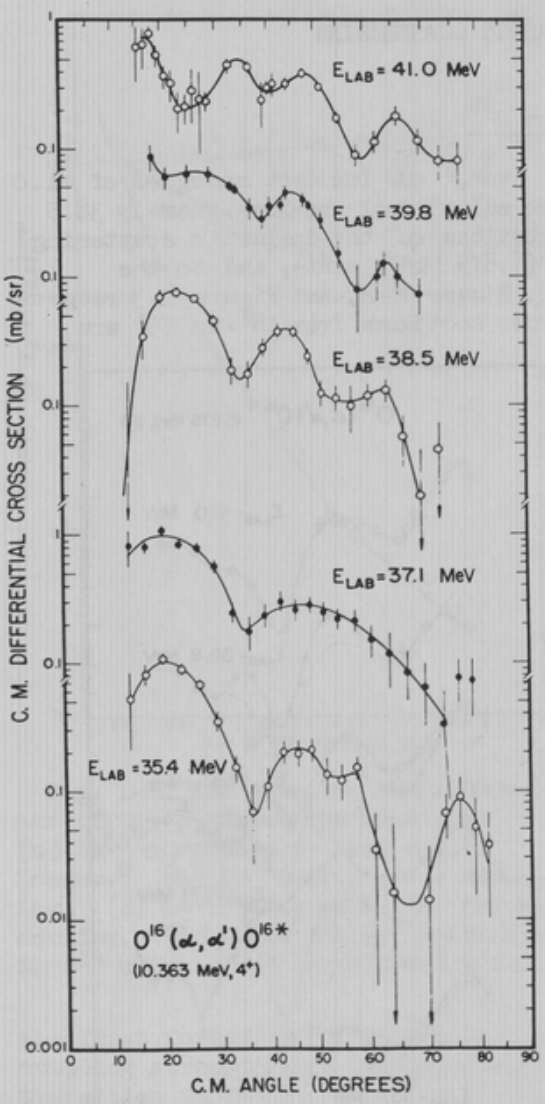

Fig. 2-3 C.M. differential cross sections of the $O^{16}(\alpha,\alpha')O^{16*}$ (4^+ -10.363 MeV) reaction at the five incident energies studied. The comments on Figure 2-1 also apply here.

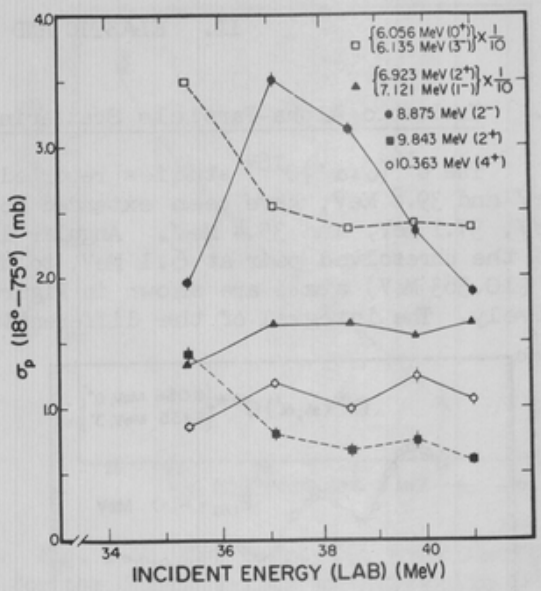

Fig. 2-4 Partial integrated C.M. cross sections from 18° to 75° plotted versus incident energy. The lines connecting the experimental points have no significance other than to serve as visual aids.

summarized in Figure 2-4. The differential cross sections are measured to ± 10%, and hence the uncertainties in the partial integrated cross sections should be no larger than this value.

Both the elastic scattering and the inelastic scattering to the unresolved pair at 6.1 MeV show diffraction-like angular distributions at the five energies studied. The angular distribution of the latter group is in phase with the elastic cross section and therefore the 0^+ contribution to the unresolved pair, if significant, has the appearance of a double excitation process. Neither the single nor double excitation of the 0^+ state are expected to be large compared to the 3^- transition. A fit to the elastic scattering and to the octupole transition (3^-) at 41.0 MeV using the adiabatic Fraunhofer theory[2] yields values for the strong absorption radius, R = 5.68F, and for the usual octupole deformation parameter, $\beta_3 R$ = 1.05F, respectively. No damping factor was required to fit the elastic cross section.

Within the accuracy of the present measurements, the elastic cross section (not shown) shows no change with energy over the energy range studied other than that expected from diffraction models. The same cannot be said about the transition to the 3^-(6.135 MeV) state. An abrupt increase in the cross section at 35.4 MeV can be seen in Figure 2-4, although the shape of the cross section remains essentially unchanged (see Figure 2-1). In view of the large increase in the absolute magnitude ($\Delta\sigma_p \simeq 10$ mb from 37.1 MeV to 35.4 MeV), it is unlikely that this effect can be attributed to the 0^+ transition. A similar increase in the cross section can also be seen in the transition to the 2^+(9.843 MeV) state. The cross sections of the transition to the unnatural parity state (2^-) at 8.875 MeV show strong energy variation both in magnitude and in shape throughout the energy interval. The change in magnitude is not monotonic as surmised earlier.[1] The cross section of the transition to the 4^+(10.363 MeV) state also shows strong energy variation although the magnitude remains roughly unchanged.

Four remarks should be made concerning results of the present study:

1) At an incident energy near 35.4 MeV, Brown et al.[3] reported an abrupt increase in the $O^{16}(\alpha,Be^8)C^{12*}$ cross sections leading to both the ground state and the first excited state of C^{12}. This increase suggested the possibility of a strongly excited (probably not isolated) level in the compound system near this energy. Since a dominating resonance of this type implies a large width for formation of a state in the compound system, it is expected that many reaction channels should show a common enhancement. However, this expectation could not be tested in their case because no reliable measurements of the (α,Be^8) cross sections to higher excited states of C^{12} could be made. The present results on inelastic scattering provide only partial support for this expectation; only the cross sections for exciting the 6.1 MeV group and the 2^+ level at 9.84 MeV show any increase at E = 35.4 MeV.

2) Collective states, such as the 3^- state at 6.135 MeV in O^{16}, are expected to be strongly excited by alpha-particle bombardment and such excitation has heretofore been interpreted fairly well with direct interaction models.[4] It is seen here that the cross section of the 3^- transition does show some change with energy and if one attempts to fit this transition at 35.4 MeV with a simple direct interaction calculation, the parameters obtained would be misleading. Thus, even though an angular distribution indicates that a process is predominantly direct in character, a study of the cross section as function of energy is always helpful if not essential in making reliable estimates of the nuclear matrix elements.

3) There is a strong energy variation in the cross sections leading to weakly excited states such as the 2^+(9.843 MeV) and the 4^+(10.363 MeV) levels. The nature of the reaction mechanism in these transitions is rather speculative, but it is a reasonable surmise that compound nuclear contributions are very important.

4) There is also considerable variation in the cross section leading to the (2^-) unnatural parity state at 8.875 MeV, again suggesting large compound nuclear contributions. Nonetheless it is interesting to note that the angular distribution for angles less than about 40° shows little change and

indeed shows some correspondence to the adiabatic prediction[5] for the unnatural parity excitation, 2^-, that the maxima and minima are those of the function, $J_1^2(kR\theta)$. (J. S. Blair, N. Cue, and D. Shreve)

---

1 Errata: in Cyclotron Research (University of Washington, 1964), p. 5. A more accurate measurement of the beam energy has been made and the incident energies should read, after subtracting energy loss in target, 39.8 MeV and 41.0 MeV instead of 40.0 MeV and 41.2 MeV respectively. Also, the quoted integrated cross sections from 18° to 70° for transitions to the 2^-(8.875 MeV) and the 4^+(10.363 MeV) states are in error. For corrected values see Figure 2-4 in text above.

2 J. S. Blair, Phys. Rev. 115, 928 (1959).

3 R. E. Brown, D. Bodansky, J. S. Blair, N. Cue, and C. D. Kavaloski, Phys. Rev. (to be published).

4 See for example J. S. Blair, in Proceedings of the International Conference on Nuclear Structure, edited by D. A. Bromley and E. W. Vogt (University of Toronto Press, Toronto, 1960), p. 824.

5 J. S. Blair, Comptes Rendus du Congrès International de Physique Nucléaire, Paris, 2-8 Juillet, 1964, Vol. II, p. 853.

---

3. Inelastic Scattering of Alpha Particles from Ne^{20}

Analysis of the experiment[1] $Ne^{20}(\alpha,\alpha')\ Ne^{20*}$ has been completed and the results will be published shortly. (J. S. Blair, N. Cue, G. W. Farwell, and D. C. Shreve)

---

1 Cyclotron Research, University of Washington (1964), p. 8.

---

4. Elastic and Inelastic Scattering of Alpha Particles by Mg^{24}, Mg^{25}, Mg^{26}, and Al^{27}

Additional analyses have been made of essentially all the data obtained in previously reported experiments.[1] Two further theoretical models for the reaction mechanism have been considered:

1) The distorted wave Born approximation for excitation of collective surface modes.[2] Computations have been carried out using the TSALLY code[2] furnished by the Oak Ridge group.

2) A simple modification[3] of the Fraunhofer inelastic diffraction model which includes effects due to a smooth transition at the edge of the nucleus from complete to no absorption.

Values of the nuclear deformation parameters, $\delta_L \equiv \beta_L R$, extracted using these two models are in fairly good accord; specifically, for the low excited

states the values of δ_L found with the modified Fraunhofer analysis are typically only about 10% less than those obtained with the more sophisticated distorted wave analysis although this discrepancy increases to 20 - 30% when the excitation energy is of the order of 5 MeV or larger. (J. S. Blair, G. W. Farwell, and I. M. Naqib)

---

1 Cyclotron Research, University of Washington (1962), p. 4 and (1963), p. 10.
2 R. H. Bassel, G. R. Satchler, R. M. Drisko and E. Rost, Phys. Rev. 128, 2693 (1962).
3 E. V. Inopin and Yu. A. Berezhnoy, Nucl. Phys. 63, 689 (1965).

---

5. Alpha Particle Scattering from Si^{28}

As a natural extension of previous studies[1] with targets in the middle of the s-d shell, an investigation has been initiated of elastic and inelastic scattering of alpha particles from Si^{28}. This study is particularly germane in that inelastic scattering leading to low even parity states in Al^{27} has been attributed[1] to excitation of the Si^{28} core.

A preliminary experiment with a natural silicon target has yielded angular distributions to the ground state and to the 1.78, 4.62, 4.98, 6.32, and 6.88-6.89 MeV levels. However, all of the cross sections, except those to the ground state and the 1.78 MeV level, contained substantial contamination from levels of Si^{29} and Si^{30} present in the natural target, and this circumstance made intensive analysis of the data premature. For example, the small yield to the 6.32 MeV (3^+) level in Si^{28} was almost submerged in the contamination background. An isotopically pure (> 98% pure) Si^{28} target is being made to overcome these difficulties.

One of the interesting results from this experiment is the strong excitation of the doublet at 6.88-6.89 MeV. The intensity of this group is exceeded only by the elastic scattering and by excitation of the 1.78 MeV (2^+) level. The angular distribution of this unresolved doublet has a characteristic single excitation shape and its maxima are in phase with the maxima of the elastic and angular distribution. An analysis in terms of the Fraunhofer diffraction model suggests that one level, with either spin 1^- or 3^-, dominates. These assignments are in conflict with some determinations[2] made using other techniques. (J. S. Blair, W. J. Braithwaite, W. A. Kolasinski, and E. Preikschat)

---

1 I. Naqib, Ph.D. Thesis, University of Washington (1962).
2 R. Nordhagen and A. Tveter, Nucl. Phys. 63, 529 (1965).

---

6. Alpha Particle Scattering from Nuclei with 20 Protons or 28 Neutrons

The elastic and inelastic scattering of 42 MeV alpha particles from Ca^{42}, Ca^{44}, V^{51}, Cr^{52}, and Fe^{54} has been studied at laboratory angles from 13° to 70° with an energy resolution ranging from 90 keV to 160 keV. The experimental angular distributions are being compared to the Fraunhofer, optical model, and parameterized phase shift theories.

Figure 6-1 shows a typical spectrum from Ca^{42}. The large peaks from C^{12} and O^{16} are due to the mylar backing of the target. In Figure 6-2 are shown fits of the damped Fraunhofer,[1] optical model,[2] and phase shift analyses[3] to the elastic scattering from Ca^{44}. The fact that the damped Fraunhofer theory leads to fits which are inferior to those of the other models is largely due to its neglect of Coulomb scattering. The parameters for all three models are listed in Table 6-1.

Many levels have been found in the even targets, and some preliminary values for their spins, parities, seniorities, and transition rates are listed in Table 6-2. The spin and parity can be deduced from the phasing of the angular distributions, and states which have seniority equal to 4 are recognized by the double

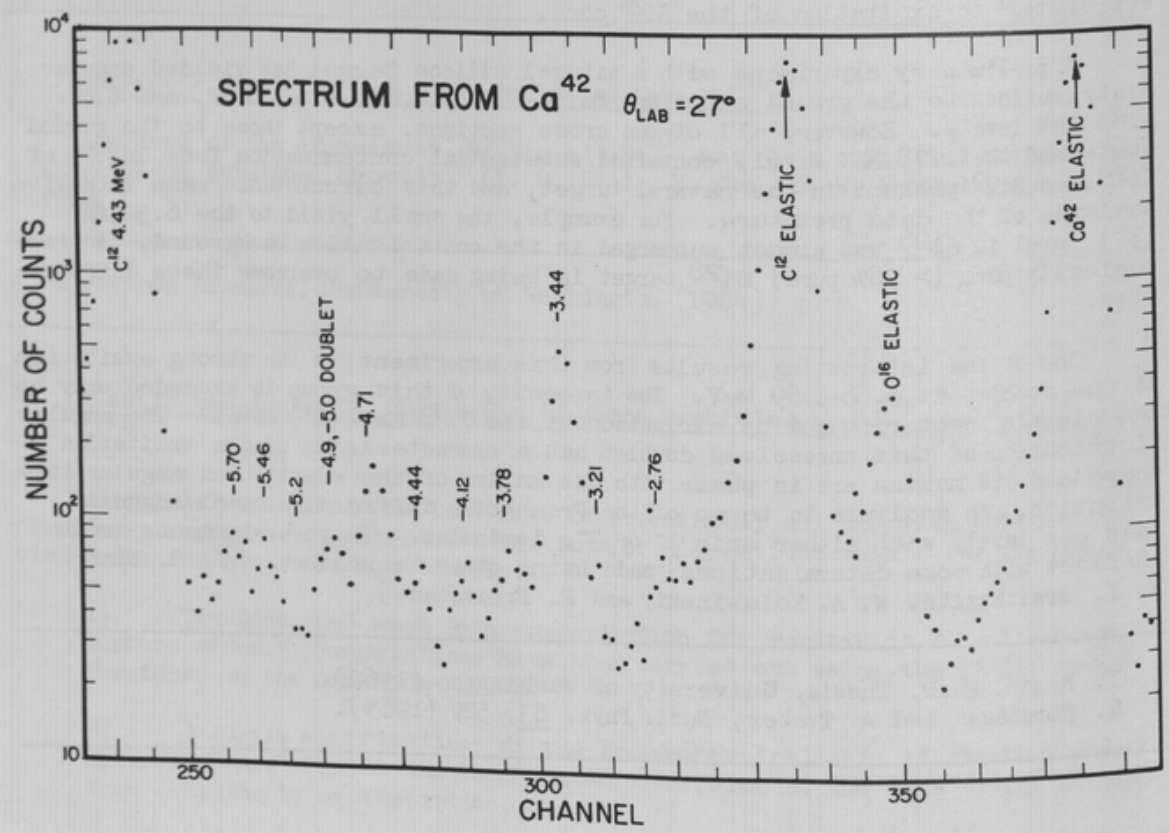

Fig. 6-1 A typical spectrum of 42 MeV alpha particles scattered from Ca^{42}.

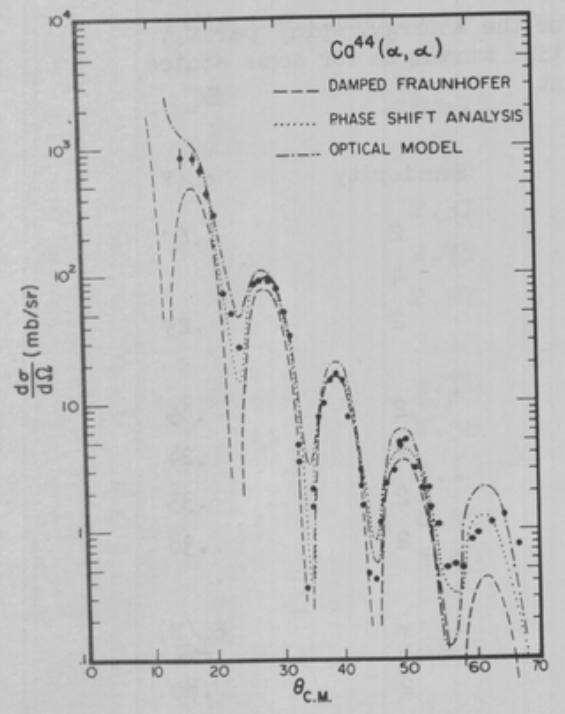

Fig. 6-2 The fits of the damped Fraunhofer, optical model, and phase shift analyses to the elastic scattering from Ca^{44}. The parameters used are listed in Table 6-1.

excitation nature of their differential cross sections.[4] The transition strengths (δ_I's) in the table are extracted from the smooth-cutoff Fraunhofer approximation, and are in approximate agreement with those from an adiabatic shift analysis.[5] It is worth noting that for each target there are several 2^+ and 3^- states with fairly large cross sections.

One odd nucleus, V^{51}, has been studied. It is known that the low-lying states of V^{51} are well-described by the j-j coupling shell model with an $(f_{7/2})^3$ configuration. Within this configuration, excitation of each state can proceed by several values of the angular momentum transfer, L, the weighting of each angular momentum being determined by the detailed wave functions for the ground and excited levels.[6] For example, the $9/2^-$ state at 1.81 MeV is primarily excited by L = 4, and the $11/2^-$ state at 1.61 MeV by L = 2. Figure 6-3 shows that curves computed using the appropriate weightings of L = 2, 4, and 6 reproduce the data quite closely, especially at small angles, where the predictions are most

Table 6-1. Parameters used to fit the elastic scattering of 42 MeV alpha particles from Ca^{44}.

Fraunhofer	Optical Model	Phase Shift
$x = 2kR \sin \theta/2$	$r_0 = 1.20$ F	$L_A = 16.18$
R = 6.63 F	R = 1.70 F	$\Delta L_A = .876$
$f' = 2J_1(y)/y$	R = 5.936 F	$\delta = .748$
$y = 2k\Delta \sin \theta/2$	V = -40 MeV	$L_\delta = 16.47$
Δ = 1.16 F	W = -15 MeV	$\Delta L_\delta = 1.47$
	D = .50 F	

Table 6-2. Preliminary results for the energy, spin, parity, seniority, and transition strength for some states seen in this experiment.

Ca^{42}	-Q(MeV)	I^{π}	Seniority	$\delta_I(F)$
	1.53	2^+	2	.69
	1.84	0^+	4	
	2.43	2^+	2	.29
	2.76	(4^+)		
	3.44	3^-	2	.69
	3.78	3^-	2	.24
	4.12	5^-	2	.33
	4.71	3^-	2	.38

Ca^{44}	-Q(MeV)	I^{π}	v	$\delta_I(F)$
	1.16	2^+	2	.80
	1.88	0^+	(4)	
	2.28	(4^+)		
	2.66	2^+	2	.22
	3.04	2^+	2	.14
	3.35	3^-	2	.56
	3.73	$1^-,3^-$	2	
	3.98	(5^-)	2	
	4.44	$1^-,3^-$	2	
	4.73	4^+	2	.26
	5.07	$1^-,3^-$	2	
	5.39	$1^-,3^-$	2	
	5.87	3^-	2	.25
	6.8	$1^-,3^-$	2	

Table 6-2. (continued)

Cr^{52}	-Q(MeV)	I^{π}	v	$\delta_I(F)$
	1.43	2^+	2	.68
	2.37	4^+	2	.24
	2.75	4^+	2	.20
	2.97	2^+	4	
	3.12	2^+	2	.26
	3.78	2^+	2	.35
	4.56	3^-	2	.61
	5.1	4^+	2	
	6.46	3^-	2	.18
	7.03	3^-	2	.21

Fe^{54}	-Q(MeV)	I^{π}	v	$\delta_I(F)$
	1.41	2^+	2	.52
	2.53	4^+	2	.21
	2.95	2^+	2	.35
	3.16	2^+	2	.20
	3.3	4^+	2	.13
	3.82	4^+	2	.20
	4.05	4^+	2	.10
	4.26	4^+	2	.17
	4.58	2^+	2	.16
	4.76	3^-	2	.21
	4.95	1^-	2	.11
	6.34	3^-	2	.31

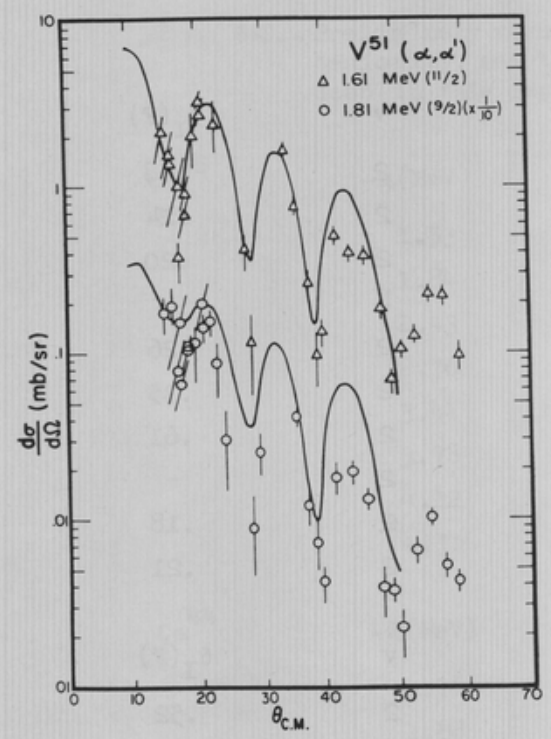

Fig. 6-3 Data from the scattering to the 1.61 MeV ($11/2^-$) and 1.81 MeV ($9/2^-$) states of V^{51}, compared to the predictions of the $(f_{7/2})^3$ configuration and the Fraunhofer approximation, with $x = 2kR \sin \theta/2$, R = 6.66 F, Δ = .83 F.

sensitive to L. To deepen the theoretical minima, perhaps the magnitude of the L = 2 component should be increased. The theoretical curve uses the Fraunhofer approximation for the differential cross section for each L. The total strength of the interaction is the only new parameter, and is the same for all states; the ratio of the $9/2^-$ and $11/2^-$ predictions is given by the model.

It is planned to study the scattering from Ca^{48} to complete this study of the nuclei with a closed $f_{7/2}$ shell, and to utilize more fully available theoretical methods in the interpretation of the data. (R. J. Peterson)

1 E. V. Inopin and Yu. A. Berezhnoy, Nucl. Phys. 63, 689 (1965).
2 J. G. Wills, Ph.D. Thesis, University of Washington (1962).
3 J. Alster, Ph.D. Thesis, University of California Radiation Laboratory Report UCRL-9650 (1961).
4 J. S. Blair in "Lectures on Nuclear Interactions," Herceg-Novi 1962, Volume II (Federal Nuclear Energy Commission of Yugoslavia, Belgrade, 1964).
5 N. Austern and J. S. Blair, to be published.
6 H. O. Funsten, N. R. Roberson, and E. Rost, Phys. Rev. 134, B117 (1964).

7. Alpha Particle Scattering from Sr^{88} and Y^{89}

The motivation and results of a preliminary investigation of the experiment $Y^{89}(\alpha,\alpha')Y^{89*}$ were reported earlier.[1] This year, by using a thin Y^{89} target[2] the experiment was completed. Also, a previous measurement of inelastic alpha particle scattering from natural Sr performed at this laboratory[3] was not accurate enough to permit consistent comparisons to be made between $Y^{89}(\alpha,\alpha')$ and $Sr^{88}(\alpha,\alpha')$. The latter measurement was therefore repeated using an enriched Sr^{88} target[4] and improved energy resolution.

The results of these experiments are shown in Figures 7-1, 7-2, 7-3, and 7-4. The angular distributions for the 2^+(1.84 MeV) and 3^-(2.74 MeV) states in Sr^{88} (Figure 7-1) have oscillations with the phasing expected from the Blair phase rule.[5] The strongly excited states in Y^{89} show similar oscillations.

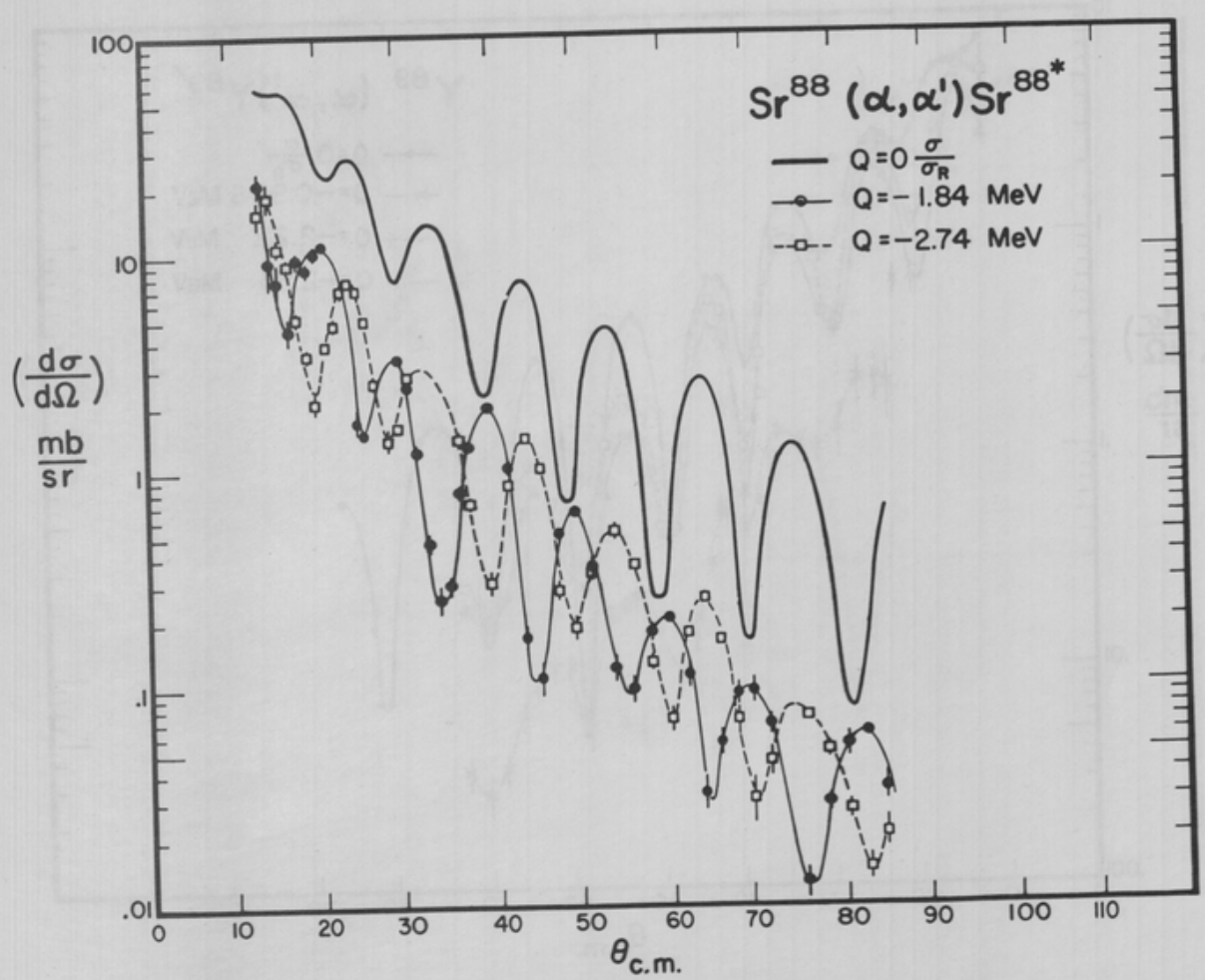

Fig. 7-1 Angular distributions for the elastic scattering divided by the Rutherford cross section and the inelastic scattering from the 1.84 MeV (2^+) and 2.74 (3^-) states in Sr^{88}.

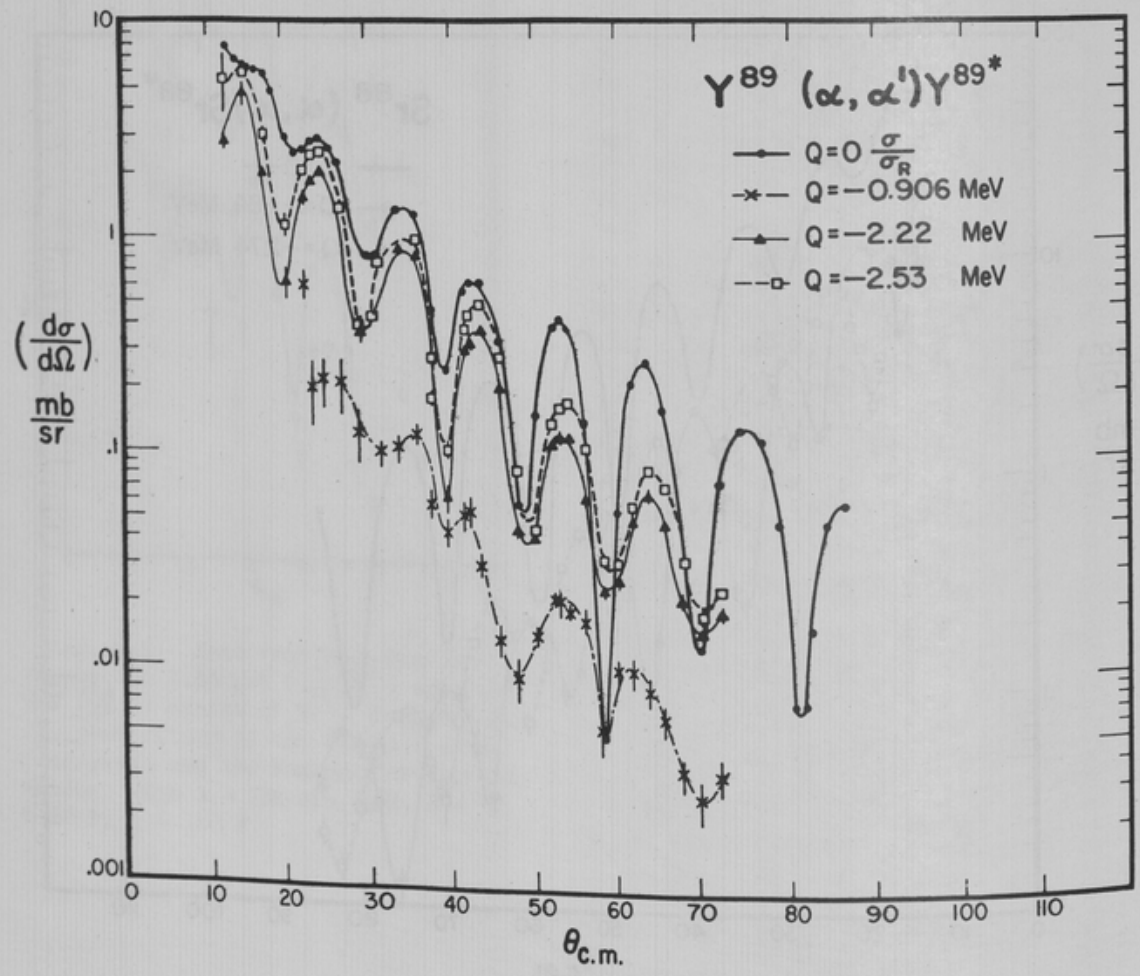

Fig. 7-2 Angular distributions for the elastic scattering divided by the Rutherford cross section and the inelastic scattering from the 0.906 MeV $(9/2^+)$, the 2.22 MeV $(5/2^+)$, and the 2.53 MeV $(7/2^+)$ states in Y^{89}.

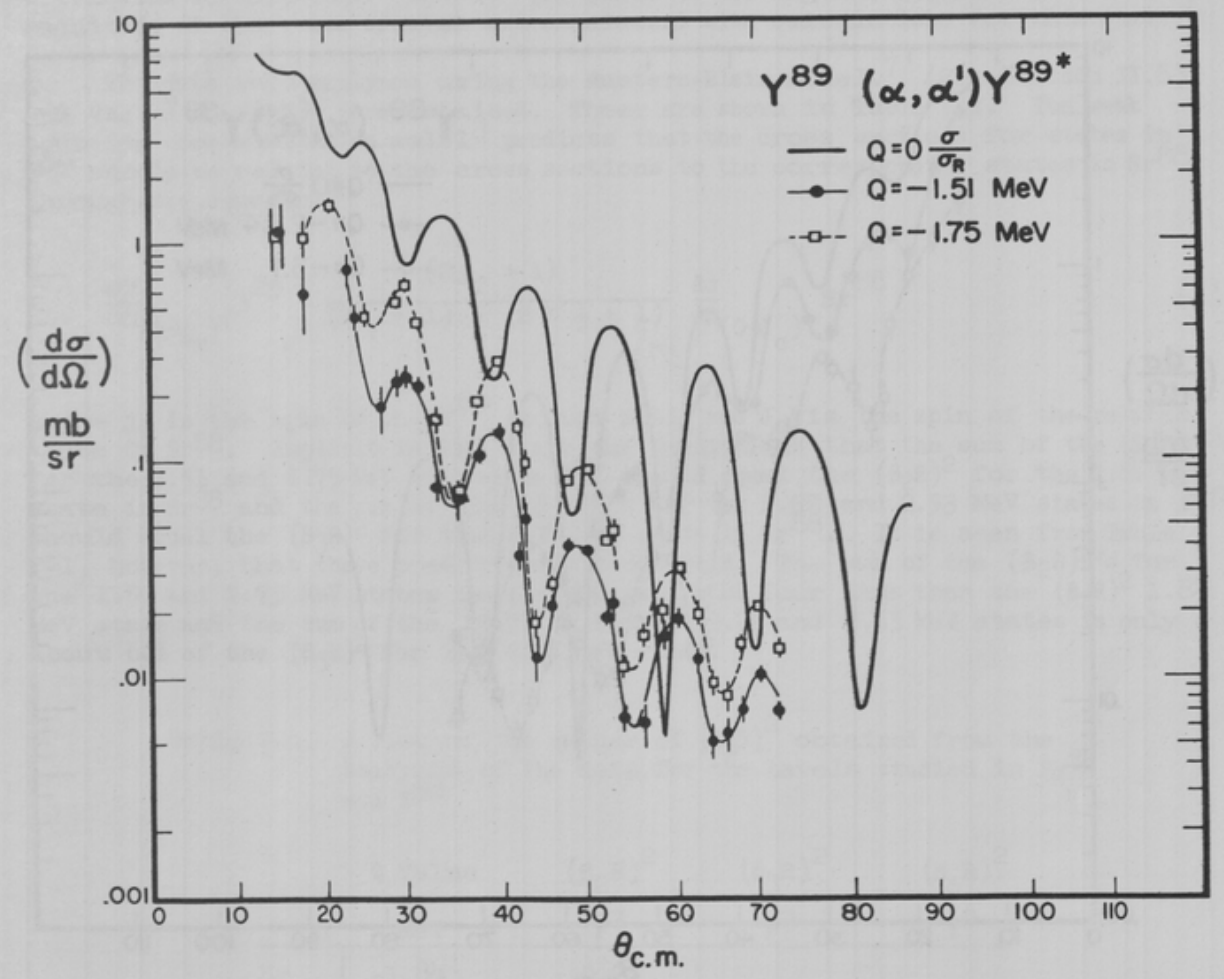

Fig. 7-3 Angular distributions for the inelastic scattering from the 1.51 MeV $(3/2^-)$ and the 1.75 MeV $(5/2^-)$ states in Y^{89}. The elastic cross section divided by the Rutherford cross section is shown for comparison.

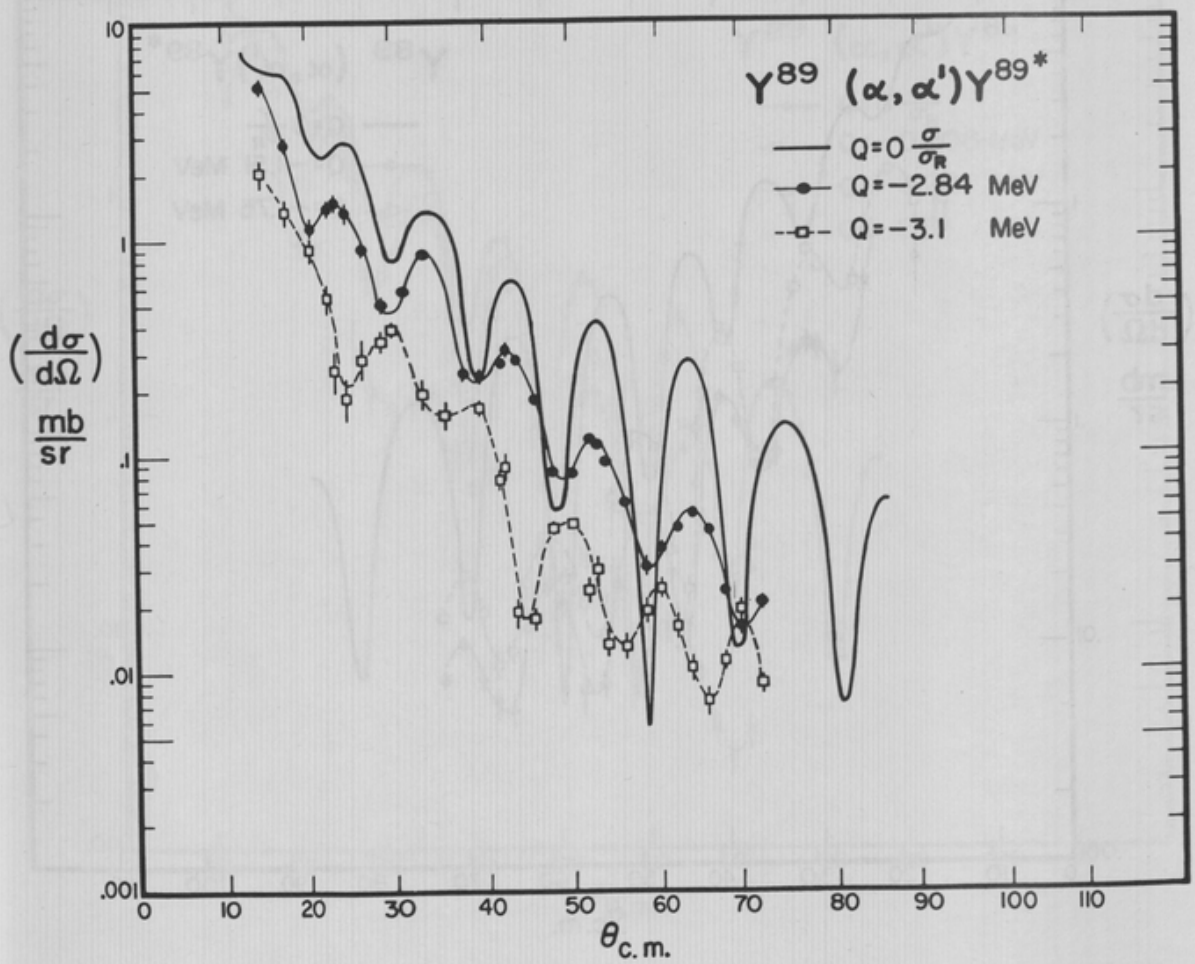

Fig. 7-4 Angular distributions for the inelastic scattering from the 2.84 MeV and 3.1 MeV states in Y^{89}. The elastic cross section divided by the Rutherford cross section is shown for comparison of the phasing.

The 0.906 MeV $(9/2^+)$ state in Y^{89} is a pure $g_{9/2}$ single particle state. In Figure 7-2 it is seen that the angular distribution to this state has regular oscillations in phase with the elastic cross section much like the angular distributions to collective states. The shape of the angular distribution and the magnitude of the cross section are consistent with calculations for this state.[6]

The data were analyzed using the Austern-Blair model.[7] (See Section II.8) and values of $(\beta_I R)^2$ were obtained. These are shown in Table 7-1. The weak coupling core-excitation model[8] predicts that the cross sections for states in Y^{89} should be related to the cross sections to the corresponding states in Sr^{88} through the equation[9]

$$\frac{d\sigma}{d\Omega}_{(\frac{1}{2}\rightarrow j_f)}^{Y^{89}} = \frac{(2j_f + 1)}{(2J_c + 1) \cdot (2 \times \frac{1}{2} + 1)} \frac{d\sigma}{d\Omega}_{(0\rightarrow J_c)}^{Sr^{88}} \qquad (1)$$

where j_f is the spin of the Y^{89} excited state and J_c is the spin of the related state in Sr^{88}. Implicit in Eq. 1 are the predictions that the sum of the $(\beta_2 R)^2$'s for the 1.51 and 1.75 MeV states in Y^{89} should equal the $(\beta_2 R)^2$ for the 1.84 MeV state in Sr^{88} and the sum of the $(\beta_3 R)^2$'s for the 2.22 and 2.53 MeV states in Y^{89} should equal the $(\beta_3 R)^2$ for the 2.74 MeV state in Sr^{88}. It is seen from Table 7-1, however, that these predictions do not hold. The sum of the $(\beta_2 R)^2$'s for the 1.51 and 1.75 MeV states is about a factor of four less than the $(\beta_2 R)^2$ 1.84 MeV state and the sum of the $(\beta_3 R)^2$'s for the 2.22 and 2.53 MeV states is only about 60% of the $(\beta_3 R)^2$ for the 2.74 MeV state.

Table 7-1. A list of the values of $(\beta_I R)^2$ obtained from the analysis of the data for the levels studied in Sr^{88} and Y^{89}

	Q Value	$(\beta_2 R)^2$	$(\beta_3 R)^2$	$(\beta_5 R)^2$
	MeV	F^2	F^2	F^2
Sr	-1.84	0.25		
	-2.74		0.30	
	-3.2	~ 0.02		
	-0.906			0.01
	-1.51	0.02		
Y	-1.75	0.04		
	-2.22		0.07	
	-2.53		0.11	
	-2.84		0.06	
	-3.1	0.025		

Also implicit in Eq. 1 is the prediction that the cross sections to states of a doublet in Y^{89} should be in phase. The cross sections to the 2.84 and 3.1 MeV states in Y^{89} have opposite phase (Figure 7-4) indicating that they cannot be members of a doublet corresponding to the 2^+ (3.21 MeV) state in Sr^{88} as suggested by Shafroth.[10]

The results of this experiment seem to rule out the core-excitation model for the 1.51 and 1.75 MeV states in Y^{89}. The magnitudes of the $(\beta_2 R)^2$'s for these states are comparable with the $(\beta_5 R)^2$ for the $g_{9/2}$(0.906 MeV) single particle state which might suggest that they are hole states in the $p_{3/2}$ and $f_{5/2}$ proton subshells. Such a description might explain the discrepancy between the sum of the $(\beta_2 R)^2$'s for these states and the $(\beta_2 R)^2$ for the 2^+ (1.84 MeV) state in Sr^{88}. The 2.22, 2.53, and 2.84 MeV states in Y^{89} all have the same parity and the sum of their cross sections almost equals the cross section to the 2.74 MeV state in Sr^{88} but the existence of three positive parity states is not explained by the simple core-excitation model.

The results of this experiment have been reported[11] and a complete paper will be published shortly. (J. Alster and D. C. Shreve)

---

1 Cyclotron Research, University of Washington (1963), p. 11.
2 The Y target was obtained from F. Karasek.
3 J. S. Blair, G. W. Farwell, and D. K. McDaniels, Nucl. Phys. 17, 641 (1960).
4 J. Sauer, to be published in Rev. Sci. Instr. 1965.
5 J. S. Blair, Phys. Rev. 115, 928 (1959).
6 D. F. Jackson, Phys. Letters 14, 118 (1965).
7 N. Austern and J. S. Blair, to be published.
8 A. de-Shalit, Phys. Rev. 122, 1530 (1961).
9 J. S. Blair, Proceedings of the Symposium on Nuclear Spectroscopy with Direct Reactions, Argonne, Illinois, 1964 ANL-6878.
10 S. M. Shafroth, P. N. Trehan and D. M. VanPatter, Phys. Rev. 129, 704 (1963).
11 J. Alster and D. C. Shreve, Bull. Am. Phys. Soc. 10, 130 (1965).

---

8. Inelastic Scattering of 42 MeV Alpha-Particles from Pb^{207}, Pb^{208} and Bi^{209}

The work reported in the previous progress report[1] was completed. The identical behavior of the levels at 2.6 MeV in the three nuclei is now more firmly established, and was recently published.[2] (See also Figure 8-1.) Using the Austern-Blair[3] model for inelastic scattering $\beta_I R$ values were obtained for all the levels identified in the spectra, and are tabulated in Table 8-1. The results show that the collective strength for all the measured levels in Pb^{208} is present, to the same extent, in the neighboring nuclei Pb^{207} and Bi^{209}.

A complete account of this experiment is now being prepared for publication. Partial results on the excitation of the levels in Pb^{206} have been obtained. (J. Alster)

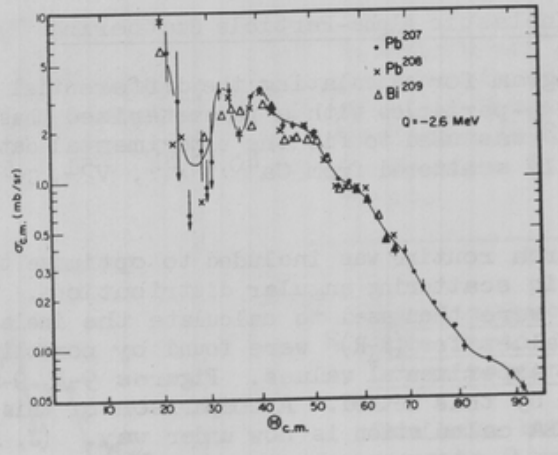

Fig. 8-1 Angular distributions for inelastically scattered alpha particles from the 2.60 MeV level in Pb^{207}, the 2.615 MeV level in Pb^{208} and the sum of the 2.50 and 2.67 MeV levels in Bi^{209}.

Table 8-1. List of $(\beta_I R)$ values obtained from the Austern-Blair model

	Pb^{207}		Pb^{208}		Bi^{209}	
I	E_{exc}	$\beta_I R$	E_{exc}	$\beta_I R$	E_{exc}	$\beta_I R$
	MeV	F	MeV	F	MeV	F
3	2.60	0.74	2.61	0.75	2.50 2.67	0.76
5	3.4 3.6	0.34	3.20	0.32	3.10	0.32
2(4)	4.07 4.27	0.55	4.12 4.40	0.45	--	--

1 Cyclotron Research, University of Washington (1964), p. 10.
2 Proceedings of the Congrès International de Physique Nucléaire II; Editions du Centre National de la Recherche Scientifique, Paris 1964, p. 450.
3 N. Austern and J. S. Blair; to be published in Annals of Physics. See also Section 9.

9. Calculation of Inelastic Alpha-Particle Scattering

The computer program for calculating the differential cross section of inelastically scattered α-particles with a parameterized phase shift model[1] described previously,[2] was used to fit the experimental data[3] of 42 MeV α-particles inelastically scattered from $Ca^{40,42,44}$, V^{51}, Cr^{52}, Sr^{88}, Y^{89}, Pb^{207}, Pb^{208}, and Bi^{209}.

An automatic search routine was included to optimize the parameters used in calculating the elastic scattering angular distributions. The phase shifts obtained in this manner were then used to calculate the inelastic scattering angular distributions. Values for $(\beta_I R)^2$ were found by normalizing the calculated cross sections to the experimental values. Figures 9-1, 9-2, and 9-3 show some typical fits obtained by this method. A comparison of this parameterized phase shift model with a DWBA calculation is now under way. (J. Alster)

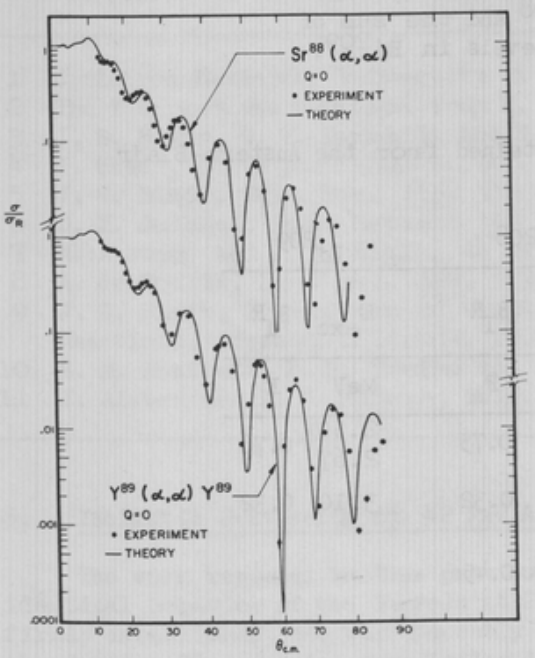

Fig. 9-1 Calculation for elastic scattering of 42 MeV α particles from Sr^{88} and Y^{89}.

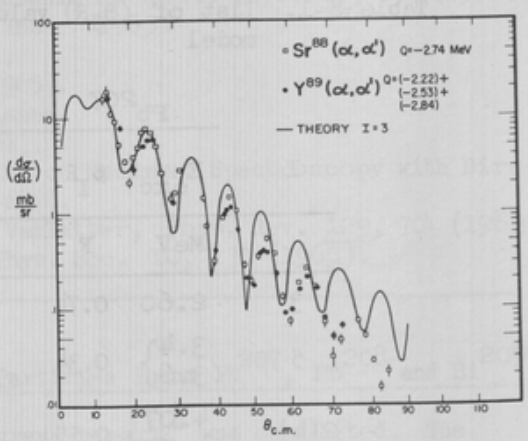

Fig. 9-2 Calculation for inelastic scattering of 42 MeV α particles from the 2.74 MeV level in Sr^{88} and the sum of the 2.22, 2.53 and 2.84 MeV levels in Y^{89}.

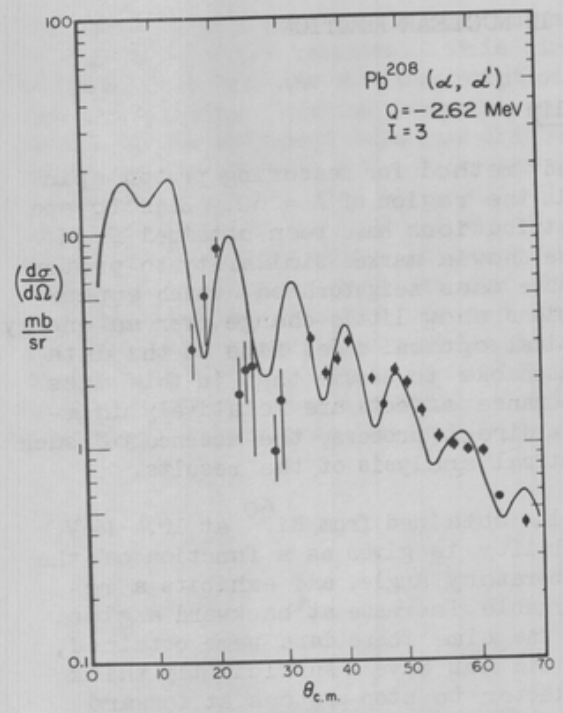

Fig. 9-3 Calculation for inelastic scattering of 42 MeV α particles from the 2.615 MeV level in Pb^{208}.

1 N. Austern and J. S. Blair, to be published in Annals of Physics.
2 Cyclotron Research, University of Washington (1964), p. 12.
3 See Sections 6, 7, and 8 of this report.

10. Magnetic Spectrometer Analysis of Alpha-Particle Scattering: Q Value Determinations

Data have been obtained to determine accurate Q values for states excited in inelastic alpha scattering from Cr^{52}. Q values and relative intensities are listed below for scattering at a laboratory angle of 20°. All uncertainties in Q values are ± 10 keV. Data obtained from Si^{28} and Ge^{72} have not been analyzed due to a lack of scanning staff. (R. J. Peterson)

-Q(MeV)	Intensity (Arbitrary Units)
1.434	180
2.774	35
3.156	45
3.774	120
4.050	20
4.585	45
4.720	30
5.109	15
5.446	40
5.705	25
6.210	20
6.588	25
7.026	50
7.503	25
7.764	30

III. ANGULAR CORRELATIONS IN NUCLEAR REACTIONS

11. Proton Angular Correlations and Spin Flip

We are applying the previously described[1] method for measuring proton spin flip during inelastic scattering to nuclei in the region of A = 60. Elastic and inelastic (Q = -1.33 MeV) proton angular distributions have been obtained from Ni^{60} at 10.4 MeV incident beam energy. These show a marked similarity to proton angular distributions from elements in the same mass neighborhood, which appear in the paper by Buck.[2] The latter distributions show little change over an energy range from 10 MeV to 17 MeV, and the theoretical optical model fits to the data are reasonably good. It therefore seems reasonable to assume that in this mass region, at proton energies above 10 MeV, resonance effects are relatively unimportant. If spin flip can be attributed to a direct process, the absence of such resonance effects should simplify the theoretical analysis of the results.

Figure 11-1 shows some preliminary results obtained from Ni^{60} at 10.4 MeV incident proton energy. The spin-flip probability is given as a function of the laboratory angle, and exhibits a remarkable increase at backward angles. At the time these data were obtained, we did not have a sufficiently thick detector to stop protons at forward angles - hence the absence of data at these angles. The equipment for performing the above measurements is ready for use in conjunction with the tandem Van de Graaff accelerator, which is scheduled for operation in the very near future. (W. J. Braithwaite, J. G. Cramer, W. A. Kolasinski, E. Preikschat and F. H. Schmidt)

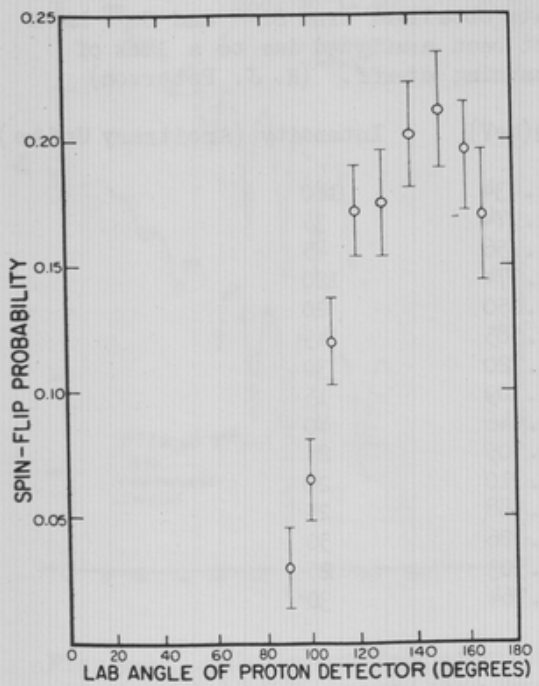

Fig. 11-1 Proton spin-flip probability in inelastic scattering to the first excited state of Ni^{60}, at 10.4 MeV incident proton energy.

1 F. H. Schmidt, R. E. Brown, J. B. Gerhart, and W. A. Kolasinski, Nucl. Phys. 52, 353 (1964).
2 B. Buck, Phys. Rev. 130, 712 (1963).

12. Angular Correlations in (d,pf) Reactions

In a nuclear stripping reaction such as the d,p reaction it is possible to leave the residual nucleus with sufficient excitation energy for fission to occur. The direction of emission of the fission fragments is dependent on

the direction of the angular momentum vector characterizing the residual nucleus following the d,p reaction. This direction is in turn determined by the stripping process. In a plane wave description of the stripping process the in-plane angular correlation (fission fragment angular distribution observed in the plane defined by the incident deuteron and the stripped proton) is expected to be symmetric about an axis defined by the direction of motion of the recoil nucleus following the stripping reaction. The out-of-plane correlation (fission fragment angular distribution measured in the plane perpendicular to the recoil or symmetry axis) will be isotropic. In observations[1] of the $(\alpha,\alpha'f)$ reaction in which the in-plane fission fragment angular distributions showed substantial anisotropies, the out-of-plane fission fragment angular distributions were isotropic. However, for the modest particle energies and high-atomic-number targets employed in d,pf studies,[2,3] Coulomb distortion effects may be severe. Distorted-wave calculations[4] indicate that appreciable deviations from the simple plane-wave predictions will occur when the proton is observed at angles forward of 140°.

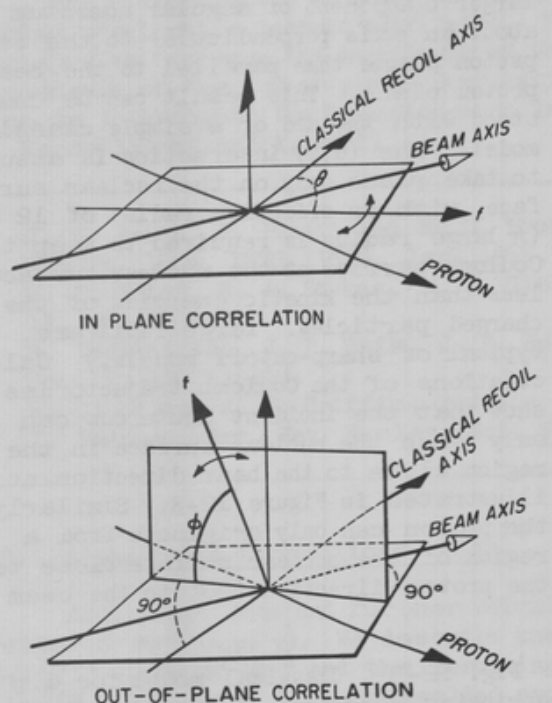

Fig. 12-1 Sketch of experimental detector configuration.

Previous (d,pf) experiments have only explored in-plane correlations. These experiments[2,3] have been consistent with the symmetry axis for the angular correlations coinciding with the classical recoil direction, even for proton angles appreciably smaller than 140°.

An experiment to measure the out-of-plane correlation has been initiated. The apparatus consists of a thick Li-drifted solid state detector for observing the proton. Four thin surface barrier detectors mounted at 0°, 30°, 60°, and 90° to the beam-proton plane are used to detect the fission fragments. A sketch of the experimental arrangement is shown in Figure 12-1. The signals from the fission fragment detectors are used to route the proton signal to the appropriate quadrant of a multichannel analyzer. This technique permits a measurement of the out-of-plane angular correlation for all proton energies in a single run.

Preliminary experiments have been performed in which the 21 MeV deuteron beam from the cyclotron was degraded to 15 MeV by means of degrader foils placed in the beam collimator assembly. This resulted in a lowered beam intensity and a high neutron flux in the scattering chamber which severly handicapped the experiment. A fairly thick target of U^{235} was required and insufficient data were obtained to divide the proton spectrum into energy bins. The preliminary results, however, were quite interesting. With the proton counter fixed at 90°, the out-of-plane anistropy, for proton energies between 8.5 and 14.5 MeV (corresponding to fission occurring at an excitation energy

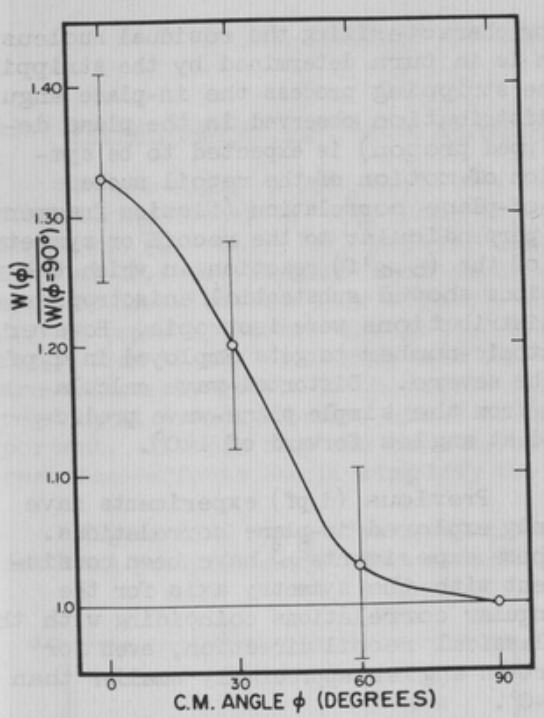

Fig. 12-2 Fission fragment anisotropy as a function of the azimuthal angle with respect to the beam-proton plane.

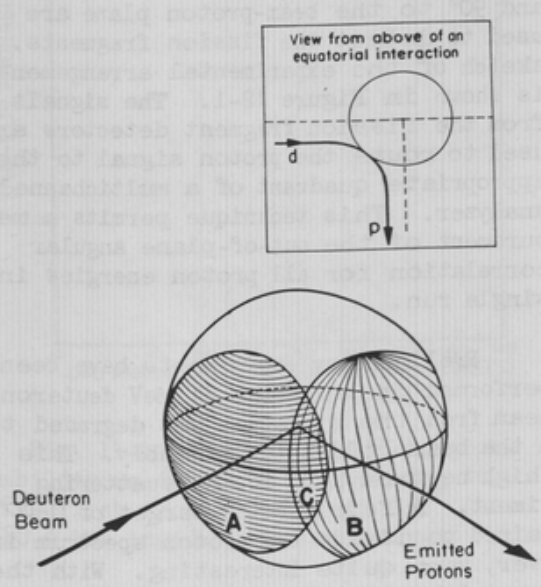

of 6 MeV or less above the fission threshold) is shown in Figure 12-2. When the proton detector is moved back to 140°, the out-of-plane correlation decreases but does not disappear.

The out-of-plane angular correlation for a proton angle of 90° showed more fission fragments were emitted per unit solid angle in the beam-proton plane than at 90° with respect to the plane. Since fission fragments are known[5] to be emitted preferentially at angles perpendicular to the angular momentum vector of the fissioning nucleus, this observation implies that the d,p interaction produces nuclei with a larger component of angular momentum about an axis perpendicular to the beam-proton plane than parallel to the beam-proton plane. This result can be understood with the aid of a simple classical model. The (d,p) interaction is assumed to take place only on the nuclear surface, with an effective radius of 12 F. (A large radius is required to keep the Coulomb barrier at the nuclear surface less than the kinetic energies of the charged particles. Large radii are typical of sharp-cutoff models.) Calculations of the Coulomb trajectories show that the incident deuterons can only reach the nuclear surface in the region close to the beam direction as is illustrated in Figure 12-3. Similarly the proton can only originate from a region of the nuclear surface close to the proton direction (90° to the beam

Fig. 12-3 Classical model for d.p stripping reaction. Region A is the region of the nuclear surface accessible to the incoming deuteron, region B is the region of the nuclear surface from which protons can originate and end up at 90° with respect to the deuteron beam, and region C is the region where a (d,p) interaction can occur. The inset shows an equatorial collision as viewed from above the deuteron-proton plane.

direction). The d,p interaction can then only take place where these two regions overlap, namely on a small region of the nuclear surface which is centered on the beam-proton plane (region C of Figure 12-3). Momentum transfer leading to angular momentum about an axis perpendicular to the beam-proton plane arises primarily from the large component of the proton-deuteron momentum mismatch which is perpendicular to the radius vector lying in the beam-proton plane. An equatorial collision results in no component of angular momentum parallel to the beam-proton plane. An interaction occurring above or below the equator can produce a component of angular momentum parallel to the beam-proton plane, but calculations show that the region of nuclear surface on which the interaction can occur does not extend far enough above or below the equator to yield as large an angular momentum component parallel to the beam-proton plane as perpendicular to this plane. It is interesting to note that this qualitative picture of the reaction mechanism implies a polarization of the fissioning nucleus, although the experimental measurements are incapable of detecting polarization.

These experiments will be continued under more favorable conditions when the tandem accelerator becomes available. Targets with smaller nuclear spins can be employed to increase the magnitude of the anisotropy. It is planned to study the dependence of the out-of-plane correlation on the proton angle in more detail and also to investigate the dependence on incident deuteron energy. (W. Loveland, R. Vandenbosch, and K. Wolf).

---

1 H. C. Britt, F. Plasil and S. G. Thompson, Nuclear Chemistry Division Annual Report, 1964, UCRL 11828, Jan. 1965.
2 H. C. Britt, R. A. Stokes, W. R. Gibbs, and J. J. Griffin, Phys. Rev. Letters 11, 343 (1963).
3 R. Vandenbosch, J. P. Unik, J. R. Huizenga, and B. D. Wilkins, Bull. Am. Phys. Soc. 9, 422 (1964).
4 W. Gibbs and J. J. Griffin, private communication.
5 I. Halpern, Ann. Rev. Nuclear Sci. 9, 245 (1959).

---

13. Alpha-Gamma Correlations on Mg^{24}

Additional data and further calculations have been added to the previous results[1] on $Mg^{24}(\alpha,\alpha'\gamma)$. We describe the correlation pattern for exciting the 1.37 MeV(2^+) state of Mg^{24} and the resulting de-excitation gamma radiation by $A + B \sin^2(\theta - \theta_0)$, with θ_0 the so-called symmetry angle. Special attention was paid in relating the results to the adiabatic model predictions.[2]

In Figure 13-1 the experimental dependence of θ_0 on θ_α, the direction of the inelastically scattered alpha particle, is compared to a prediction of Wills and Cramer,[3] the result in the plane-wave Born approximation (labeled recoil angle), and the prediction of the adiabatic approximation. Wills and Cramer assume that only one incoming particle wave L_{in} contributes to the scattering, and that $L_{out} = L_{in} - 2$. The results of a previous experiment[4] on $C^{12}(\alpha,\alpha'\gamma)$ are also shown.

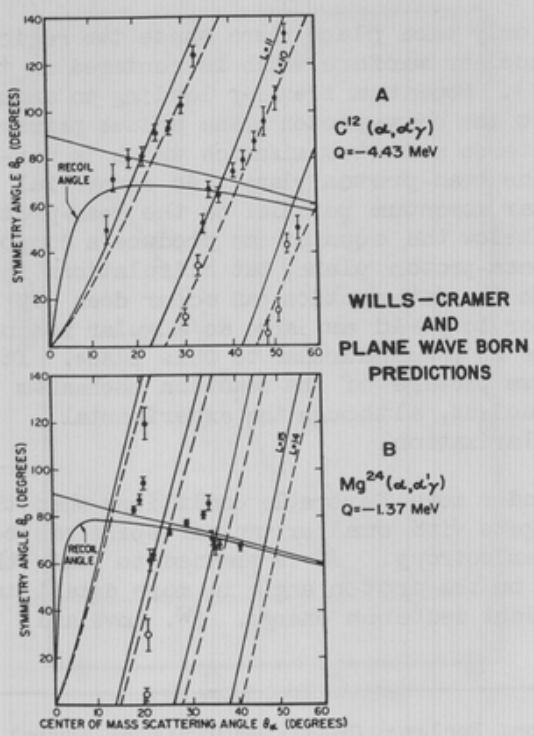

Fig. 13-1 Predictions of the Wills-Cramer and plane-wave Born approximation for the symmetry axis.

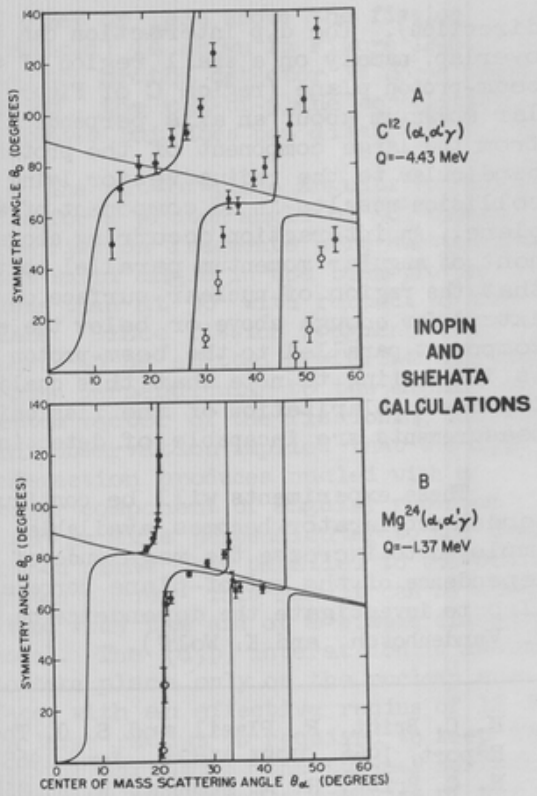

Fig. 13-2 Predictions of the Inopin and Shehata calculations for the symmetry angle.

Figure 13-2 compares to the prediction of Inopin and Shehata,[5] who extend the adiabatic theory to first order in the non-adiabaticity. Adiabatic here is used to mean that the nuclear wave function changes only slightly while the alpha particle senses the nuclear potential. This prediction may be contrasted with that of the extremely non-adiabatic Wills-Cramer model.

Figure 13-3 shows the comparison with a distorted-wave Born approximation calculation[6] and a coupled channel calculation.[7] Two sets of optical parameters gave equivalent fits to the angular distribution of $C^{12}(\alpha,\alpha')^8$, but one is clearly preferred by the correlation data. The parameters involved are listed in the table.

It is seen that the simpler theories do not account for the observed excursions of the symmetry angle, and that in particular, these excursions seem to be due to the influence of the non-adiabatic part of the scattering amplitude. Excitation of the Mg^{24} 1.37 MeV state better fulfills the adiabatic approximation than does excitation of the 4.43 MeV state of C^{12}, and it can be seen that the more adiabatic theories fit the Mg^{24} data better, while the extremely

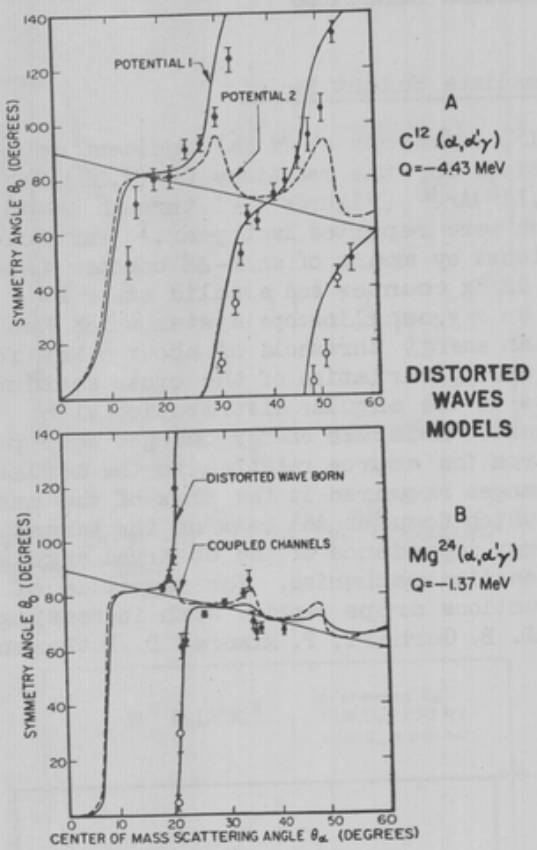

Fig. 13-3 The predictions for the symmetry angle of several calculations based on the optical model.

non-adiabatic theory of Wills and Cramer gives better agreement with C^{12}. While the inelastic scattering of medium energy alpha particles has been well accounted for by the adiabatic theories,[9,10] it is seen that the angular correlation of the de-excitation gamma rays must also take into account the non-adiabatic components of the scattering amplitude. (G. W. Farwell, D. L. Hendrie, and R. J. Peterson)

---

1 Cyclotron Research, University of Washington (1964), p. 19. D. L. Hendrie, Ph.D. Thesis, University of Washington (1964).

2 J. S. Blair and L. Wilets, Phys. Rev. 121, 1493 (1961).

3 J. G. Wills and J. G. Cramer, Jr., Argonne National Laboratory Report ANL-6848 (1964).

4 Cyclotron Research, University of Washington (1962), p. 9.

5 B. V. Inopin and S. Shehata, Nucl. Phys. 50, 317 (1964).

6 R. H. Bassel, R. M. Drisko, and G. R. Satchler, Oak Ridge National Laboratory Report ORNL-3240.

7 J. G. Wills, Ph.D. Thesis, University of Washington (1963).

8 I. Naqib, Ph.D. Thesis, University of Washington (1962).

9 J. S. Blair, Phys. Rev. 115, 928 (1959).

10 N. Austern and J. S. Blair, to be published.

IV. PICKUP AND STRIPPING REACTIONS

14. (d,Li^6) Reactions on Light and Intermediate Weight Nuclei

Continuing our investigation of (d,Li^6) reactions at 21 MeV incident deuteron energy, we have obtained angular distributions for the reactions $C^{12}(d,Li^6)Be^8$, $F^{19}(d,Li^6)N^{15}$, $S^{32}(d,Li^6)Si^{28}$, and $Ca^{40}(d,Li^6)Ar^{36}$ (Figures 14-1 through 14-4) in addition to the $O^{16}(d,Li^6)C^{12}$ results which were reported last year.[1] Particle detection and identification were accomplished by means of an E-ΔE counter telescope employing a gas-filled proportional dE/dx counter and a solid state E-detector, used with a pulse stretcher and an x-y oscilloscope system which has been described earlier.[2] This system has an energy threshold of about 6 MeV for lighium particles. Figure 14-5 shows the energy variation of the cross section of the $O^{16}(d,Li^6)C^{12}$ reaction at six points in the angular distribution with statistical uncertainties of about 6 per cent. Moderate energy changes were produced by moving the position of the cyclotron ion source relative to the deflector and were indicated by the corresponding changes required in the flux of the analyzing magnet of the external beam system which focuses the beam on the target. The forward peaking and lack of strong energy dependence of the observed angular distributions are suggestive of a direct reaction mechanism. The magnitude of the integrated cross sections for these reactions drops rapidly with increasing target mass as is shown in Figure 14-6. (J. B. Gerhart, P. Mizera, D. Patterson, and F. Slee).

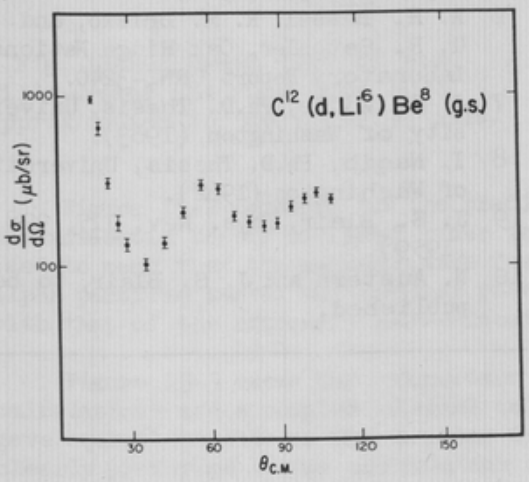

Fig. 14-1 $C^{12}(d,Li^6)Be^8$ angular distribution.

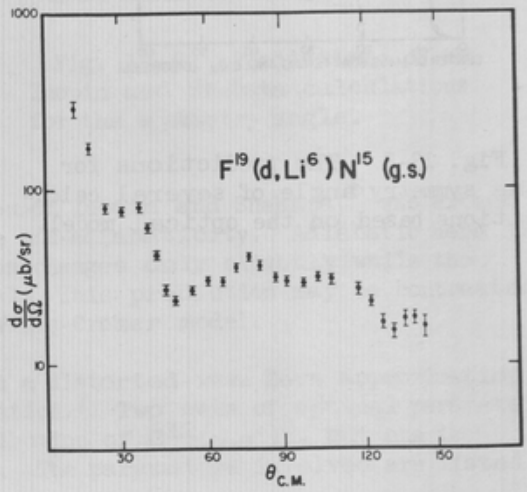

Fig. 14-2 $F^{19}(d,Li^6)N^{15}$ angular distribution.

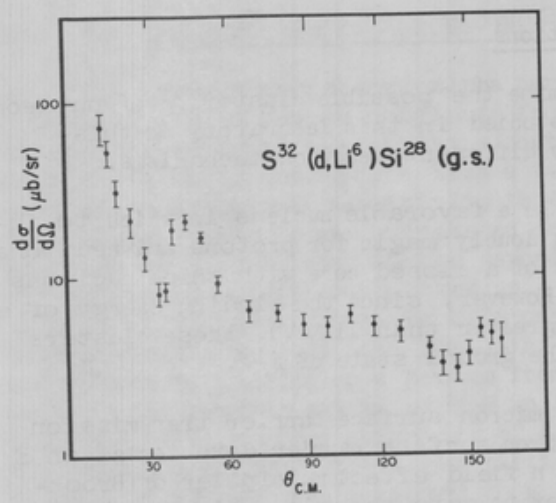

Fig. 14-3 $S^{32}(d,Li^6)Si^{28}$ angular distribution.

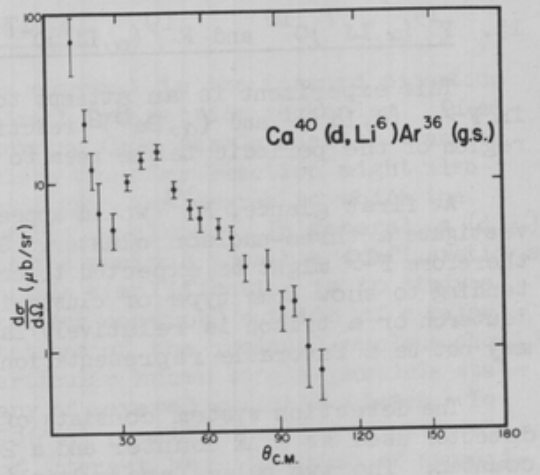

Fig. 14-4 $Ca^{40}(d,Li^6)Ar^{36}$ angular distribution.

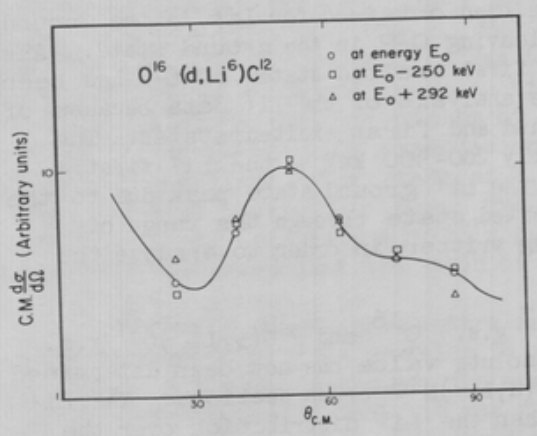

Fig. 14-5 $O^{16}(d,Li^6)C^{12}$ differential cross-section variation with incident energy.

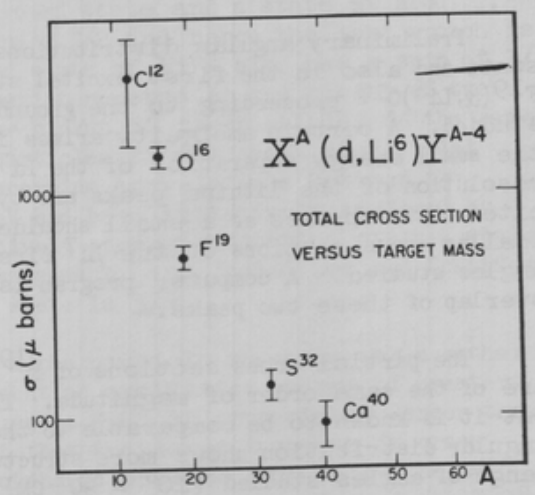

Fig. 14-6 Total cross section for the (d,Li^6) reaction versus target mass.

---

1 Cyclotron Research, University of Washington (1964), p. 21.
2 Cyclotron Research, University of Washington (1962), p. 39.

---

15. $F^{19}(\alpha,Li^7)O^{16}$ and $F^{19}(\alpha,Li^6)O^{17}$ Reactions

This experiment is an attempt to examine the possible clustering of nucleons in F^{19}. (d,Li^6)[1] and (α,Be^8)[2] reactions studied in this laboratory in this region of the periodic table seem to imply different reaction mechanisms.

At first glance, F^{19} would appear to be a favorable nucleus in which to investigate a three-nucleon cluster. O^{16} is doubly magic for protons and neutrons; therefore F^{19} might be expected to consist of a closed core with three nucleons tending to show some type of clustering. However, since the binding energy of a deuteron or a triton is relatively large (greater than 11 MeV), these clusters may not be a favorable representation of the ground state of F^{19}.

The detection system consists of a 25 micron surface barrier transmission detector used as a ΔE counter and a 200 micron surface barrier detector as an E counter. The two pulses are multiplied in a field effect multiplier of Brookhaven design and an electronic window is set to gate the pulse height analyzer with detected lithium ions. This system gives a threshold of approximately 12 MeV for the lithium ions. The targets consist of a thin layer of CaF_2 evaporated on thin polystyrene to minimize the energy spread due to target thickness effects.

Preliminary angular distributions have been obtained for Li^7 in the ground state and also in the first excited state leaving O^{16} in the ground state. Also $F^{19}(\alpha,Li^6)O^{17}$ proceeding to the ground and first excited states of O^{17} has been studied. A certain ambiguity arises in the analysis of the Li^7 data because of the small energy separation of the Li^7 ground and first excited states. The resolution of the lithium peaks are typically 200-300 keV so the Li^7 first excited state appears as a small shoulder on the Li^7 ground state peak due to the smaller cross sections of the Li^7 first excited state through the range of angles studied. A computer program is being written in order to analyze the overlap of these two peaks.

The partial cross sections of $F^{19}(\alpha,Li^7$ g.s.$)$ O^{16} and $F^{19}(\alpha,Li^6)O^{17}$ g.s. are of the same order of magnitude. The absolute value has not been determined but it is known to be comparable to the $F^{19}(d,Li^6)N^{15}$ cross section.[1] The Li^7 angular distribution shows more structure than the Li^6 distribution over the range of angles studied (10° - 90° CM).

An investigation of possible fluctuations in the angular distribution at various angles through the range of 42 to 40.4 MeV shows no strong variations in the cross sections. This excitation investigation will be continued in more detail and over larger energy ranges. (J. B. Gerhart, P. Mizera, and F. Slee)

---

1 See Section 14 of this report.
2 R. E. Brown, J. S. Blair, D. Bodansky, N. Cue, and C. D. Kavaloski; Phys. Rev. (to be published).

---

16. $Cu^{63}(d,\alpha)Ni^{61}$ and $Cu^{63}(d,He^3)Ni^{62}$ Reactions

One expects high energy alpha particles observed in the forward direction from a (d,α) reaction to originate from a direct interaction mechanism. In addition to the usual selectivity effects occurring in a single nucleon transfer direct reaction, one expects that a two-nucleon transfer reaction might also exhibit an additional selectivity that depends upon the degree to which the transferred nucleons are correlated in the target nucleus.[1] In general, a (d,α) reaction can excite many states depending on the various possible configurations of the neutron and proton picked up. A possible simplification is to study a (d,α) reaction where there is only one proton (or neutron) outside of a major closed shell. In this case low-lying excitations of the residual nucleus should correspond to picking up a proton from a particular known single-particle state, whereas the neutron may be picked up from any of several possible states. To test this idea, an investigation of the $Cu^{63}(d,\alpha)$ reaction has been initiated. For 21 MeV deuterons, the alpha particles of interest have energies of approximately 30 MeV and were detected by a solid-state detector. The cross sections observed were small (about 50 μb at 30° for the strongest transition) and only partial angular distributions were obtained. Two interesting features were observed in the energy spectrum of the emitted alpha particle. First of all, although more than a dozen levels below 2 MeV of excitation energy in the residual nucleus Ni^{61} are known,[2] only the ground state and a state at about 1.2 MeV were strongly excited. Cu^{63} has a spin of 3/2 and hence the last proton is expected to be in a $p_{3/2}$ state. The ground state of Ni^{61} also has a spin of 3/2, and the ground state transition can then be interpreted as the pickup of two $p_{3/2}$ particles. A larger cross section for pickup of two particles in the same shell model state than for pickup of two particles in different shell model states is consistent with expectations concerning correlations between the picked-up particles. The state at 1.19 MeV had been tentatively assigned by Cohen et al.,[2] as a $p_{1/2}$ state. The relatively strong excitation of this state, however, is more consistent with a $p_{3/2}$ assignment, and indeed Lee and Schiffer[3] have recently shown that the spin of this state is 3/2.

The other interesting feature in the alpha particle spectrum was a rather sudden increase in cross section to states at an excitation energy of greater than about 3.2 MeV. Although the energy gap at N=28 is appreciably larger than 3.2 MeV for neutron states, it was thought that the large increase in cross section at 3.2 MeV might correspond to picking up protons from below the Z=28 closed shell. It was decided to try to find the energy separation at the Z=28 closed shell by studying the $Cu^{63}(d,He^3)$ reaction. Preliminary measurements showed that the (d,He^3) cross sections were appreciably larger than the (d,α) cross sections, and several excited states were clearly visible. A somewhat surprising observation was that the cross section for excitation of the first excited 2+ state in Ni^{62}, usually described as a collective vibrational state, was only reduced by a factor of about 3 from that of the ground state. In a very recent publication by Hiebert et al.,[4] similar results were reported. Hiebert et al.,[4] have also measured angular distributions for higher excited states and find states at about 4 MeV of excitation whose angular distribution is consistent with pick-up of a proton from below the Z=28 closed shell. (C. J. Bishop and R. Vandenbosch).

1 N. K. Glendenning, Ann. Rev. Nuclear Sci. 13, 191 (1963).
2 B. L. Cohen, R. H. Fulmer and A. L. McCarthy, Phys. Rev. 126, 698 (1962).
3 L. Lee and J. P. Schiffer, Phys. Rev. Letters 12, 108 (1964).
4 J. C. Hiebert, E. Newman and R. H. Bassel, Phys. Letters 15, 160 (1965).

17. Nuclear Reactions to High Excitations in Heavy Nuclei

In the study of alpha-particles inelastically scattered from heavy nuclei the existence of a broad maximum was established corresponding to excitation energies in the region of 12 MeV.[1] The considerable size of the cross section, compared with the expected evaporative yield, and the forward dependence with scattering angle indicate that a direct nuclear reaction mechanism is responsible. It is of interest to compare the systematics of this reaction with those of other direct processes leading to high residual excitation energies. In particular, with the (α,t) and (d,α) reactions at the incident energies available at the cyclotron it should be possible to reach excitation energies in excess of 12 MeV before the Coulomb barrier of the outgoing particle seriously begins to limit the yield. Relatively little is known about this aspect of direct interactions and details of how the cross sections depend on angle, incident energy, target species, projectile, etc., are largely unknown. If one wants a better understanding of the nature of the mechanism or mechanisms involved one must begin by exploring these main dependences. Preliminary data are reported here on both the (α,t) and (d,α) reactions for the target nuclei previously used in the inelastic scattering study: tantalum, gold and bismuth.

In the (α,t) work the incident energy was 42 MeV. A conventional dE/dx-E detection system[2] unambiguously identified tritons among the reaction products for all energies above 7 MeV, the minimum energy required for a triton to penetrate the thin detector. Typical triton energy spectra are shown in Figure 17-1.

The same targets were used in the study of the (d,α) process initiated with 21 MeV deuterons. A particle identification arrangement similar to the above was used to record the α-particle spectra. No attempt was made to exclude He^3 ions. The Q-value is typically 13 MeV less for (d,He^3) than for (d,α) so any He^3 contribution would appear at the low-energy end of the α-spectrum. Visual displays of the dE/dx and E signals indicated that this contribution was small.

Typical Q-values for the (d,α) reactions are +12 MeV and +15 MeV for the nuclei studied yielding α-particles up to 36 MeV. Q-values for the common contaminants, C^{12} and O^{16}, are -1.3 and +3.11 MeV respectively. These, together with the recoil energy loss, generally ensured that the alpha groups associated with these contaminants lay below the region of interest.

This point is illustrated in Figure 17-2 which shows energy spectra taken at 50° for the three targets. The effect of the Coulomb barrier is strikingly demonstrated. Peaks from carbon and oxygen are prominent and the energies corresponding to ground state He^3 particles are indicated.

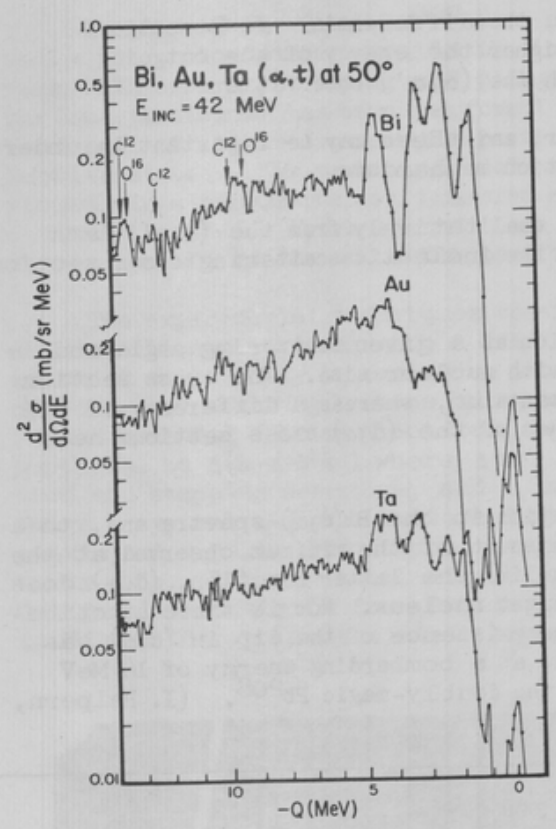

Fig. 17-1 Energy spectra of tritons emitted at 50° from bismuth, gold and tantalum bombarded with 42 MeV alpha-particles.

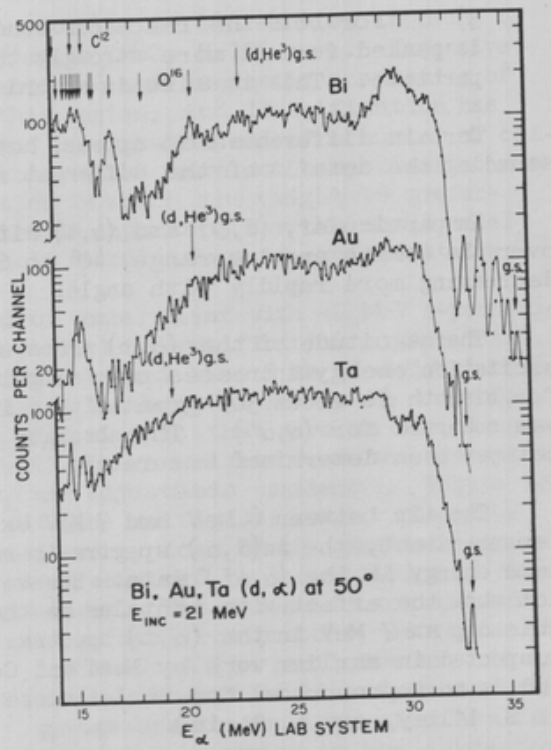

Fig. 17-2 Energy spectra in the laboratory system of alpha-particles emitted at 50° from bismuth, gold and tantalum bombarded with 21 MeV deuterons.

In common with the inelastic scattering results, both these processes exhibit several features which may be typical of this type of direct interaction:

1) Above about 7 MeV the reaction probability does not decrease with the excitation energy of the residual nucleus, until the Coulomb barrier begins to inhibit the escape of the outgoing ion. Indeed there are indications that the (d,α) cross section would continue to increase with residual excitation in the absence of the Coulomb barrier.

2) In a given reaction, the energy spectra and differential cross sections for one nucleus are qualitatively the same as those for any other nucleus in this region of the periodic table. This suggests that, as in compound nuclear processes, details of nuclear structure are unimportant at residual excitation energies greater than a few MeV.

3) For both the reactions studied, the differential cross section is peaked forward more strongly the higher the energy of the outgoing particle. This is also in accord with the (α,α') observations.

Certain differences do appear, however, and these may be important in understanding the details of the different reaction mechanisms.

In particular, (d,α) and (α,t) differ qualitatively from the (α,α') data over the common angular range, 40° to 60°; the inelastic scattering cross section decreasing more rapidly with angle.

The magnitude of the (α,t) cross section at a given scattering angle and excitation energy increases only slightly with nuclear size. The cross section for bismuth is about 30% greater than for tantalum, whereas a difference of 80% was observed for (α,α'). The absolute values of the (d,α) cross sections have not yet been determined accurately.

The dip between 6 MeV and 7 MeV excitation in the $Bi(d,\alpha)$ spectra and, to a lesser extent, the $Au(d,\alpha)$ spectra is reminiscent of the minimum observed at the same energy in the (α,α') data. However, unlike the latter reaction, (d,α) does not show the effect with tantalum as the target nucleus. Nor is there a noticeable dip at 7 MeV in the (α,t) spectra. The existence of the dip in (d,α) was suspected in earlier work by Mead and Cohen[3] at a bombarding energy of 16 MeV and is most pronounced for nuclei close to the doubly-magic Pb^{208}. (I. Halpern, J. S. Lilley, and N. Stein)

---

1 Cyclotron Research, University of Washington (1964), p. 13.
2 See Section 18 of this report.
3 J. B. Mead and B. L. Cohen, Phys. Rev. 125, 947 (1962).

---

18. (α,t) Reactions in the Lead Region

In contrast to the large amount of nuclear structure information available from neutron transfer reactions,[1] much less is known about (1) low lying energy levels corresponding to single proton excitations and (2) unstable nuclei that can be reached by the addition of a proton to a target nucleus. The usefulness of the (d,n) stripping reaction for such studies has not yet been exploited to the extent of the (d,p) reaction mainly because of the difficulties involved in measuring neutron spectra with good resolution. The increasing number of laboratories with facilities for accelerating He^3 has prompted the study of the (He^3,d) reaction, but the results are only now beginning to appear.[2] A third possible proton stripping reaction is the (α,t) process which has been least studied of the three. The availability of 42 MeV α-particles from the cyclotron provides two advantages for studying this reaction. First, outgoing tritons over a wide energy can be obtained despite the large negative Q values characteristic of the (α,t) reaction (between -10 and -19 MeV). Second, heavy nuclei with 20 MeV Coulomb barriers for He projectiles can be studied easily with 42 MeV incident energy.

Targets of Pb^{208} and Bi^{209} were chosen for the (α,t) reaction in order to study the proton states outside the doubly magic Z=82, N=126 core. Extensive work with neutron stripping and pickup reactions[3] and inelastic scattering of various particles[4] has been performed in this region, and identification has been made of the neutron single particle and hole states and of a number of collective states. The proton particle and hole states have not been observed previously in a single nucleon transfer reaction in which they might be preferentially excited. Knowledge of these states is important for the shell model theory[5] and forms the basis for particle-hole calculations of excited states.[6]

The experimental techniques consisted of bombardment with 42 MeV α-particles and detection of tritons with a (dE/dx)-E particle identification system. A 0.2 mm thick solid state transmission detector was backed by a 2 mm Li-drifted silicon detector allowing tritons with energies up to about 30 MeV to be stopped. Pulses were fed into an electronic multiplying circuit that gave an output proportional to $\Delta(k_1\Delta+E+k_2)$ where Δ and E are the pulse heights from the transmission and stopping detectors, and k_1 and k_2 are adjustable constants. Figure 18-1 shows a typical x-y oscilloscope display with the multiplier output along the y-axis and a pulse proportional to the total energy loss of the particle along the x-axis. Accurate total energy pulses were obtained by the addition of carefully balanced signals from the Δ and E detectors. The three horizontal bands in Figure 18-1 indicate a clear separation of pulses from protons, deuterons and tritons. Alpha particles are off scale. The solid line from which the groups branch consists of pulses from particles stopping in the Δ detector. The folding back of the proton band is caused by protons which penetrate both detectors. For data acquisition the multiplier output was fed to a differential pulse height analyzer which was adjusted with the aid of the x-y display to produce coincidence pulses corresponding to tritons. The width of the alpha window is indicated by the nearly vertical line passing through the triton group in Figure 18-1. Total energy spectra were obtained by gating a 512 channel analyzer with a triple coincidence formed by Δ, E and multiplier pulses from the triton window.

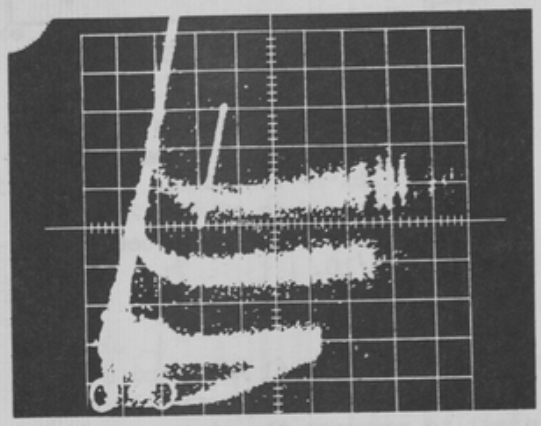

Fig. 18-1 x-y oscilloscope display of multiplier output (y-axis) versus total energy-loss of particle. Separation into protons (lowest group), deuterons and tritons is clearly indicated.

A typical energy spectrum for $Pb^{208}(\alpha,t)Bi^{209}$ obtained at a laboratory angle of 30° from a 1.5 mg/cm^2 target is shown in Figure 18-2. Four strong peaks appear with widths equal to the 170 keV experimental resolution. They correspond to the Bi^{209} ground state and excited states at 0.90, 1.61, and 2.83 MeV. Weaker excitations are evident at 2.6, 3.1, and 4.2 MeV. Angular distributions at 2.5° degree intervals between 27.5° and 75° for five of the states are shown in Figure 18-3.

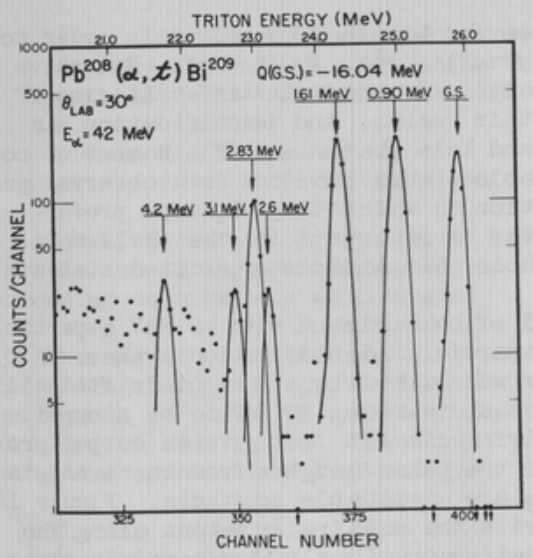

Fig. 18-2 Energy spectrum of tritons emitted in the $Pb^{208}(\alpha,t)Bi^{209}$ reaction at 30°.

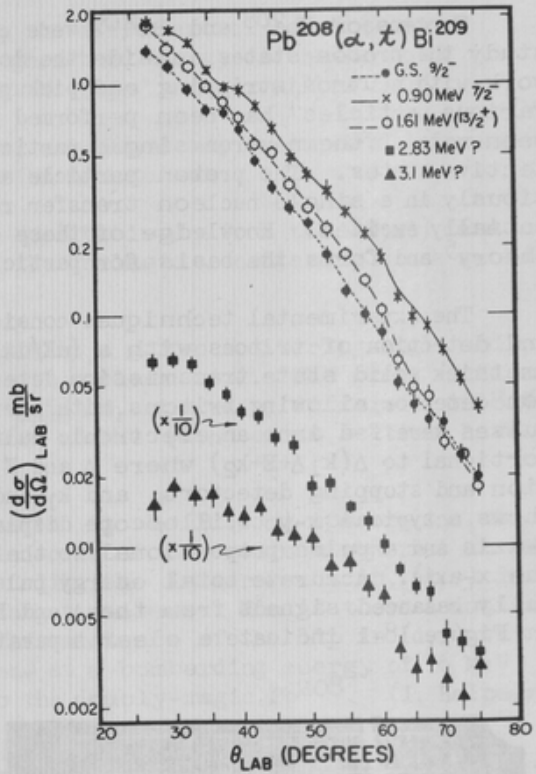

Fig. 18-3 Angular distributions of five triton groups from the $Pb^{208}(\alpha,t)Bi^{209}$ reaction. For clarity the cross sections of the 2.83 and 3.1 MeV transitions have been multiplied by 1/10.

The spins and parities of the ground state and 0.90 MeV state in Bi^{209} have been reported as $9/2^-$ and $7/2^-$, respectively.[7] Based on the shell model, they have been identified[5] with the $1h_{9/2}$ and $2f_{7/2}$ proton single-particle states which are expected in the major shell 83-126. The next shell model state is predicted[5] in Bi^{209} as a $1i_{13/2}$ proton state at about 1.3 MeV. Since the only known level between 0.90 and 2.48 MeV is the one at 1.61 MeV, and a $13/2^+$ assignment has been found consistent with (n,n') data,[8] it may actually be the $1\ i_{13/2}$ single proton state. It is of interest to compare the strong excitation of the g.s., 0.90, and 1.61 MeV states in the (α,t) reaction with (1) the much weaker excitation (by a factor of 10) of a state near 2.6 MeV which is in the vicinity of states thought to be collective due to their strong excitation by inelastic scattering and (2) the very weak excitation of the 0.90 and 1.61 MeV states by inelastic scattering reactions.[4] These results taken together, strongly support a "single particle" interpretation for the first three states in Bi^{209}, assuming that the (α,t) reaction preferentially excites single proton states.

The present results also imply another strong single particle state at 2.83 MeV. Although a number of levels have been observed in that region in (n,n') experiments,[7] a single particle state has not been reported there previously. This location disagrees with existing shell model calculations[5] which predict

that the remaining states in the shell, $2f_{5/2}$, $3p_{3/2}$ and $3p_{1/2}$, are unbound and lie above 3.5 MeV. (This disagreement may not be surprising since the $1i_{13/2}$ state was calculated at 1.3 MeV.) A fifth single particle excitation may be the state at 3.1 MeV which is weaker than the four discussed above, but still prominent, especially at large angles.

The angular distributions of the $Pb^{208}(\alpha,t)$ cross sections for 42 MeV alphas decrease rapidly with angle and lack pronounced structure. If the level assignments for the g.s. and first two excited states are used to identify the ℓ-values of the stripped protons, then there appears to be no marked variation of the angular distributions as a function of ℓ in the angular range 27.5°-75°. The only discernible trend is that the ℓ=6 angular distribution has a steeper slope than the ℓ=3, with the ℓ=5 slope intermediate between the two. The lack of sensitivity to ℓ makes it difficult to identify the 2.83 and 3.1 MeV transitions by comparison with known transitions.

Of the remaining shell model states, the 2.83 and 3.1 MeV levels are more likely to be the $2f_{5/2}$ or $3p_{3/2}$ states rather than the $3p_{1/2}$ state which would be expected to lie highest. However, neither of the angular distributions is very similar to the $2f_{7/2}$ transition, so that a j-dependence may be indicated if, as seems likely, one of the levels is the $2f_{5/2}$ state. Distorted wave calculations will be attempted to determine if the angular distributions can be predicted. In addition, further data may be obtained over a wider angular range.

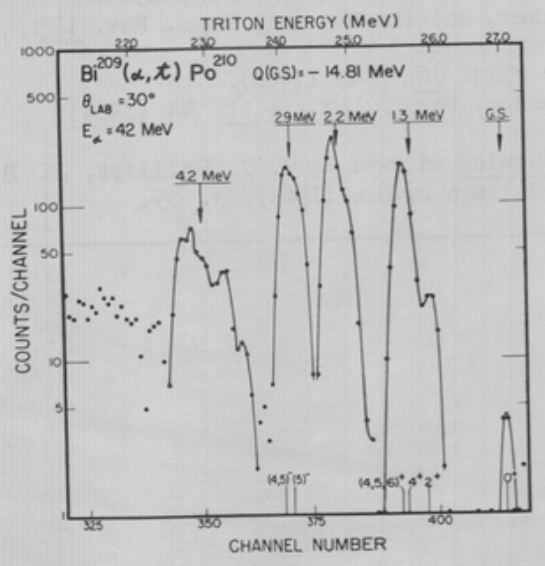

Fig. 18-4 Energy spectrum of tritons emitted in the $Bi^{209}(\alpha,t)Po^{210}$ reaction at 30°. Vertical lines along the horizontal axis indicate the previously known states in Po^{210}.

The $Bi^{209}(\alpha,t)Po^{210}$ reaction provides one of the few ways for studying the energy levels of Po^{210}. A typical triton spectrum, obtained at 30° (Figure 18-4) shows the ground state, very weakly excited, and four strong peaks broader than the experimental resolution. When compared with the (α,t) results leading to Bi^{209}, several striking similarities are evident. First, the intervals between the strong peaks in Po^{210} are very similar to the spacing between the g.s., 0.90, 1.61 and 2.83 MeV states in Bi^{209}. Second, within the experimental errors, the four peaks in Po^{210} have about the same cross sections and angular distributions as do the corresponding states in Bi^{209}. Thus the Bi^{209} ground state corresponds closely to the lowest energy Po^{210} group at 1.3 MeV, the 0.90 MeV Bi^{209} state to the 2.2 MeV group in Po^{210}, etc. Cross sections for the 2.6, 2.83 and 3.1 MeV states in Bi^{209} were summed for comparison with the broad group in Po^{210} at 4.2 MeV.

These results suggest a simple interpretation for the low lying states in Po^{210} excited by (α,t). Groups of levels are formed by stripping a proton into the different shell model states where each couples to the $1h_{9/2}$ proton in the Bi^{209} ground state. The coupling appears to be weak enough that the groups remain relatively narrow and distinguishable. Thus the 1.3 MeV group can be expected to contain the even spin positive parity states due to a $(1h_{9/2})^2$ configuration where the 0^+ member has been depressed by the pairing energy to form the ground state. The group centered at 2.2 MeV probably consists of the positive parity states formed by the $(1h_{9/2}, 2f_{7/2})$ configuration and the 2.9 MeV group consists of the negative parity states in the $(1h_{9/2}, 1i_{13/2})$ configuration. Information about the structure of the group near 4.2 MeV will depend upon the identity of the 2.83 and 3.1 MeV states in Bi^{209}. Only five excited states in Po^{210} are listed in the nuclear data cards. These are shown as vertical lines at the bottom of Figure 18-4. The energies, spins and parities are in good agreement with the grouping and configurations suggested above. (J. S. Lilley and N. Stein).

---

1 B. L. Cohen, R. H. Fulmer, A. L. McCarthy, and P. Mukherjee, Rev. Mod. Phys. 35, 332 (1963).
2 A. G. Blair, Proceedings of the Symposium, Nuclear Spectroscopy with Direct Reactions, II., Argonne, Illinois, 1964, p. 115.
3 P. Mukherjee and B. L. Cohen, Phys. Rev. 127, 1284 (1962).
4 J. Alster, Proceedings of Congrès International de Physique Nucléaire II; Editions du Centre National de la Recherche Scientifique, Paris, 1964. H. Crannell, R. Helm, H. Kendall, J. Oeser, and M. Yearian, Phys. Rev. 123, 923 (1961).
5 J. Blomqvist and S. Wahlborn, Arkiv For Fysik 16, 545 (1960).
6 V. Gillet, A. M. Green, and E. A. Sanderson, Phys. Letters 11, 44 (1964).
7 Nuclear Data Sheets.
8 L. Cranberg, Progress in Fast Neutron Physics edited by G. C. Phillips, J. B. Marion and J. R. Risser, University of Chicago Press (1963), p. 89.

V. COMPOUND NUCLEAR REACTIONS

19. Low-Energy Proton Emission in Compound-Nuclear Reactions

The studies of low-energy (sub-Coulomb-barrier) proton emission discussed in previous progress reports[1,2] have been completed.

One phase of this study was concerned with measurements of proton spectra in (p,p') reactions with Al^{27}, natural Ti, Co^{59}, natural Ni, and Cu^{63} targets, at 10.5 MeV bombarding energy. Because emphasis was placed on the measurement of the spectrum shapes at energies well below the Coulomb barrier, a special detector system, with low threshold, was developed.[1] This system, which utilized both dE/dx-E and time-of-flight information for particle identification, was potentially useful to energies as low as 1 MeV, but the useful lower limit in the present experiments was higher (about 2 MeV), due to target contamination, background and small yield.

The proton emission spectra were found to be consistent with a statistical mechanism, as indicated by (a) the isotropy of the observed angular distributions, (b) the consistency of observed and predicted absolute yields, subject to some uncertainties introduced by the presence of direct reaction contributions and also to some uncertainties in the correction of excitation energies for pairing and shell effects, and (c) the good agreement of predicted and observed spectral shapes.

Because "second proton" emission was essentially absent at the bombarding energy of 10.5 MeV, it was possible to compare quite simple statistical theory predictions and experimental spectra over a wide spectral range. Typical results of such comparisons are shown in Figures 19-1 and 19-2, where experimental evaporation spectra are shown in comparison with arbitrarily normalized theoretical spectrum shapes. The theoretical curves were found from statistical theory predictions based upon a modified Fermi-gas model of nuclear level density[3] and upon inverse reaction cross sections found from conventional continuum theory and optical model calculations. The theoretical curves plotted in Figures 19-1 and 19-2 were calculated from values of a, the nuclear level density parameter, found to be reasonable from other experiments;[3] the effects of variations of a on the characteristic emission temperature of the spectra are evident.

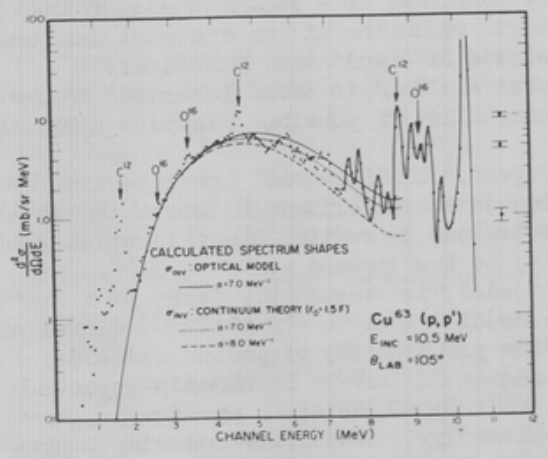

Fig. 19-1 Comparisons of calculated and experimental Cu^{63}(p,p') spectrum shapes. Normalization of the theoretical curves is such that their low-energy portions coincide.

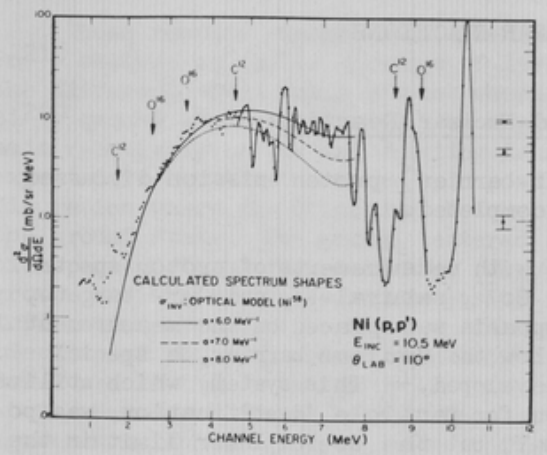

Fig. 19-2 Experimental Ni(p,p') spectrum, in comparison with theoretical shapes, obtained as indicated in the figure, for Ni^{58}.

Both temperature effects and effects due to details of the inverse reaction cross-section model are shown in Figure 19-1. The different theoretical $Cu^{63}(p,p')$ spectra shown for the same value of the level density parameter ($a = 7.0\ MeV^{-1}$) reflect differences in penetrability for optical model and continuum theory predictions of inverse reaction cross sections. It is to be noted that the predicted spectra for the two models are not very different.

Below the peaks of the evaporation spectra the energy dependence of the inverse reaction cross section dominates the spectral shape. Because agreement between observed and predicted shapes in the low energy region is good, and because agreement in the higher-energy region (where level density effects are more important) is good for reasonable choices of the level density parameter, it was concluded that conventional proton reaction cross sections successfully describe barrier penetration in the emission of protons from nuclei with moderate excitations, down to proton energies as low as 2 MeV.

The relative probabilities of proton and gamma-ray emission from levels near the particle emission threshold in Cu^{63} were examined in a second phase of the present studies. The probabilities of particle emission at low energies has been a subject of particular interest in the analysis of excitation functions. Grover[4] and Delorme[5] have carried out analyses similar to those described below to explain excitation functions near the thresholds of possible reaction channels.

As described in detail in a previous report,[2] differential cross sections for the $Cu^{63}(p,2p)Ni^{62}$ reaction were measured in an experiment in which the observation of the energies of the coincident protons permitted identification of the events as proceeding, almost exclusively, to the ground state of Ni^{62}. On the assumption that the (p,2p) reaction proceeded via sequential decay of a Zn^{64} compound nucleus, comparisons of the $Cu^{63}(p,2p)Ni^{62}$ and $Cu^{63}(p,p')Cu^{63*}$ differential cross sections were used to determine the probability of proton emission from excited states in the proton trapping region of Cu^{63}. Previously-reported results[2] have been somewhat revised through additional data; in particular, a correction was introduced for an observed anisotropy between the coincident proton angle pairs (90° - 90°) and (135° - 135°). A revised value of 0.12 ± 0.05 was obtained for the average probability for emission of 2.08-MeV protons from levels in Cu^{63} (at 8.19 MeV excitation).

Statistical model calculations showed that this rather small probability can be understood in terms of the competition of gamma-ray de-excitation. The ratio of proton and gamma ray emission widths, $(\Gamma_p/\Gamma_\gamma)_J$, is a strong function of

the spin, J, of the emitting levels. A prediction of the expected proton emission probability can be carried out through the following sequence of steps: (1) $(\Gamma_p/\Gamma_\gamma)_{1/2}$ is found from statistical theory calculations of absolute radiation widths (which are comparable with semi-empirical values) and absolute proton widths, at $J = \frac{1}{2}$; (2) $(\Gamma_p/\Gamma_\gamma)_J$ is found from (1) and from calculated values of $(\Gamma_p)_J/(\Gamma_p)_{1/2}$, with the assumption that Γ_γ is independent of J; (3) the spin population of emitting Cu^{63} levels is calculated for 10.5-MeV incident protons; (4) the proton emission probability, averaged over the spin population, is found by combining (2) and (3). The result of such a calculation, for an excitation energy of 8.19 MeV, gives a theoretical average proton emission probability of 0.14 ± 0.05, in good agreement with the experimental result.

The problem can also be couched in terms of the extraction of an "experimental" value of $(\Gamma_p/\Gamma_\gamma)_{1/2}$. Here all steps of the previous calculation are carried out, except that $(\Gamma_p/\Gamma_\gamma)_{1/2}$ is considered unknown, to be adjusted to give agreement with the experimental emission probability. The "experimental" result was $(\Gamma_p/\Gamma_\gamma)_{1/2} = 9^{+10}_{-6}$. The theoretical value of this quantity was 13 ± 7. Again the results agree, but fractional uncertainties are much greater. This is natural, because when the ratio of widths is large, the observed proton yield is insensitive to the value of the ratio. Although $(\Gamma_p/\Gamma_\gamma)_{1/2}$ is large, the overall value of Γ_p/Γ_γ is small, because the proton emission width decreases rapidly with increasing spin, and the mean spin of the Cu^{63} levels is considerably greater than 1/2 (about 3).

The comparison of experiment and theory discussed above included an accounting for fluctuations in emission probability arising from a Porter-Thomas distribution of proton widths about an average value. Significantly less satisfactory agreement between experiment and theory resulted from neglect of the width distribution.

The work reported here illustrates a rather direct experimental method for determining proton emission probabilities. Although here the protons were only in competition with gamma rays, the method could also be used when other particles compete. The agreement found between the calculated and experimental results provides further evidence that the statistical model, with conventional parameters, is capable of accounting for particle and gamma ray emission probabilities. (D. Bodansky and E. R. Parkinson)

---

1 Cyclotron Research, University of Washington (1963), p. 40.
2 Cyclotron Research, University of Washington (1964), p. 28.
3 D. W. Lang, Nucl. Phys. 434 (1961).
4 J. R. Grover, Phys. Rev. 123, 267 (1961); 127, 2142 (1962).
5 J. Delorme, Nucl. Phys. 47, 544 (1963).

---

20. The $O^{16}(\alpha,Be^8)C^{12}$ Reaction

The experimental study of the energy dependence of the $O^{16}(\alpha,Be^8)C^{12}$ reaction was continued, and the measurements were extended to include angular

distributions at nine bombarding energies between 35.5 and 41.9 MeV. The results, for transitions to both the ground state and the first excited state of C^{12}, confirmed the earlier indications of marked fluctuations in cross section as the incident energy was varied.

A paper describing these results and their possible interpretation has been submitted to The Physical Review. In brief summary, it was concluded that the observations could be qualitatively understood in terms of Ericson fluctuations, within the framework of the statistical theory of compound nuclear reactions, although a substantial non-statistical contribution to the yield could not be excluded. (J. S. Blair, D. Bodansky, R. E. Brown, N. Cue, and C. D. Kavaloski)

21. Investigation of the $Si^{28}(He^4, O^{16})O^{16}$ Reaction

The experiment described previously[1] has been continued. A 100 $\mu gm/cm^2$ evaporated silicon target supported on a thin nickel backing is mounted perpendicular to the 42 MeV helium ion beam. The oxygen fragments emitted at 90° in the center of mass system appear in the laboratory system at about 60°. A thin (40 micron) transmission-mounted detector is placed on one side of the beam. A large-area surface barrier detector with a thin depletion region is placed on the other side of the beam. The second detector subtends a large enough area to intercept the partner of an oxygen particle detected by the first counter. The 40 micron detector is thick compared to the range of the O^{16} fragments but thin enough that alphas and other light particles cannot deposit more than 7 MeV in the detector. Pulse shape discrimination in the second detector helps to discriminate against lighter particles of longer range. The pulse heights from coincident events are recorded in a two-dimensional analyzer.

The first experiment was designed to measure the relative cross sections for formation of O^{16} nuclei in various ground or excited-state combinations. This experiment was performed by varying the forward-folding angle of the two detectors, which were kept at equal angles with respect to the beam. Kinematic effects result in oxygen nuclei formed in their ground states at 90° in the center of mass to appear in the laboratory at 66° with respect to the beam, whereas if one of the oxygen nuclei is formed in a 6 MeV excited state, the fragments appear at 63° in the laboratory. Figure 21-1 shows the differential cross section at 90° in the C.M. as a function of the laboratory angle. In Figure 21-1 all coincidences with energies consistent with equal mass partners have been included. The energy resolution, however, is very poor as even the 100 $\mu gm/cm^2$ target used is fairly thick for the low energy oxygen ions, which can lose as much as 2.5 MeV of their initial kinetic energy of 10 to 16 MeV in the target. The total acceptance angle of the angle-defining detector was 2.7°. The large cross section for giving a total excitation of approximately 12 MeV to the fragments must be attributed to processes in which the excitation energy is shared between the fragments rather than all concentrated in one fragment, as an O^{16} nucleus excited to 12 MeV is particle unstable with respect to emission of alpha particles. It is impossible with the present energy and angular resolution to identify exactly which states of O^{16} are being excited. A 0+ and a 3- state are known at 6.06 and 6.13 MeV, respectively, and a 2+ and a 1- state are known at 6.93 and 7.13 MeV, respectively. The increased yield of the excited states

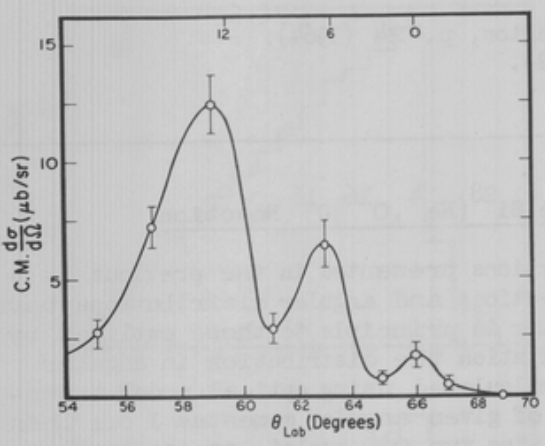

Fig. 21-1 The center of mass differential cross section at 90° as a function of laboratory angle. The upper scale indicates the total residual excitation energy corresponding to several laboratory angles.

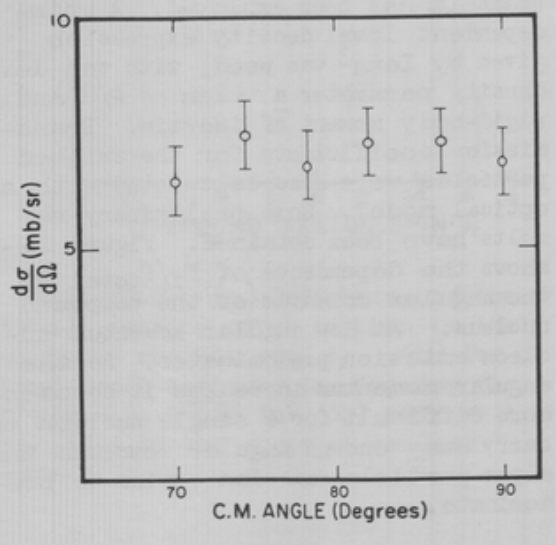

Fig. 21-2 Center-of-mass differential cross section for the reaction $Si^{28}(\alpha,O^{16})O^{16*}$ where the excitation of one of the fragments is approximately 6 MeV.

compared to the ground state can be at least partly attributed to the number and statistical weights of these excited states.

After learning of the sizeable variations in yield with bombarding energy for the $O^{16}(\alpha,Be^{8})C^{12}$ reaction,[2] a search for an energy dependence in the present experiment was performed. The yield of the $Si^{28}(\alpha,O^{16})O^{16*}$ (6 MeV) reaction at four bombarding energies between 40.8 MeV and 42.4 MeV indicated a gradual decrease of almost a factor of two, although the statistical accuracy was not sufficient to exclude the possibility of no dependence on bombarding energy. Care was taken, however, to hold the bombarding energy constant when measuring angular distributions.

The angular distributions of heavy products from similar nuclear reactions in lighter nuclei have been reported.[3,4] The structure in the angular distributions has indicated that at least for certain bombarding energies, compound states of a single angular momentum are predominant. An experiment to look for such an effect was performed for the case where one O^{16} nucleus was formed in the ground state and the other O^{16} nucleus was excited to about 6 MeV. (The angular and energy definition was not sufficient to exclude any contribution from the states at about 7 MeV of excitation.) The resulting angular distribution is shown in Figure 21-2. The angular region investigated, although small, was large enough to exclude the possibility that compound states with a single large spin value predominate.[5] (C. J. Bishop, C. T. Ratcliffe, R. Vandenbosch, and K. Wolf)

---

1 Cyclotron Research, University of Washington, p. 41 (1964).
2 See Section 20 of this report.

3 Cyclotron Research, University of Washington, p. 24 (1964).
4 N. O. Lassen, Phys. Letters 1, 161 (1962).
5 See Section 22 of this report.

---

22. Statistical Model Calculations for the $Si^{28}(He^4, O^{16})O^{16}$ Reaction

As an aid in understanding the observations presented in the previous section,[1] theoretical calculations of cross sections and angular distributions have been initiated. The calculations are similar in principle to those outlined by Hauser and Feshbach.[2] In the present calculation the distribution in angular momentum of the compound nucleus is first calculated using optical model transmission coefficients. Each compound state of given angular momentum J can then decay to either the state of interest involving two O^{16} nuclei, or can decay using other exit channels which may involve emission of neutrons, protons, or alpha particles. Since the residual nuclei may be left at high excitation energies, a statistical description of the final states reached in the neutron, proton, and alpha particle exit channels has been employed. A spin-dependent level density expression given by Lang[3] was used, with the level density parameter a taken as A/8 and a rigid-body moment of inertia. Transmission coefficients for the emitted particles were also calculated with an optical model. Some preliminary results have been obtained. Figure 22-1 shows the dependence of Γ_i/Γ_{total} on the angular momentum of the compound nucleus. At low angular momentum nucleon emission predominates. As the angular momentum increases it becomes more difficult for a single nucleon to carry away enough angular momentum and alpha particle emission begins to predominate.

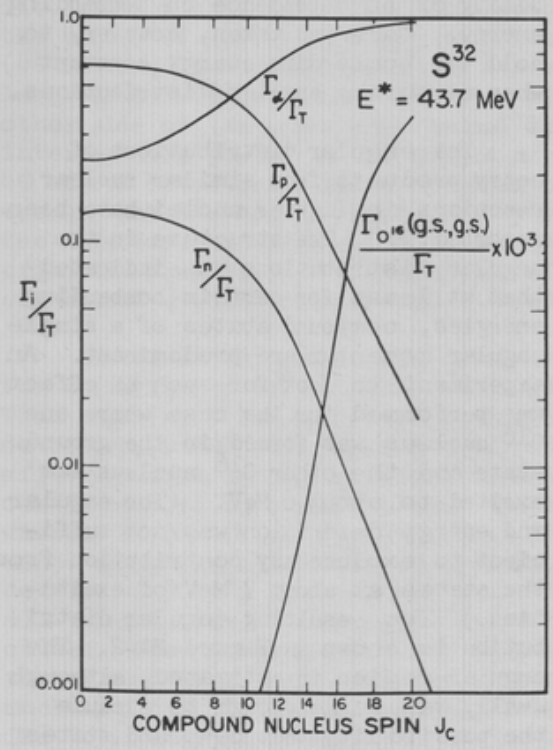

Fig. 22-1 Calculated dependence of Γ_i/Γ_T on the compound nuclear spin J_c. Γ_n, Γ_p, and Γ_α are the total widths for emission of these particles, whereas Γ_{O-16} is the width for the O^{16}(g.s.), O^{16}(g.s.) pair only. The compound nucleus is S^{32} at an excitation energy of 43.7 MeV.

The ratio of the width for forming O^{16} nuclei in their ground state relative to the total width never becomes very large because of the many competing channels, but is largest for the very highest angular momentum states of the compound nucleus. Figure 22-2 shows the contribution of different J_c states of the compound nucleus to the cross section for forming an O^{16}(g.s.),O^{16}(E*=6.0 MeV, I=0+)

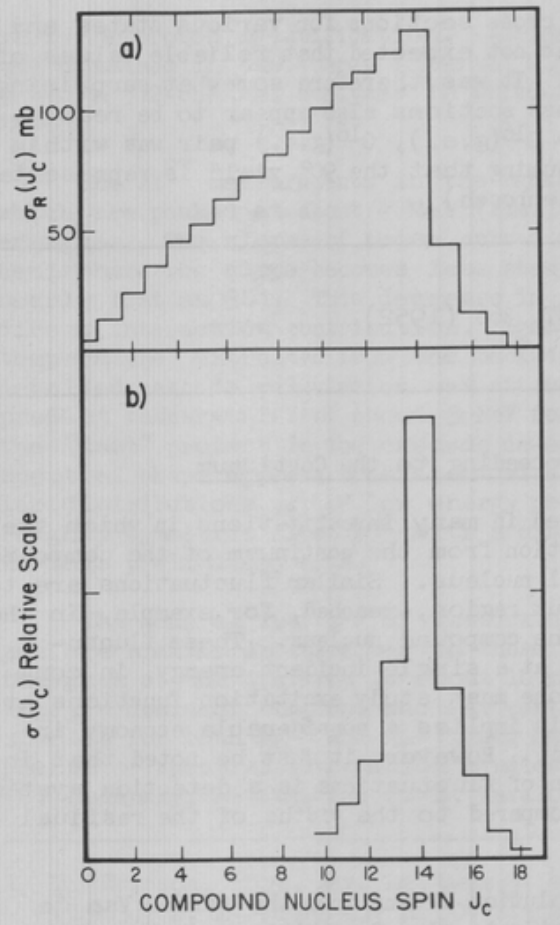

Fig. 22-2 (a) Dependence of the total reaction cross section on the compound nuclear spin J_c. (b) Partial cross sections for forming the O^{16}(g.s.), O^{16}(6 MeV, 0+) pair as a function of the compound nuclear spin J_c.

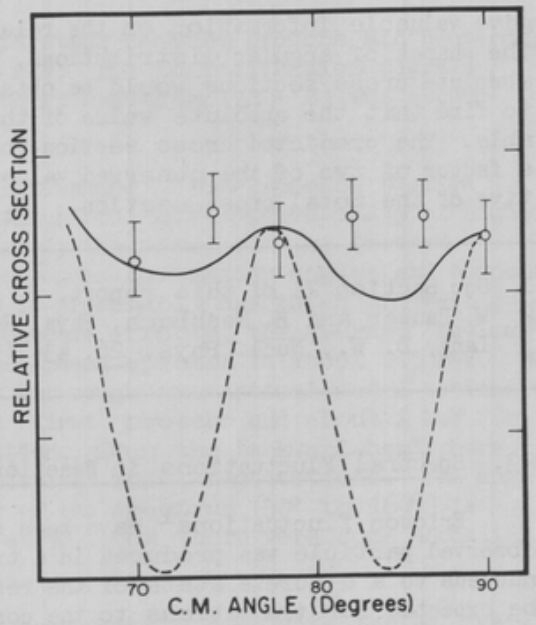

Fig. 22-3 The full curve is the calculated curve for the O^{16}(g.s.), O^{16}(6 MeV, 0+) pair, normalized to the experimental data at 90°. The dashed curve shows the angular distribution expected if only $J_c = 14$ were to contribute.

pair. The dependence of the total reaction cross section on the spin of the compound nucleus is also shown for comparison. The predominance of states with high angular momentum is demonstrated, but the calculation indicates that compound states with several J_c values rather than states with a single J_c value are expected to contribute significantly. This result is consistent with the measured angular distribution. The calculated angular distribution for forming an O^{16}(g.s.), O^{16*}(6.0 MeV, I = 0+) pair is indicated by the full curve in Figure 22-3. If instead the above reaction proceeded only through J = 14 compound states the angular distribution would have the shape indicated by the dashed line. A calculation of the angular distribution assuming the excited state has spin and parity 3- rather than 0+ is in progress, but is not expected to be qualitatively different if compound states with several J values contribute.

Although it was hoped that calculations of the type described here would

give valuable information on the relative cross sections for various states and the shapes of angular distributions, it was not expected that reliable values of absolute cross sections would be obtained. It was therefore somewhat surprising to find that the absolute value of the cross sections also appear to be reasonable. The predicted cross section for the O^{16}(g.s.), O^{16}(g.s.) pair was within a factor of two of the observed value, assuming that the 90° yield is representative of the total cross section. (R. Vandenbosch)

---

1 See Section 21 of this report.
2 W. Hauser and H. Feshbach, Phys. Rev. 87, 366 (1952).
3 Lang, D. W., Nucl. Phys. 26, 434 (1961).

---

23. Spectral Fluctuations in Reactions Proceeding to the Continuum

Ericson fluctuations[1] have been studied in many investigations in which the observed particle was produced in a transition from the continuum of the compound nucleus to a discrete state of the residual nucleus. Similar fluctuations are to be expected for transitions to the continuum region, reached, for example, in the first step of a cascade de-excitation of the compound nucleus. These fluctuations would be exhibited in spectra taken at a single incident energy, in contrast to the conventional situation where one must study excitation functions at many closely spaced incident energies. This implies a considerable economy in data collection time for the continuum study. However, it must be noted that in this case a requirement for the observation of fluctuations is a detection system with an energy resolution which is small compared to the widths of the residual nuclear levels.

The imminent availability of high resolution beams from the tandem Van de Graaff accelerator has prompted us to investigate the feasibility of observing this type of fluctuation. With the incident energies which will first be available (about 16 MeV for singly charged particles, (d,p) reactions appear to be the most promising choice, particularly because of their positive Q-values. Relatively high residual excitation energies are needed, so that the level widths are not too narrow to observe. For example, with a 16 MeV incident beam one anticipates widths of about 30 keV using an Al^{27} target and observing 4 MeV protons. Another possibly desirable target is Mg^{24} which, because of its zero spin ground state, should lead to fluctuations of larger magnitude.

A preliminary run has been carried out in which the (d,p) reaction in Mg^{24} and Al^{27} was studied, using the 21-MeV deuteron beam from the cyclotron. The resolution was relatively poor in this run and there was no prospect of observing fluctuations. The main objective was to survey the general characteristics of the (d,p) reaction to the continuum. Previous work[2] has indicated that most of the forward-hemisphere proton yield comes from the direct breakup of deuterons near the nuclear surface. Particular attention was paid in the present run to the backward hemisphere, where compound nuclear contributions may be expected to be more prominent.

A ΔE-E system, which incorporated a conventional multiplier circuit, was

used for proton identification. A clean separation between protons and deuterons was attained in the energy interval 2.5-9.0 MeV. The identification signals gated a 512-channel analyzer in which the energy spectrum ($\Delta E + E$) was accumulated.

The Al^{27} measurements in the backward hemisphere yielded proton spectra which are peaked at about 4 MeV (c.m.) and which fall off exponentially at higher energies. The slopes of these curves are nearly the same. In the forward hemisphere the slope becomes less steep as one goes to smaller angles and becomes nearly flat at 30°. This decrease in slope is presumably due to an increasing direct interaction contribution. Ignoring cascade effects, the average "nuclear temperature" extracted from the backward-hemisphere spectra is about 2.5 MeV. No detailed cascade calculation was attempted, but rough statistical model estimates predict temperatures of about 3 MeV for the "first" protons and about 2 MeV for the "last" protons in the cascade de-excitation. Thus the backward-hemisphere spectral shape appears consistent with statistical model expectations. The angular distributions of the low energy portion of the spectrum (30° to 160°) is roughly symmetric about 90° with a minimum at 90°, but there were some anomalies in this preliminary data.

The general features of less extensive measurements made with the Mg^{24} target are similar in character to those obtained with Al^{27}. The proton yield at the peak of the spectrum is about 10 mb/sr-MeV for both targets. These results imply a dominant compound nuclear contribution to the backward-hemisphere (d,p) spectra for both Mg^{24} and Al^{27}, and have encouraged us to proceed with detailed plans for spectral fluctuation studies with the tandem Van de Graaff accelerator. (D. Bodansky, N. Cue, and C. D. Kavaloski)

---

1 T. Ericson, Phys. Rev. Letters 5, 430 (1960); Ann. Phys. (N.Y.) 23, 230 (1963); D. M. Brink and R. O. Stephen, Phys. Letters 5, 77 (1963).

2 See, e.g., E. W. Hamburger, B. L. Cohen and R. E. Price, Phys. Rev. 121, 1143 (1961); and F. Udo, H. R. E. Tjin A. Djie and L. A. Ch. Korts, Nucl. Phys. 63, 657 (1965).

---

24. Investigation of Rotational States in the Rare-Earth Region

The investigation of rotational states in the rare earth region by observation of conversion electrons with the Toroidal β-ray spectrometer has been continued.[1] Source charging caused by secondary electron emission resulting from the cyclotron beam and the consequent apparent shifts of the spectrometer calibration in time have delayed progress on this experiment until recently. (J. B. Gerhart and J. S. Heagney)

---

1 Cyclotron Research, University of Washington (1964), 34.

VI. PHOTONS FROM NUCLEAR REACTIONS

25. Angular Distributions of Rotational Quanta Produced in Bombardments by 42 MeV Alpha Particles

In a continuation of the work begun last year[1] the distributions of rotational quanta from rare earth distorted nuclei have been measured in alpha particle bombardments. More specifically the quantities measured were the yields and angular distributions of the rotational lines in the ground state bands of the residual nuclei in $(\alpha,3n)$ reactions produced with 42 MeV alpha particles. It should be remarked at this point, that as has already been found,[2-6] the ground state band is the only band strongly excited in the residual nucleus. In fact the cross section for the lower lines of this band approaches the full $(\alpha,3n)$ cross section. That is to say, most de-excitations in the $(\alpha,3n)$ reaction pass through the ground state band of the residual nucleus. As a result, the observed photon spectra appear as a series of sharp lines on an otherwise smooth continuous spectrum - which arises from the unresolved photons which precede the emission of the rotational quanta.

A study of the relative yields of the rotational lines tells one what fraction of the angular momentum originally deposited in the reaction is left after the evaporation of 3 neutrons and a number of photons. A study of the angular distribution of the rotational lines measures the degree of orientation of the radiating nuclei and hence the amount of disorientation of the angular momentum direction brought about by the evaporation of the particles and photons. In short, the rotational cascade in question, by giving information about the angular momenta at the tail-end of the evaporation cascade, provides important insights about the course of that cascade.

A typical pulse height spectrum as measured with a NaI crystal in an anticoincidence annulus is shown in Figure 25-1. This spectrum is converted on the basis of the pulse-height vs. photon energy matrix to a photon spectrum as mentioned elsewhere (See Section 26) and since one wants to know actual state populations and not just photon intensities, each line intensity is corrected for internal conversion.

Figure 25-2 shows a typical angular distribution for several individual rotational lines determined after the subtraction of the smooth continuous photon background. It should be said that the spectrum of the background that one chooses to subtract is to a certain degree arbitrary and is perhaps one of the greatest sources of uncertainty in the determination of the yields and angular distributions. The observed angular distributions were, as expected, symmetric around the plane perpendicular to the beam. The quadrupole angular distributions are expected to have the form

$$W(\theta) = A + BP_2(\cos\theta) + CP_4(\cos\theta).$$

Values of B/A and C/A will be extracted from the data by least squares analysis. Values of the anisotropy, $\sigma(0°)/(90°)$, have already been extracted from the data and are given in Table 25-1 for a number of lines in the decay of Dy^{156} formed

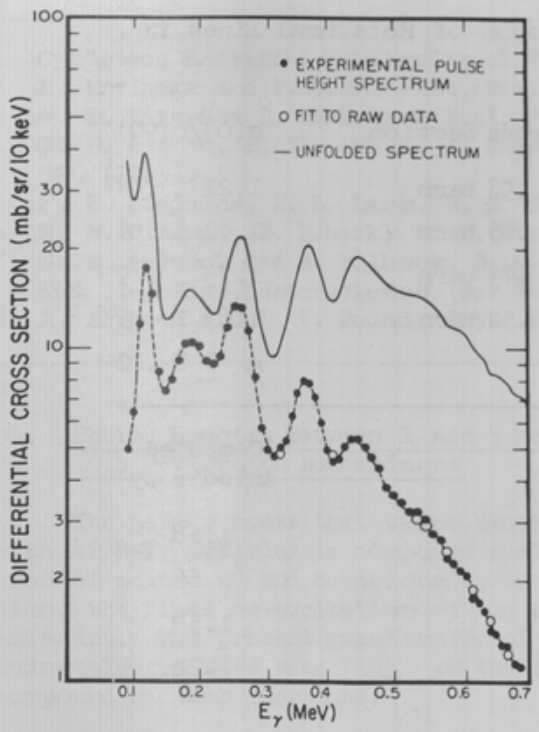

Fig. 25-1 Pulse height and deduced gamma ray spectrum from 42 MeV alpha particle bombardment of Gd^{155} (giving Dy^{156}).

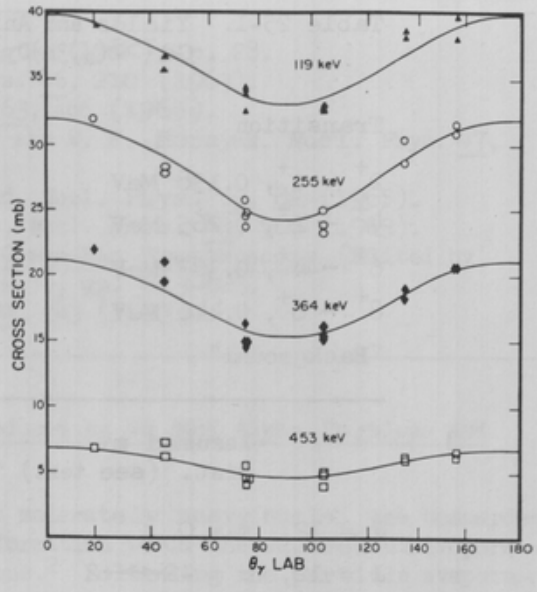

Fig. 25-2 Preliminary angular distribution for rotational levels in Dy^{156}.

by the $(\alpha, 3n)$ reaction on enriched Gd^{155}. The spins involved in the transitions are also indicated as well as the cross sections for the particular transitions. The absolute errors of the cross sections are fairly large because of the uncertainties mentioned above, but they show that the yields increase as one goes further down the band. This is of course to be expected since all higher transitions are necessarily followed by lower ones, and besides one can feed the band at any J from levels not in the band.

The analysis and interpretation of these data are just beginning, but the following qualitative features seem to emerge.

The angular momentum which is deposited in the nucleus by the bombardment is not severely reoriented as a result of the evaporations that take place. If one ignores the target spin, the angular momentum just before evaporation can be described by m = 0 taking the quantization direction along the beam axis. It can be shown that the successively emitted quanta in a rotational cascade emerge with unchanged angular distributions.[7] It is also easy to show that for reasonably large initial values of the angular momentum J at the start of the cascade and m = 0, the $0°/90°$ ratio is roughly 1.7. Due to the evaporation, one expects some disorientation which gives rise to a distribution in starting m values still centered about m = 0. The entries below the line in Table 25 1 give the expected values for B/A, C/A and the $0°/90°$ ratio for distributions corresponding to J = 12

Table 25-1. Yields and Anisotropies of Rotational Lines in $Gd^{155}(\alpha,3n)Dy^{156}$

Transition	Cross Section	$\sigma(0)/\sigma(90)$
$2^+ \rightarrow 0^+$, 0.138 MeV	.98 barn	$1.21 \pm .08$
$4^+ \rightarrow 2^+$, 0.265 MeV	.85 barn	$1.41 \pm .04$
$6^+ \rightarrow 4^+$, 0.363 MeV	.73 barn	$1.73 \pm .19$
$8^+ \rightarrow 6^+$, 0.446 MeV	.50 barn	$1.63 \pm .75$
"Background"		$\approx 1 \pm .02$

Assumed m Dist. (see text)	Computed Anisotropy
J = 12, m = 0	1.68
J = 12, m = -2↔+2	1.66
J = 12, m = -5↔+5	1.59
J = 12, m = -12↔+12	1.22

(arbitrarily chosen) and distributions of m as follows: (1) just m = 0, (2) m in a triangular distribution about m = 0 extending between m = ±2, (3) a triangular distribution between m = ±5 and finally (4) a triangular distribution between m = ±12. It is $\langle(m/J)^2\rangle^{1/2}$ that measures the rms angle of the angular momentum vector with respect to the beam and the given calculated ratios would therefore be roughly the same for different choices of the initial J and m distributions scaled according to J.

It is seen that for the higher J transitions the angular momentum vectors at the start of the rotational cascade must still be fairly close to the m = 0 plane. Preliminary estimates show that this is in accord with theoretical expectations. The lower J transitions are more isotropic than the higher J ones. This can be due in part to the feeding of these levels from outside the band, from levels in initially less oriented nuclei, but the observed diminution in anisotropy exceeds what one can legitimately expect from this effect when one takes into account the measured amount of "side-feeding" into the band. The most reasonable explanation of the anomalously low anisotropy in the 2→0 transition seems to be that the nuclei in the 2+ state are disoriented by the interaction of the nuclear quadrupole moments and the crystalline electric fields in the target. Estimated precession periods in typical fields are of the order of 1 $nanosecond^8$ and the lifetime of the 2+ state is of the same order. The lifetime of higher states are at least an order of magnitude less and the distributions of their radiation is therefore not expected to suffer significantly from this type of disorientation. (I. Halpern, B. J. Shepherd, and C. F. Williamson)

1 Cyclotron Research, University of Washington (1964), p. 28.
2 H. Morinaga and P. C. Gugelot, Nucl. Phys. 46, 210 (1963).
3 N. L. Lark and H. Morinaga, Nucl. Phys. 63, 466 (1965).
4 G. B. Hansen, B. Elbeck, K. A. Hagemann, and W. F. Hornyak, Nucl. Phys. 47, 529 (1963).
5 F. S. Stephens, N. L. Lark, R. M. Diamond, Nucl. Phys. 63, 82 (1965).
6 R. M. Diamond, B. Elbeck, F. S. Stephens, Nucl. Phys. 43, 560 (1963).
7 S. R. deGroot and A. Tolhoek, Beta- and Gamma-Ray Spectroscopy (Edited by Kai Siegbahn), Interscience (New York, 1955), pp. 613-623.
8 A. Abragam and R. V. Pound, Phys. Rev. 92, 943 (1953).

26. Photon Spectra Between 1 and 5 MeV Produced by 42 MeV Alpha Particle and 10.5 MeV Proton Bombardment

The main process that takes place when moderately heavy nuclei are bombarded with 42 MeV particles is compound nuclear formation with the subsequent evaporation of neutrons[1] and occasionally of protons.[2] Following the particle evaporation, the final de-excitation of the struck nucleus takes place through photon emission. The present examination of the yields and spectra of photons was undertaken to shed some light on the final stages of the de-excitation process in compound nuclear reactions.

The data were obtained using a NaI crystal with the anticoincidence annulus detector system described in last year's progress report. A number of targets extending in atomic weight from Co to Pb were studied with 42 MeV α particles and 10.5 MeV protons. Rare earth targets received especial attention because they were being examined anyhow for the rotational lines excited in the same bombardments (see Section 25). The detector was about a yard from the target and all targets were studied at 135° to the beam. Some were studied at other angles as well.

To convert the observed pulse height distributions to photon spectra, the backgrounds including that from oxygen contamination were subtracted and use was made of the measured response matrix of the detector system. The absolute efficiency of the system was checked by comparing the yield of the 4.43 MeV gamma ray in $C^{12}(\alpha,\alpha')C^{12*}$ to the first excited state with the known total inelastic scattering cross section.[3] It was found that at higher energies all spectra fell off with increasing energy smoothly and approximately exponentially. The resolution of the detector was not good enough to show much structure in the spectrum above 1 MeV although strong lines were discernible below 1 MeV. For purposes of a preliminary survey it was therefore decided to concentrate on the photon spectra above 1 MeV. Because of the smoothness of the observed distribution and the simplicity of the response functions at all photon energies (they were essentially a δ function at the photon energy accompanied by a uniform tail of comparable area extending to zero energy), it was possible to develop an approximate unfolding procedure that is sufficiently accurate for a preliminary orientation.

Figure 26-1 shows a typical observed pulse height distribution (for the alpha particle bombardment of holmium), a few examples of response functions and

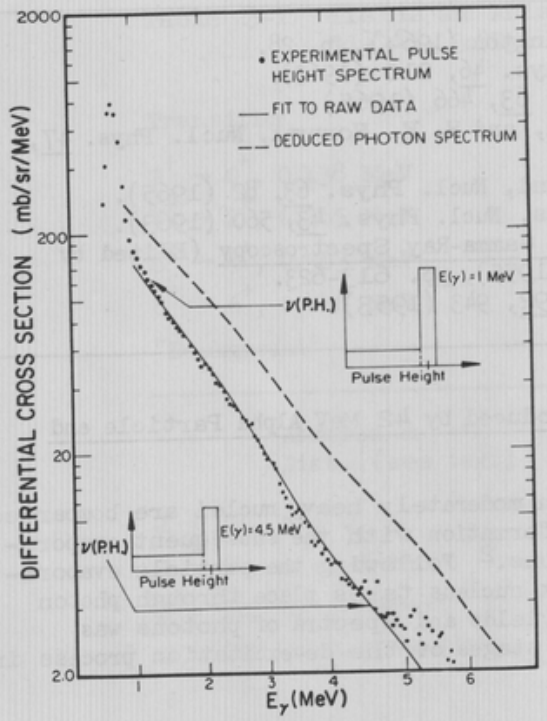

Fig. 26-1 Pulse height spectrum and deduced photo spectrum resulting from 42 MeV alpha particle bombardment of Ho^{165}. The insets show the idealized shapes of the pulse height response function at two photon energies.

the deduced photon spectrum above 1 MeV. It is seen that this spectrum decays very nearly as a pure exponential ($\sim C \exp -E/E_0$) and can therefore be characterized by two constants, C and E_0. All of the other measured spectra showed the same character.

Figures 26-2 and 26-3 show some of deduced spectra observed at 135° for the alpha particle and proton bombardments. Preliminary indications are that the spectral shapes and total yields do not change strongly with the angle of observation. Table 26-I gives the mean photon energies above 1 MeV (namely $\bar{E}_{>1} = 1 + E_0$) for the spectra studied so far. Each entry is based on at least two runs and the standard error assigned to each $\bar{E}$ is about 10%.

In addition to the values for mean photon energies, Table 26-I lists the values for the mean number of quanta with E > 1 MeV emitted per nuclear reaction. To determine this number the total photon producing cross section was divided by the known total reaction cross section. It was assumed that the photon emission is isotropic and computed values[4,5] (listed as σ_α and σ_p) were used for the reaction cross sections. The final columns in the table give the total energies carried off by quanta above 1 MeV per reaction.

Although the data in the table are preliminary and the analysis is just beginning, it is worth remarking about a few of the most striking features.

1. Some of the entries for the total energy carried off by quanta over 1 MeV exceed the neutron binding energies of the nuclei involved. Since the total photon energy (including quanta below 1 MeV) carried off per reaction is even larger, it is clear that a measurable number of photons are being emitted at excitation energies the binding energy of the last emitted particle. This observation is in accord with earlier ones, especially those made in bombardments with heavy ions.[6]

2. Although the mean energies $\bar{E}_{>1}$ in the proton bombardments are roughly equal to those observed in slow neutron capture,[7] the shapes of the spectra are very different. The exponential fall off in the latter

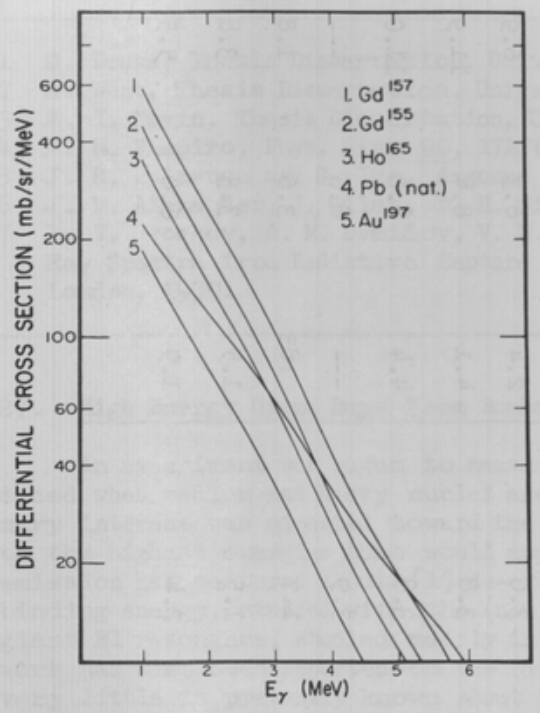

Fig. 26-2 Typical preliminary deduced photon spectra from alpha particle bombardment.

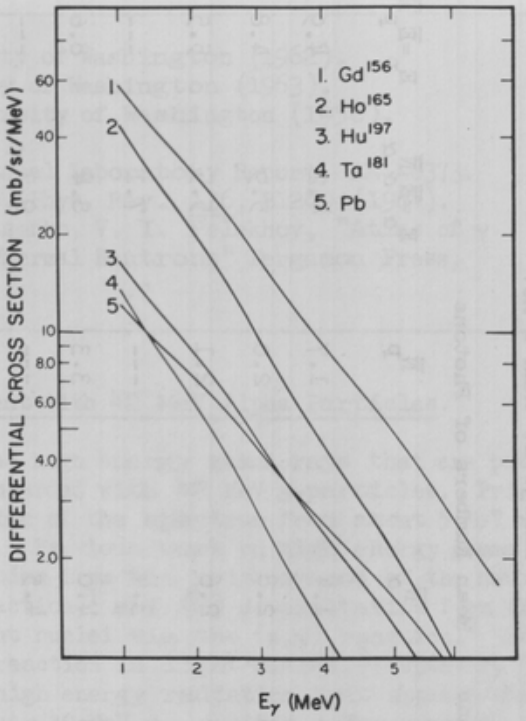

Fig. 26-3 Typical preliminary deduced photon spectra from proton bombardment.

does not begin until about 2 MeV. Thus, there seem to be many more soft quanta in the present bombardments than in the thermal neutron capture studies.

3. A comparison of the total energies carried away by photons in the proton and the alpha particle bombardments suggests that the excitation energy of the nucleus which remains after the last particle evaporation is not broadly distributed and that its average value varies significantly in the different bombardments. One implication of this conclusion that should be checked is that this total photon energy should be very sensitive to changes in bombarding energy of a few MeV.

4. The photon spectra seem to be sensitive to shell effects.

5. There are some entries in the table (for example, the small tantalum photon yields) which are admittedly suspect and although no sufficiently large possible sources of error have been uncovered so far that might account for the anomalies, it is clear that further studies and checks are necessary. (I. Halpern, B. J. Shepherd, and C. F. Williamson)

Table 26-I. Energies Removed by Photons More Energetic than 1 MeV

Target	Mean Photon Energies		Reaction Cross Sections		Mean Numbers of Photons			
	$\bar{E}_\alpha$	$\bar{E}_p$	σ_α	σ_p	$\bar{N}_\alpha$	$\bar{N}_p$	$E_\alpha=\bar{E}_\alpha\bar{N}_\alpha$	$E_p=\bar{E}_p\bar{N}_p$
Co	2.2	2.9	1.66	.706	1.4	1.7	4.2	4.9
Zu	2.1	2.4	1.70	.693	2.8	2.0	5.9	4.8
Rh	2.1	2.6	1.802	.574	2.6	2.1	5.5	5.5
Gd^{155}	2.1	---	1.865	---	3.4	---	7.1	---
Gd^{156}	2.1	2.6	1.865	.353	4.0	3.3	8.4	8.6
Gd^{157}	2.1	---	1.865	---	4.5	---	9.5	---
Dy^{161}	2.1	---	1.865	---	3.2	---	6.7	---
Ho^{165}	2.1	2.3	1.865	.317	3.0	2.4	6.3	6.9
Er^{167}	2.2	2.9	1.865	.310	3.8	4.1	8.4	11.9
Yb^{171}	2.1	2.5	1.864	.29	3.8	4.4	8.0	11.0
Hf^{174}	2.2	---	1.860	---	3.9	---	8.6	---
Ta	2.1	2.2	1.855	.251	1.7	.83	3.6	1.8
Au	2.2	2.5	1.825	.208	1.5	1.5	3.3	3.8
Pb	2.5	2.9	1.812	.156	2.4	1.9	6.0	5.5

1 D. Drake, Thesis Dissertation, University of Washington (1962).
2 R. West, Thesis Dissertation, University of Washington (1963).
3 A. I. Yavin, Thesis Dissertation, University of Washington (1958).
4 M. M. Shapiro, Phys. Rev. 90, 171 (1953).
5 J. R. Huizenga and G. Igo, Argonne National Laboratory Report, ANL-6373.
6 J. M. Alexander, J. Gilat, D. H. Sisson, Phys. Rev. 136, B1289 (1964).
7 L. V. Groshev, A. M. Demidov, V. N. Lutsenko, V. I. Pelekhov, "Atlas of γ Ray Spectra from Radiative Capture of Thermal Neutrons" Pergamon Press, London, 1959.

27. High Energy Gamma Rays from Bombardment with 42 MeV Alpha Particles.

An experiment was begun to measure the high energy gamma rays that are produced when medium and heavy nuclei are bombarded with 42 MeV α-particles. Primary interest was directed toward the region of the spectrum from about 5 MeV up to the highest energies that would appear. Previous work on high energy gamma emission has centered about (1) de-excitation from the neighborhood of the neutron binding energy, studied with the (n,γ) reaction,[1] and (2) de-excitation from the giant El resonance, studied mainly in light nuclei via the (p,γ) reaction.[2] Some work has also been reported on the (α,γ) reaction in light nuclei.[3] However, very little is presently known about the high energy radiation that appears when a heavy nucleus at an excitation energy near 40 MeV de-excites. For example, do the highest energy quanta correspond to giant resonance transitions or are there higher energies in the spectrum? Another question of current interest is the mechanism for radiative capture. Information about the high energy spectra is relevant to this since direct[4] or semi-direct[5] mechanisms would be expected to proceed via high energy radiation.

Preliminary data were obtained using a 3" x 6" NaI(Tl) crystal surrounded by an anti-coincidence annulus shield.[6] Targets of cobalt, silver and gold were bombarded with 42 MeV alpha particles and measurements were made at 105° to the incident beam. Pulses associated with neutrons from the target, and non-target background, were reduced by time-of-flight requirements. A preliminary gamma ray spectrum above 4 MeV for silver is shown in Figure 27-1. Of principal interest is the observation of a significant number of gamma rays up to about 16 MeV and the sharp change in slope which occurs at about 10 MeV. These energies are approximate because of uncertainties regarding saturation effects in the detection system. For this reason a high energy limit on the emitted gamma rays cannot be given based on these data. The spectra from cobalt and gold are qualitatively similar to silver. The major difference is that gamma rays may extend to somewhat higher energies as the nuclear mass decreases. Very rough estimates of the total cross sections near 15 MeV are of order 0.3 mb/MeV for Co and Ag and 0.1 mb/MeV for Au. It is clear that before any interpretations can be made and conclusions drawn, much more data will be required. However, a possible indication of these results is that in the de-excitation of highly excited nuclei, gamma rays appear in significant quantities only up to giant resonance energies. It would be interesting to learn between which excitation energies these giant resonance transitions occur.

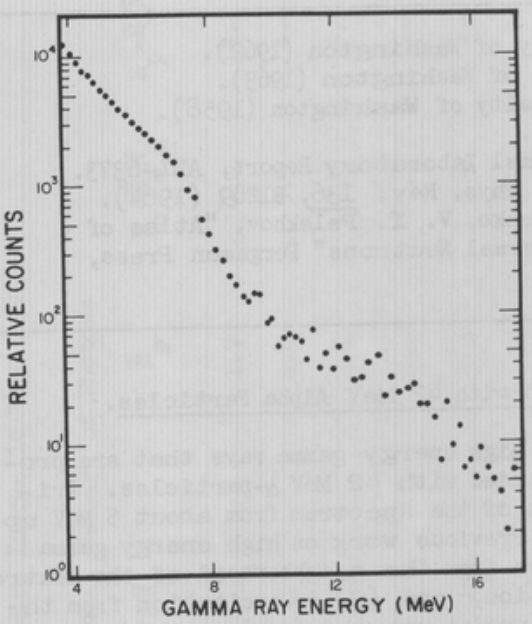

Fig. 27-1 Pulse height spectrum of gamma rays produced at 105° by bombarding a 25 mg/cm^2 natural silver target with 42 MeV alpha particles. The energy scale is only approximate.

The preliminary results seem interesting enough that further experiments, with possibly improved techniques, are being planned. (I. Halpern, D. Johnson, N. Stein, and C. F. Williamson)

1 G. A. Bartholomew, Ann. Rev. Nucl. Sci., 11, 259 (1961).
2 N. W. Tanner, G. C. Thomas, and E. D. Earle, Nucl. Phys. 52, 29 (1964).
3 C. Van der Leun and G. Wieders, Nucl. Phys. 52, 104 (1964). L. Meyer-Schutzmeister, Z. Vager, and R. E. Segal, Bull. Am. Phys. Soc. 10, 463 (1965).
4 A. M. Lane, Nucl. Phys. 11, 625 (1959).
A. M. Lane and J. E. Lynn, Nucl. Phys. 11, 646 (1959).
5 G. E. Brown, Nucl. Phys. 57, 339 (1964).
6 B. J. Shepherd and C. F. Williamson, Cyclotron Research, University of Washington (1964), p. 52.

28. Radiative Capture

Together with the measurements of high energy quanta produced by 42 MeV alpha bombardment,[1] a comparison study has been initiated to measure cross sections for radiative capture as a function of incident energy. By measuring the residual activity characteristic of the target plus incident particle, knowledge is obtained of the probability for capturing the particle and subsequent de-excitation solely by gamma ray emission. This is closely related to the high energy radiation experiment since some of the energetic gamma rays may be involved in the mechanism for radiative capture.

Advances in gamma ray detection techniques should allow much more extensive measurements of residual radio-activity by gamma counting than previously possible. With the advent of the tandem Van de Graaff accelerator, which will provide several projectiles with variable energy, systematic studies of radiative capture throughout the periodic table may become feasible.

At present, a target box has been assembled for irradiation of targets in the cyclotron, and a study of possible targets has been made with easily measured half lives a prime consideration. (I. Halpern, D. Johnson, and N. Stein)

1 See Section 27 of this report.

VII. NUCLEAR FISSION

29. The Emission of Charged Particles During Nuclear Fission

The experimental studies of charged particle emission during nuclear fission have been continued during the past year. Since it is difficult to make quantitative predictions about the process using any of the models for the process now in vogue, the program of varying one possible characteristic parameter for the process (keeping all others constant) and noting the resultant change in the probability of charged particle emission has been followed. The results of such studies are summarized below:

A. Variation of Probability of Charged Particle Emission During Nuclear Fission with the Excitation Energy of the Compound Nucleus.

Figure 29-1 shows the variation in probability of charged particle emission during nuclear fission with the excitation energy of the compound nucleus. No attempt has been made to correct for any (Z,A) dependence of the probability of charged particle emission because the fissioning species were all roughly the same and the (Z,A) dependence isn't too strong for this group of fissioning species (see B). One sees that the probability of charged particle emission falls sharply with an initial increase in E^*_{CN} and gradually levels off at higher E^*_{CN}. Simple considerations of the fission-neutron evaporation competition show that the charged particle emission taking place at high E^*_{CN} is not merely a consequence of last chance (low E^*_{CN}, high probability for particle emission) fission. This picture of the process seems roughly consistent with data obtained by a Russian group and a group at Princeton.[1]

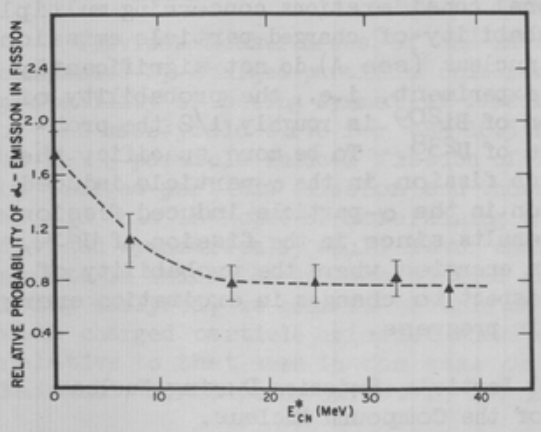

Fig. 29-1 The relative probability of charged particle emission during nuclear fission as a function of the excitation energy of the compound nucleus. No attempt is made to correct for any (Z,A) dependence of the emission probability or the broadened angular correlation between the charged particle and fission fragment directions of motion (see D).

However, it should be mentioned that other workers have observed a different trend.[2] This is shown in Figure 29-2. Here one sees an initial sharp decrease in charged particle emission probability followed by a sharp upswing in probability at higher E^*_{CN}. We feel, however, these data do not represent a true picture of what is going on in charged particle emission during nuclear fission. Our feelings are based on the fact that in the studies utilizing protons, no attempt was made to correct for (direct interaction, fission) reactions such as $(p,\alpha f)$ and in the studies of α-particle induced fission, the cross

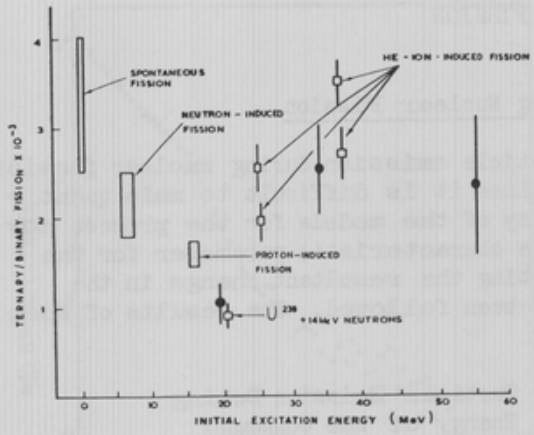

Fig. 29-2 Probability of ternary fission relative to binary fission as a function of the excitation energy of the initial compound nucleus. A variety of nuclei from californium to thorium is represented, but with one exception no attempt is made to identify them.

section for the $(\alpha,\alpha'f)$ reaction seems to have been underestimated. This assertion that the $(\alpha,\alpha'f)$ cross section was underestimated is based on our measurements of this cross section which are consistent with the known values of the (α,α') cross sections and estimates of Γ_f/Γ_t. If one makes corrections for the $(p,\alpha f)$ reaction based on known (p,α) cross sections and known values for F_f/F_t, one obtains a behavior of the emission probability which is in agreement with the data shown in Figure 29-1.

B. Variation of Probability of Charged Particle Emission During Nuclear Fission with the (Z,A) of the Compound Nucleus.

The work can be summarized by saying that the relative probability of charged particle emission during nuclear fission for U^{238}, Th^{232}, and Bi^{209} (all excited with 42 MeV alpha particles) is $1\pm0.1/1\pm0.1/0.5\pm0.2$. Additional considerations concerning multiple chance fission and the variation of the probability of charged particle emission with the excitation energy of the compound nucleus (see A) do not significantly change the qualitative conclusions of this experiment, i.e., the probability of charged particle emission during the fission of Bi^{209} is roughly 1/2 the probability of such an occurrence in the fission of U^{238}. To be more specific, the fact that one is dealing with multiple chance fission in the α-particle induced fission of U^{238} and with first chance fission in the α-particle induced fission of Bi^{209} doesn't qualitatively affect the results since in the fission of U^{238}, over 90% of the nuclei fission at excitation energies where the probability of charge particle emission is constant with respect to changes in excitation energy. Further experiments with other targets are in progress.

C. Variation of Probability of Charged Particle Emission During Nuclear Fission with the Angular Momentum of the Compound Nucleus.

The compound nucleus, Pu^{239*}, was formed at an excitation energy, 30.3 MeV, in two different ways (U^{235} + 35.5 MeV α-particles and Np^{237} + 21.0 MeV deuterons). The mean square angular momentum in the α-particle bombardment was $110\hbar^2$ and in the deuteron bombardment $55\hbar^2$, i.e., a factor of 2 difference in the value of $\overline{\ell^2}$. (It should be noted that these values of $\overline{\ell^2}$ were calculated using optical model potentials[3,4] where the quantities in question were the total reaction cross sections rather than the cross sections for formation of a compound nucleus. However considerations involving the ℓ values associated with the direct interactions, the amount of direct reactions, and the relative amounts of these reactions in the α-particle and deuteron bombardments leads one to conclude that the

aforementioned values of the angular momentum are probably correct within ±10%.) The results show that within 10% (the statistical uncertainty in the data) the probability of charged particle emission is the same in both bombardments.

D. Behavior of the Fission Fragment - Charged Particle Angular Correlation with Excitation Energy of the Compound Nucleus.

One of the most prominent features of the process of charged particle emission during nuclear fission is the sharp right angle correlation which exists between the fission fragment and charged particle direction of motion. Feeling that this correlation and the energetics concerned with it are very sensitive indicators of the dynamics of the process under study, we, as well as other workers, have attempted to explore the correlation and its energetics under a variety of circumstances. Our angular correlation data for Th^{232} + 10.5 MeV protons and Th^{232} + 42 MeV α's do not show any significant difference between them. The correlation is broader than that seen in the spontaneous fission of Cf^{252} and appears to be narrower than that of Thomas[1] observed in the 17.5 MeV proton bombardment of U^{238} although the uncertainties in the data do not permit any definite conclusion at this time. The data showing angular correlation of various energy charged particles and the variation of charged particle and fission fragment energies as a function of the included angle between the directions of motion has been obtained and is being analyzed.

E. Variation in Probability of Charged Particle Emission During Nuclear Fission as a Function of the Relative Asymmetry of the Mass-Yield Curve.

Previous measurements of the mass-yield curve for those fission events accompanied by charged particle emission have been for situations in which the probability of seeing symmetric fission was very low. We have made measurements of the mass-yield curve for the 10.5 MeV proton induced fission of Th^{232} and the 42 MeV α-particle induced fission of Th^{232} for those fission events accompanied by charged particle emission and those events not accompanied by such emission. We did this in hopes of determining whether or not events in which the nucleus divided symmetrically would favor charged particle emission relative to those events in which the nucleus divided asymmetrically. Although the data are still being analyzed, we seem to be able to say that the mass yield curve associated with charged particle emission shows no large enhancement of symmetric fission relative to that seen in the mass yield curve for "normal" fission. (A. W. Fairhall, I. Halpern, and W. D. Loveland)

---

1 T. D. Thomas (private communication), 1965.

2 See for example, A. W. Fairhall, "Proton Induced Fission," P.L.A. Progress Report, 1964, Rutherford High Energy Laboratory, NIRL/R/81, p. 60.

3 J. R. Huizenga and G. J. Igo, "Theoretical Reaction Cross Sections for Alpha Particles with an Optical Model," ANL-6373, May, 1961.

4 R. Bassel, R. Drisko and G. Satchler, "The Distorted-Wave Theory of Direct Nuclear Reactions," ORNL-3240, 1962.

---

30. Kinetic Energy Release in Symmetric Fission

In proton-induced fission of bismuth using 50 and 30 MeV protons the kinetic energy of the fission fragments shows a distinct shift with 50 MeV proton-induced fission having 2.5 MeV/fragment more kinetic energy than for 30 MeV proton-induced fission.[1] Allowance for the kinetic energy carried off by post fission neutrons increases this difference even further. This is the first instance where the kinetic energy release in fission apparently varies with the energy of the fission-inducing projectile.

In an attempt to verify this result, a Bi target was bombarded with 42 MeV and 35.5 MeV α-particles. Fission fragments were detected in a surface-barrier detector at an angle of 135° to the beam. Energy calibration of the detector was made using a Cf spontaneous fission source and corrections for kinetic energy defects as a function of mass were made using the data of Schmitt.[2]

Because of the lower fission cross section at the lower bombarding energy the counting statistics are rather poor. Using a computer, the mean fragment kinetic energies as measured in the laboratory frame of reference are 62.9±0.3 and 64.4±0.8 MeV at 42 MeV and 35.5 MeV, respectively. Transformation to the center-of-mass frame gives for the mean fragment kinetic energies 70.3±0.3 and 71.3±0.8 MeV, respectively. Allowance for one extra neutron evaporated from the fragments at the higher bombarding energy increases the kinetic energy release per fragment at 42 MeV to 70.6±0.3 MeV. Thus within the experimental error there appears to be no dependence of the kinetic energy release on the bombarding energy. However, the magnitude of the expected effect is of the same order as the experimental uncertainties. On the other hand, the results for proton-induced fission imply an increase in fragment kinetic energy with increasing bombarding energy whereas for the α-induced fission the kinetic energy is, if anything, less at the higher bombarding energy. Thus the α-induced fission of Bi appears to be in agreement with previous observations and the proton-induced fission of Bi is anomalous. (A. W. Fairhall and W. D. Loveland)

---

1 A. W. Fairhall, P.L.A. Progress Report, Rutherford High Energy Laboratory, Chilton, England, p. 60 (1964).

2 H. W. Schmitt, W. E. Kiker and C. W. Williams, Phys. Rev. 137, B837 (1965).

---

31. Isomeric Yields of Nb^{95g}/Nb^{95m} from Proton-Induced Fission of Uranium

The relative independent yields of high and low spin isomeric states produced in fission are useful in determining the initial angular momentum of the primary fission fragments.[1,2] A recent set of values for the non-shielded Nb^{95g}/Nb^{95m} pair obtained from proton-induced fission of uranium are in disagreement with other isomeric ratios at similar bombarding energies.[3] A calculation based on the statistical model, with an initial fragment spin distribution which qualitatively fits other experimentally determined isomeric yields,[1,2] predicts a ratio of Nb^{95g}/Nb^{95m} with a higher population of the ground state in disagreement with the experimental value of 0.06 obtained[3] from 15 MeV proton-induced fission of uranium.

In the present investigation, uranium oxide was bombarded with 10 microamps of 10 MeV protons for two hours. Niobium was initially precipitated from the dissolved target solution as the insoluble oxide using 10 mg. of Nb carrier and 10 mg. each of Zr, Mo, and Te as hold-back carriers. Purification with successive $BaZrF_6$ and sulfide precipitations insured removal of Zr, Te and other contaminants. The gravimetric yield of Nb carrier in the chemical separation was about 30-50 per cent. The Nb oxide was mounted on a thin Mylar film for counting.

Nb^{95g} was determined by measuring the 768 keV gamma ray with an integral line assembly 3" x 3" NaI(Tl) crystal. The isomeric state, Nb^{95m}, decays primarily by interval conversion to the ground state. An integral line assembly 1" x 1/32" NaI(Tl) crystal was used to determine the x-ray from the K-conversion of the isomeric transition. Background corrections were made in both cases by subtracting a linear slope under the peaks.

Since the calculated independent yield of Nb^{95} from uranium fission is several orders of magnitude lower than the cumulative yield of its β^- unstable parent, Zr^{95}, it is necessary to determine the fractional chain yield of Nb^{95} from Zr^{95} between the time of bombardment and the separation of Nb from Zr, to obtain the true value for the independent yield of Nb. The growth rate of Nb^{95} from Zr^{95} decay was obtained by milking the Nb from the original uranium solution several hours after the initial Nb separation. This Nb sample was purified and counted in the same manner as the initial sample.

A Zr contamination in the uranium oxide used was suspected due to the high activity of Nb^{92} present, presumably formed by the reaction $Zr^{92}(p,n)Nb^{92}$. Purification of the uranium will be necessary to insure no contribution from (p,xn) reactions to the yield of either Nb^{95} state.

Preliminary results from two bombardments show that the independent yield of the high spin ground state exceeds that of the low spin metastable state. This result is in much better agreement with theoretical expectations than the previously reported value. (C. T. Ratcliffe and R. Vandenbosch)

---

1 D. G. Sarantites, C. D. Coryell and G. E. Gordon, Phys. Rev. 138, B353 (1965).
2 H. Warhanek and R. Vandenbosch, J. Inorg. Nucl. Chem. 26, 669 (1964).
3 E. Hagebo, J. Inorg. Nucl. Chem. 25, 1201 (1963).

---

32. Breakup of Deuterons by Protons with 7 MeV Center of Mass Energy

The work begun last year by Hendrie, Ilakovac, and Warren,[1] who looked at the zero degree inelastic protons produced by 21 MeV deuterons incident on hydrogen, was continued at laboratory angles from 11.25 degrees to 51 degrees in three-degree steps. The hydrogen gas was contained in one of the gas cells described in Section 39 of this report. The scattering of 10.5 MeV protons incident on deuterium was also studied at laboratory angles from 11 degrees to 60 degrees and was attempted at zero degrees.

By running the reaction in both directions one can, in principle, obtain the entire angular distribution for the reaction with center of mass angles from zero to 180 degrees. It is necessary to look at the reaction with both bombarding particles as the momentum of the center of mass is large. With one particle incident, protons emitted forwards in the laboratory system with energies below the counter threshold are actually moving backwards with reasonably large energies in the center of mass system. When the other particle is incident these same center of mass protons have large laboratory energies and are detected. Furthermore, the final-state interactions between two particles with small relative momentum should effect the spectrum most at angles about zero and 180 degrees,[2] so it is important to obtain a complete angular distribution.

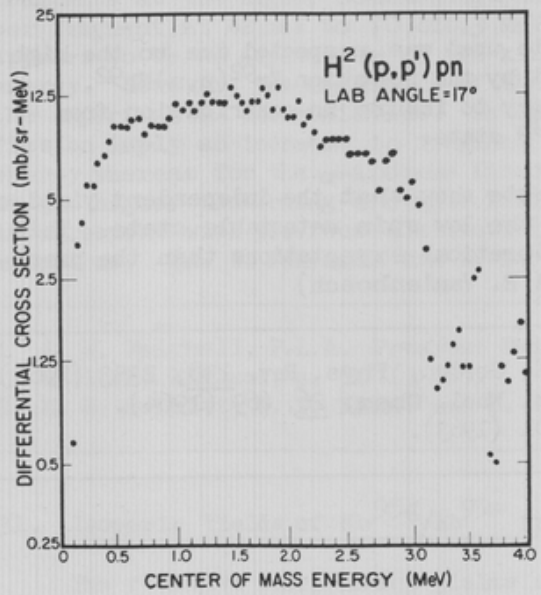

Fig. 32-1 Typical spectrum of inelastic protons from the breakup of deuterons by incident protons. Statistics are not good enough to observe final state effects which should be small at this angle.

Although we have obtained spectra at laboratory angles from 11 to 60 degrees (see Figure 32-1), we need better statistics and especially need spectra at very small angles in the laboratory system for each incident particle, in order to see the most interesting effects of the final-state interactions. We were unable to obtain a spectrum at zero degrees with protons incident due to high background. The magnet described by Ilakovac[3] separates the beam from reaction products, so if there are degraded protons in the beam, from the collimator slits for example, they are bent along with reaction protons of the same energy. These degraded protons can not be distinguished from reaction protons, as degraded beam deuterons were. However, in the Van de Graaff accelerator beam there should be many times fewer degraded particles, as it

is not necessary to use a collimator. (K. Ilakovac, J. Lilley, and D. W. Storm)

---

1 Cyclotron Research, University of Washington (1964), p. 26.
2 K. Ilakovac, L. G. Kuo, M. Petravic, I. Slaus, and P. Tomas, Nucl. Phys. 43, 254 (1963). V. V. Komarov and A. M. Popova, Nucl. Phys. 18, 296 (1960). K. M. Watson, Phys. Rev. 88, 1163 (1962).
3 Cyclotron Research, University of Washington (1964), p. 51.

---

33. Alpha Particle Induced Reactions Involving Multiple Alpha Particle Emission and Passing Through the 4.43 MeV Level of C^{12}.

Because oxygen is present in several targets used in another experiment[1] an investigation of the gamma rays following 42 MeV alpha particle bombardment of O^{16} was undertaken. The gas target[2] was used, and the anticoincidence annulus system[3] was used as the detector.

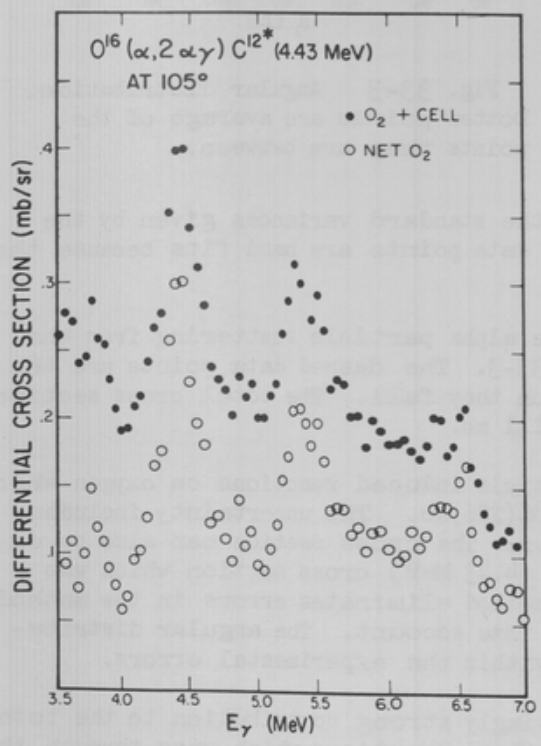

Fig. 33-1 Oxygen spectra before and after subtraction of contribution due to the gas cell.

The runs were taken in pairs at each angle, with and without gas in the target. Typical spectra are shown in Figure 33-1. An angular distribution was also taken on polystyrene to provide both an energy and efficiency calibration by measurement of the cross section for $C^{12}(\alpha,\alpha')C^{12*}$(4.43 MeV). A few preliminary runs were also taken with Ne^{20} in the gas target, using the same experimental arrangement.

The data were analyzed using ORACLE, a computer program for data reduction and analysis. The spectrum from the empty gas cell was subtracted from that of the gas cell filled with gas to obtain the net contribution due to the gas alone. Quantitative information about various features of the spectra were obtained from the parameters of a least square fit to the data.

The spectra show a prominent peak at 4.43 MeV. This peak is not due to inelastic scattering from a possible hydrocarbon film on the gas target cell, as it is absent when the cell is empty. The conclusion is that with O^{16} in the gas cell, the reaction we observe is $O^{16}(\alpha,2\alpha)C^{12*}$(4.43 MeV).

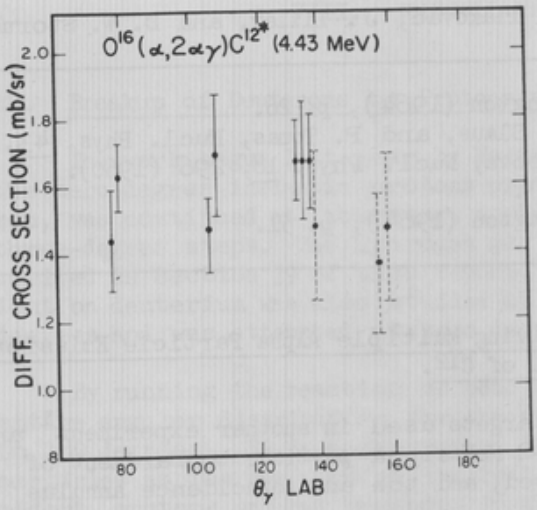

Fig. 33-2 Angular distribution. Dotted points are hand calculated from the spectra.

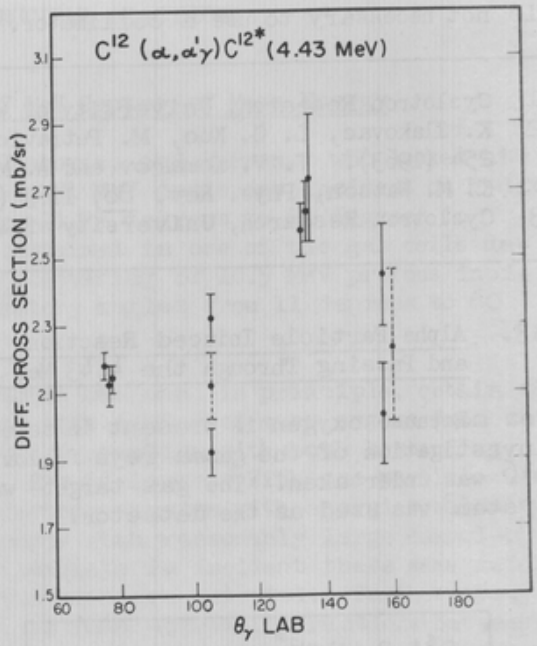

Fig. 33-3 Angular distribution. Dotted points are average of the points they are between.

This reaction has been studied both here and elsewhere by looking for the coincident alpha particles.[4,5,6] Our experimental angular distribution is shown in Figure 33-2. The error bars are the standard variances given by the least squares fitting program. The dashed data points are hand fits because the program would not converge in those cases.

The angular distribution for inelastic alpha particle scattering from the 4.43 MeV level in C^{12} are shown in Figure 33-3. The dashed data points are the average of the two data points between which they fall. The total cross section, assuming symmetry about 90 degrees, is 121±11 mb.

The total cross section for alpha particle induced reactions on oxygen which pass through the 4.43 MeV level of C^{12} is 86(±26)mb. The uncertainty includes 10% for the photo-efficiency of the detector. The cross section can also be expressed as 71% (±17%) of the $C^{12}(\alpha,\alpha')C^{12*}$ (4.43 MeV) cross section which was measured in this experiment. This second method eliminates errors in the method by which the detector efficiency was taken into account. The angular distribution of the 4.43 MeV gamma ray is flat to within the experimental errors.

The data from Ne^{20} indicates a surprisingly strong contribution to the total alpha particle reaction cross section from those reactions which pass through the 4.43 MeV level of C^{12}. If we assume isotropy, the cross section for alpha particle induced reactions on Ne^{20} passing through the 4.43 MeV level of C^{12} is 33(±17)mb. The cross section can also be expressed as 27%(±15%) of the $C^{12}(\alpha,\alpha')C^{12*}$(4.43 MeV) cross section which was measured. This value is much larger than one obtained elsewhere using different techniques at a lower incident energy.[7]
(I. Halpern, B. J. Shepherd, and C. F. Williamson)

1 See Section 26 of this report.
2 Cyclotron Research, University of Washington (1963), 41.
3 Cyclotron Research, University of Washington (1964), 52.
4 Cyclotron Research, University of Washington (1964), 24.
5 Cyclotron Research, University of Washington (1964), 26.
6 P. F. Donovan, J. V. Kane, C. Zupancic, C. P. Baker, and J. F. Mollenauer, Phys. Rev. 135, B61 (1964).
7 N. O. Lassen, Nucl. Phys. 38, 442 (1962).

IX. ACCELERATOR RESEARCH AND DEVELOPMENT

34. The Van de Graaff Accelerator Program

Progress made in installing the High Voltage Engineering Corporation model FN Van de Graaff accelerator is illustrated by the following chronology. The two stage tandem tank arrived at the laboratory on June 2, 1964. The high voltage terminal support structure was assembled during June. Beam tube and ion source vacuum system testing was carried out during July and August. Optical alignment of the accelerator components was completed in October. On November 11, the tank was first pressurized and the insulating gas handling equipment checked. The terminal was first charged to high voltage on December 8. A small but encouraging proton beam was obtained from the machinery on January 5, 1965.

Since that time work on the accelerator has centered around obtaining an intense, stable beam. The terminal has been operated at voltages from 2 to 7.5 MeV. However, at no voltage has the beam current yet been intense enough to meet design specifications. The maximum analyzed beam obtained so far is 2.5μA.

Faulty operation of the thermal-mechanical valve controlling the flow of stripper gas in the terminal made it necessary to place a locally built mechanically operated needle valve in series with the thermal-mechanical valve. This needle valve provides a much more stable and precisely controllable flow rate of stripper gas than did the thermal mechanical valve.

Work is presently going on to determine and eliminate the cause of the less than acceptable beam intensity. As an aid in diagnosis, sets of tungsten wire cross hairs have been placed at several positions in the beam tubes. These wires not only have enabled us to determine precisely the shifts in alignment of the beam tubes that occur as the tank is pressurized, but also - because the wires incandesce when heated by the beam - permit us to observe the position of the beam as it travels through the beam tubes.

The installation of this machine has been considerably impeded by a large number of manufacturing flaws in the accelerator components. These flaws range from leaky welds to incorrectly designed and constructed electrical circuits. In most cases these flaws should have been detected by normal inspection and testing of the components at the factory prior to shipment. The result has been that much time has been lost trouble shooting and field repairing of items which one would normally expect to receive in an operating condition.

Factory tests on the injector stage of the three stage system are still continuing and delivery of this portion of the accelerator has been postponed pending the successful completion of these tests. It is now estimated that this will occur in November or December, 1965 or approximately one year later than the originally scheduled delivery date.

Van de Graaff Experimental Areas

The analyzed beam from the Van de Graaff accelerator passes through a switching magnet by means of which the beam can be directed into either of the

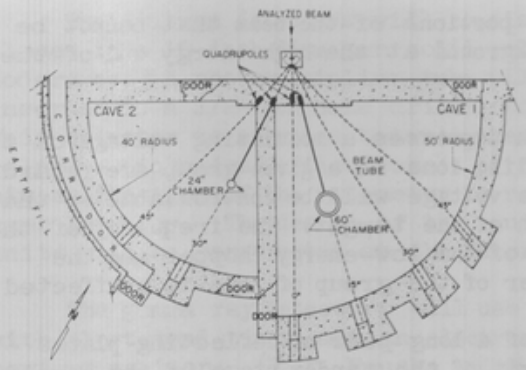

Fig. 34-1 Van de Graaff experimental cave plan.

two existing experimental cave areas. With the present magnet configuration there are four beam lines available for use in cave #1 and two beam lines into cave #2. See Figure 34-1. Magnetic quadrupole lenses and some other portions of the required beam handling hardware for four of these 6 beam lines were purchased with the accelerator and have been installed.

A 60" scattering chamber modelled after the chamber which has been in use on the cyclotron for the last few years but embodying many improvements has been constructed and installed in cave #1 and is now ready for use as soon as a useable beam is available. The 24" scattering chamber formerly used with the cyclotron has been removed from the cyclotron cave, rebuilt and improved and is installed and ready for use on the 30° beam line in cave #2. The 45° beam line in cave #2 is being set up for use in very low background experiments with the requisite equipment either designed or on order.

The 0° beam line in cave #1 is at present being used for the testing procedures on the accelerator itself. (T. J. Morgan and W. Weitkamp)

35. A Beam Bunching System for the Tandem Van de Graaff

Work is in progress to develop a system to apply bunching and chopping to the D.C. ion beam of the tandem stage of the University of Washington electrostatic generator, in order to produce short, regular bursts of ions at any desired target location. The present system is designed for proton, deuteron or alpha-particle beams. Later on it is hoped to provide an additional bunching unit for heavier ions.

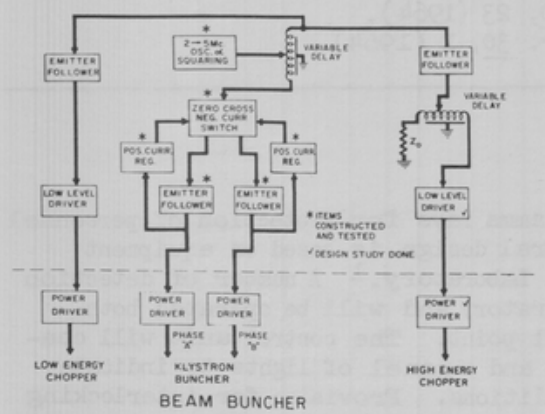

Fig. 35-1 Block diagram of beam buncher electronics.

The principles of the method are well known and have been used successfully at several laboratories.[1,2,3] The complete system incorporates three parts: (See Figure 35.1)

1. A Low-Energy Chopper which converts the low-energy D.C. beam into a series of bursts of duration variable between 20 nsec and 60 nsec and with a variable repetition rate 2 Mc/s

to 5 Mc/s. Its purpose is to remove those portions of the beam that cannot be bunched and which would be a source of background at the high-energy end of the accelerator.

2. A Three-Gap Klystron Buncher which impresses a modulating voltage on the low-energy ions in such a way that the leading ions in a given group are retarded and the trailing ions are accelerated. The voltage will be controllable so that optimum bunching will occur at the position of the target. The frequency of the modulating waveform will be locked to that of the low-energy chopper and the relative phase adjustable so that the center of the group of ions is unaffected.

3. A High-Energy Wiper will consist of a long pair of deflecting plates operating on the high-energy beam at the exit of the tandem stage of the accelerator. A periodic shaped-voltage applied to the plates will cause the beam to be swept across a variable aperture at the correct frequency and phase to transmit the bunched ions and at a variable speed to provide a fine control on the ultimate duration of the beam pulse at the target. Normally this unit will be used to clean up the incompletely bunched beam at the extreme edges of the pulse.

Most of the mechanical parts of the system have been designed and construction of the klystron buncher has already begun. The decision was reached to use a sawtooth waveform on the buncher and a rectangular waveform on the low-energy deflecting plates. Thus far the design of the variable chopping rate oscillator and the sawtooth generators with the proper phase inversion electronics has been completed. The remaining work consists of design and construction of the drivers for the choppers and buncher. Most of the design study for the high-energy chopping electronics has been completed. (W. Braithwaite, H. F. Fauska, I. Halpern, J. S. Lilley, D. Patterson, C. W. Williamson)

---

1 H. W. Lefevre, R. C. Borchers, C. H. Poppe, Rev. Sci. Inst. 33, 1231 (1962).
2 C. D. Moak, W. M. Good, R. F. King, J. W. Johnson, H. E. Banta, J. Judish, and W. H. du Preez, Rev. Sci. Inst. 35, 672 (1964).
3 D. Dandy and H. Hammond, Nucl. Instr. 30, 23 (1964).
J. H. Anderson and D. Swann, Nucl. Instr. 30, 1 (1964).

---

36. Radiation Monitoring System

A system for monitoring neutrons and gamma rays for protection of personnel is being planned and constructed. The general design is based on equipment presently in use at the Los Alamos National Laboratory.[1] A number of detection devices will be located throughout the laboratory and will be operated both manually and remotely from a central control point. The control unit will consist of count rate meters for each detector and a panel of lights to indicate quickly the existence of safe or unsafe conditions. Provision for interlocking doors to potentially unsafe areas and for shutting down the machine in the event of hazardous conditions are also being considered. The necessary electronic equipment is about one-half completed.

The neutron detectors will consist of an enriched Li^6 - I(Eu) crystal enclosed in a 10-inch diameter solid polyethylene sphere which serves as a moderator. A photomultiplier tube will view the crystal through a light pipe inserted in a 1/2-inch hole drilled to the center of the sphere. The response of this detector to energies between thermal and 7 MeV adequately simulates the relative biological effectiveness of neutrons over this range.[2,3] This will permit calibration of the ratemeter to read the neutron dose rate directly in millirems per hour. The design of the neutron monitor has been completed and the units will be constructed at the laboratory.

The gamma ray detectors will use commercially available Geiger-Muller tubes with short dead-times, and an electronic system similar to that used for the neutron monitor. (H. F. Fauska and N. Stein)

---

1 H. K. Jennings, Los Alamos National Laboratory (private communication).
2 R. L. Bramblett, R. I. Ewing, and T. W. Bonner, Nucl. Instr. and Methods 9, 1 (1960).
3 D. E. Hankins, Los Alamos Scientific Laboratory Report LA-2717 (1962).

X. INSTRUMENTATION FOR RESEARCH

37. Lithium Drifted Silicon Detector Fabrication

A program was started to fabricate lithium drifted silicon surface barrier detectors.

During the first two months of the program four detectors were produced, all having depletion depths on the order of 1.5 mm. The active areas ranged from 80 - 250 mm^2. Three of the four detectors were satisfactory and had an energy resolution of less than 100 keV (FWHM) when tested with 8.78 MeV alphas. The fourth detector with an active area of 80 mm^2 had 30 keV resolution. The reverse current for this detector was 2 μA with 400 V reverse bias.

The detectors were fabricated according to the technique described by Goulding and Hansen.[1] (J. Sauer)

---

1 F. S. Goulding and W. L. Hansen, IEEE Trans. Nucl. Sci. 11, 286 (1964).

---

38. A Flexible System for Using Lithium Drifted Germanium Detectors

The recent development[1] of solid state gamma-ray detectors of very high (< 2 keV) resolution and reasonable efficiency is revolutionizing certain aspects of gamma-ray spectroscopy. In order to take advantage of the possibilities of these detectors in this laboratory, a system has been designed and built which allows the detector to be used in any experimental arrangement presently foreseen.

The most troublesome requirement for these detectors is that they must be operated at a temperature less than 100°K. This presents no great technical problem if the counter is operated in air without NaI anticoincidence shielding. However, the use of liquid nitrogen when the counter is situated inside a vacuum chamber or an anticoincidence shield presents serious technical problems. In order to facilitate the use of the detectors under these conditions a detector mount system has been designed using a miniature Joule-Thomson cryostat.

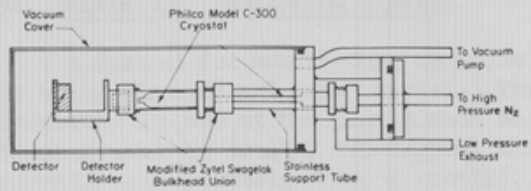

Fig. 38-1 Schematic drawing (not to scale) of the Ge(Li) detector holder system using the miniature Joule-Thomson cryostat.

A schematic diagram of the system is shown in Figure 38-1. A Philco model C-300 cryostat[2] is used to cool the detector and holder. A zytel Swagelok[3] bulkhead union is used to insulate the detector holder and provide easy interchangeability between different detectors. The zytel union was machined down to 0.030" wall thickness over 3/4" of its length in order to reduce heat conduction. This

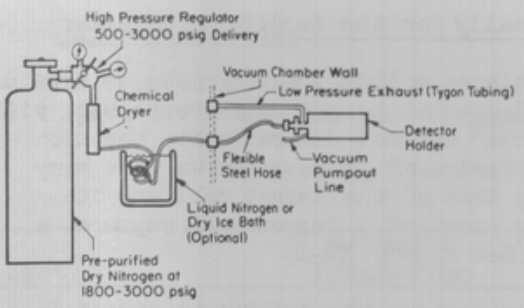

Fig. 38-2 Schematic diagram of the high pressure nitrogen delivery and purifying system.

union had been previously bored out to make a snug fit around the cryostat in order to have optimum efficiency of the heat exchange.

If the system is to be operated in air, it must be evacuated to a pressure of five microns Hg or less in order to prevent water condensation on the detector and significant thermal loading by the residual gas. For air operation, a pump is connected to the vacuum line and the low pressure exhaust is left unconnected. For operation inside a vacuum chamber, the vacuum cover may be removed or left on as desired. The vacuum line is left unconnected, and both the high and low pressure lines are connected to an outlet in the side of the vacuum chamber.

For both vacuum and air use the high pressure nitrogen is fed to the system through flexible stainless steel hose. A schematic diagram of the high pressure feed system is shown in Figure 38-2. For successful startup the model C-300 cryostat must be supplied with the highest purity nitrogen possible at a pressure of 1800 psig or higher. Initial cooldown requires 30-45 minutes, after which the delivery pressure can be lowered to 1400 psig to conserve nitrogen. The normal operating temperature is 78° K.

The system has been tested both on the bench and in an actual run inside the 60" scattering chamber. The performance was found to be satisfactory in both cases. Under continuous operating conditions two cylinders of nitrogen are required for an 18-hour day. This implies an operating cost of only $1.50/hour.

It is planned to design a high-resolution solid state preamplifier for this unit using a field-effect transistor. The latter must be cooled to below 200° K for optimum performance, and the detector holder has been designed in such a manner that this is easily accomplished. The entire preamplifier could be mounted inside the vacuum cover to reduce stray capacitance and electrical interference. It is also planned to incorporate a fast time pickoff to be used in conjunction with a pulsed-beam time-of-flight system to discriminate against neutrons and against gamma rays which are uncorrelated in time with the beam burst.
(J. Alster, T. Hayward, C. Williamson)

---

1 A. J. Tavendale and G. T. Ewan, Nucl. Inst. and Meth. 25, 185 (1963).
2 Manufactured by Philco, Lansdale Division, Lansdale, Pa.
3 Manufactured by the Crawford Fitting Co., Cleveland, Ohio.

---

39. A Gas Target System Designed Specifically for the Handling of Tritium

Due to the difficulties of using tritiated solids for targets,[1] we have designed and built a gas handling system and special target cells to be used with tritium. The gas targets designed by Shreve[2] are not desirable for use with tritium as their volume is large. In the design of this system we were very careful to minimize its volume, especially that of the target cell and its associated tubing, so that in the unlikely event of a target cell rupture, a minimum amount of tritium would escape. (See Figure 39-1)

As with Johnson's and Banta's[3] tritium system, the tritium is stored in a few grams of activated uranium in a cylinder permanently attached to the system. Heating the uranium causes the tritium to be evolved from the uranium tritide to a pressure that depends on its temperature. We have obtained hydrogen pressures up to 40 lbs./sq.in. The cold uranium will pump the system back down to about 25 microns. The system also has an additional input through which any other gas may be put into the target. This line is also used for helium leak testing. The gas cells are 1/2 in. high by 1/2 in. in diameter with a 0.00009 in. Havar[4] foil window. They are tested to 50 lbs./sq.in. before use, and some have held up to 100 lbs./sq.in. pressure.

The system was tested thoroughly with hydrogen before introducing the tritium. Eighty curies of tritium gas were obtained from Oak Ridge National Laboratory under provisions of our License No. 46-1662-1. When it was introduced into the system, very little of this tritium was absorbed in the uranium. After the tritium was removed by absorption into a very large uranium trap, the system was retested with hydrogen. A volume of hydrogen many times as great as that of the tritium was easily absorbed. Consequently we have assumed that the tritium was badly contaminated and are planning to purchase more tritium from a different source. (K. Ilakovac, D. W. Storm, C. F. Williamson)

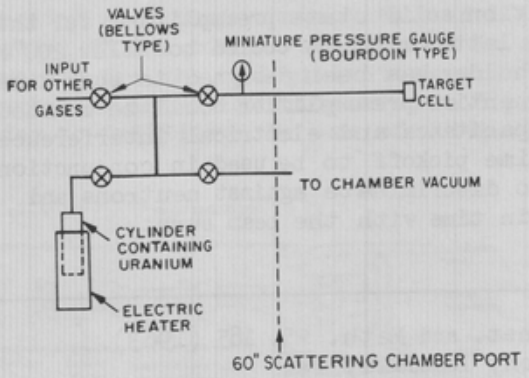

Fig. 39-1 Schematic of tritium handling system and target.

1 Cyclotron Research, University of Washington (1963), p. 25.
2 Cyclotron Research, University of Washington (1962), p. 52.
3 C. M. Johnson and H. E. Banta, Rev. Sci. Instr. 27, 132 (1956).
4 Supplied by the Hamilton Watch Company.

40. Target Preparation

The targets listed in Table 40-1 have been prepared in the past year. Only the targets different from those prepared the previous year have been listed.

Table 40-1. Targets Prepared in the Past Year

Target	Method of Preparation	Backing*	Thickness
B	pressing	s.s.	10-25 mg/cm^2
$Ca^{42,44}$	vac. evap.	thin mylar	300-500 μg/cm^2
Cr	vac. evap.	s.s.	100-200 μg/cm^2
$Cu^{63,65}$	vac. evap.	s.s.	300-1000 μg/cm^2
Dy	rolling	s.s.	15 mg/cm^2
$Fe^{54,56}$	electro-deposition	s.s.	500-1500 μg/cm^2
Ho	rolling	s.s.	27.5 mg/cm^2
Pb^{208}	vac. evap.	VYNS	100-200 μg/cm^2
Mg^{24}	vac. evap.	s.s.	70-150 μg/cm^2
Si	vac. evap.	s.s.	100-700 μg/cm^2
Sr^{88}	vac. evap.	s.s.	300-1000 μg/cm^2
Tℓ	vac. evap.	s.s.,thin nylon	1000 μg/cm^2
$Sn^{116,118,119,120}$	vac. evap.	s.s.	200-500 μg/cm^2
UF_4	vac. evap.	VYNS,thin Ni	50-100 μg/cm^2
V	vac. evap.	s.s.	100-200 μg/cm^2
Yt	rolling	s.s.	25.3 mg/cm^2

*s.s. indicates self-supporting

Only one of the more interesting techniques developed will be described in more detail.

Calcium, Magnesium and Strontium

Thin metallic, monoisotopic targets of Ca, Mg and Sr may be prepared starting either from the metal-oxide or carbonate by simultaneous reduction of the oxide to metal using aluminum metal and evaporation of the resulting metal in vacuum.[1]

Two types of sources were used. Both are available commercially.[2] The first source was a 0.005 inch thick Ta canoe-shaped crucible. In order to reduce the loss of material during evaporation, a vertically mounted Ta crucible 1/4 inch in diameter, 1 1/2 inches high and 0.005 inches thick was used.

The crucible was loaded with carbonate and cautiously heated in vacuum until the carbonate had decomposed to metal oxide and carbon dioxide. The oxide was then removed from the crucible and well mixed with an amount of aluminum metal dust sufficient to reduce the oxide (50% stoichiometric excess). This mixture was then returned to the same crucible and carefully heated to just above the melting point of aluminum (about 800°C). At this temperature the molten aluminum reduces the oxide to metal and the metal simultaneously evaporates onto the substrate.

The yield using this method of reduction was determined to be 90% or better, which is a substantial improvement over the technique reported by Allen[3] whereby the metal oxide is reduced on the surface of a hot tantalum crucible. (J. Sauer)

---

1 L. M. Pidgeon and J. T. N. Allunson, Can. Mining and Met. Bull., 429, 14 (1948).
2 R. D. Mathis Co., Long Beach, California.
3 Larry D. F. Allen, Rev. Sci. Instr. 34, 491 (1963).

---

41. On-Line Computer for Data-Handling

The AEC authorized this laboratory to take bids for an on-line computer system for real-time acquisition and processing of data from nuclear physics experiments. On the basis of bids received and further AEC approval, a contract has been signed for the purchase of the system proposed by Scientific Data Systems, Inc. This system will include an SDS 930 digital computer with an 8K memory and versatile data input, output, and display facilities. The system is scheduled for delivery in the late summer of 1965. Details of the system are described in the Technical Specifications of the bid request. Preparations for the use of the system have been initiated, and include systems programming and interface design. (D. Bodansky, J. G. Cramer, H. Fauska, J. B. Gerhart, B. J. Shepherd, and R. Vandenbosch)

42. Design, Development and Construction of Electronic Equipment

One counting bay has been placed into operation in the Van de Graaff counting room. It is being currently used for counter testing and for studies with radioactive isotopes, pending normal operation of the Van de Graaff. Most of the major units, including a 512-channel analyzer, amplifiers and coincidence systems, are commercially constructed. Certain additional units have been constructed locally and a versatile cabling system has been provided for interconnection between the experimental caves and the counting bays.

Specific items of electronic equipment constructed during the past year, for cyclotron and Van de Graaff use, include:

a. A three-parameter data recording system using a punched paper tape output has been designed and constructed. It replaces the earlier three-parameter system which used a decimal printer output. In the new arrangement the output is in a format suitable for computer input. It may also be presented directly to a typewriter. In this new system, amplified signals are fed to existing ADC's and the converted data are stored temporarily in decade scalers which are sequentially scanned, digit by digit. At present, three three-decade scalers are being used, providing for 1000 x 1000 x 1000 channel analysis, but the unit is readily adapted to expansion if either more detectors or more channels per detector are needed. The equipment uses solid state components, rather than mechanical switches, for the scanning operations. It is built with plug-in etched printed circuit cards to facilitate trouble shooting and repair.

b. A logarithmic count rate meter has been constructed for use as part of a system for monitoring alpha particles from foils of radioactive heavy isotopes. This unit, which includes a detector probe power supply, is mounted in a glove box where the foils are stored.

c. A decode display unit was designed and constructed to use with the new target changer system.

d. Design and construction of electronic equipment for the Van de Graaff accelerator beam buncher has begun. (See Section 35 for a description of this system.)

e. Several fast pre-amplifiers have been constructed on a design similar to that of Williams and Neiler.[1] The units yielded gains of ten with risetimes of approximately 6 nanoseconds. Attempts, not as yet successful, have been made to construct low-noise preamplifiers which could be placed within a vacuum.

f. Prototypes of the electronic cards for a neutron radiation monitor have been constructed and tested. Approximately ten such units will be built. The circuits are based on those developed by the Los Alamos Scientific Laboratory.[2] (See Section 36 for a description of the monitoring system.)

g. A solid state detector drifting oven has been constructed, with automatic control of ion drift rate and with sensing of the depth of drift. This unit was based on the Lawrence Radiation Laboratory design, described by Goulding and Hansen.[3]

h. Electronic scalers have been developed and built to record real time during experimental runs. These units replace a commercial electrical clock which gave occasional trouble. Time is recorded in units of 0.1 second or 0.01 minutes, as selected by a front panel switch. Three such units have been built.

i. Faster scaler driving cards and faster scaling circuits have been inserted in the front end of the scalers previously built for use in the Van de Graaff counting room.

j. A dual count rate meter circuit has been constructed to be mounted near the dual voltage-to-frequency converters used with the Faraday cup beam monitoring system. This facilitates the zero adjustment of the converters. A pre-scaler unit has also been constructed and installed to reduce possible dead-time losses in beam monitoring.

k. A multiplier system for particle identification has been constructed, following the design of Radeka and Miller.[4]

l. Other equipment which has been constructed includes: an adder-mixer unit (based on an Argonne design);[5] two four-channel slow coincidence-anticoincidence chassis; two power supplies for commercial low-noise preamplifiers; three multichannel coincidence pulsers; three portable noise meters; one precision pulse generator; a fast pre-scaler unit (25-mc resolution); and two chassis for mounting dual delay units. Some of these items represent additional copies of units developed previously and described in earlier progress reports.

Equipment purchased commercially during the past year includes: a stabiline line voltage regulator; a modified ND-160-F ADC unit; two Dymec voltage-to-frequency converters; one ORTEC Model 220 pulse analysis system; three ORTEC Model 210 solid state detector controllers; an ORTEC Model 260 time pickoff unit and control; three Tennelec Model 100-A low noise preamplifiers; a 5-channel Cosmic amplifier, discriminator and coincidence system; a 1-channel Cosmic amplifier, discriminator and coincidence power supply; two RIDL baskets with two scalers, a biased amplifier and a noise meter as plug-ins; three Nanosecond baskets with amplifiers, scaler drivers, discriminators; 1 time-to-pulse-height converter; a closed circuit t.v. system with two cameras, two monitors and one zoom lens with remote control; four 0-3 kv @ 12 ma. power designs power supplies. (L. H. Dunning, H. Fauska, Research Electronics Supervisor, K. H. Lee, G. Monge, and N. Ward)

---

1 C. W. Williams and J. H. Neiler, IRE Transactions of Nuclear Science, Vol. NS-9 No. 5 (Nov. 1962).
2 H. K. Jennings, Los Alamos Scientific Laboratory (private communication).
3 F. Goulding and W. L. Hansen, IRE Transactions on Nuclear Science, Vol. NS-11 No. 3 (June 1964).
4 G. L. Miller and V. Radeka, "Analogue Multiplication with Field-Effect Transistors," Proc. Nas. Conference on "Instrument Techniques in Nuclear Pulse Analysis," Monterey, California (1963).
5 J. A. Kopta, Argonne National Laboratory, private communication.

XI. APPENDIX

43. Statistics of Cyclotron Operation

The disposition of the time available for cyclotron operation during the period from May 16, 1964 to May 15, 1965, is given in Tables 43-1, 43-2, and 43-3.

Table 43-1. Division of Cyclotron Time Among Activities

Activity	Hours	Per Cent
Normal Operation	5260	76.1
Setup of Experiments	217	3.1
Cyclotron Testing	29	0.4
Scheduled Repairs and Modifications	68	1.0
Unscheduled Repair	433	6.3
Failure of Experimental Equipment	72	1.0
Unsatisfactory Cyclotron Operation	440	6.4
Experiments Using No Beam	136	2.0
Unrequested Time	104	1.5
Visitors	4	.1
Checkup	148	2.1
Total	6911	100.0

Table 43-2. Division of Normal Operation Time Among Normal Facilities

Projectiles	Hours	Per Cent
Alpha Particles	3649	69.4
Protons	883	16.8
Deuterons	728	13.8
Total	5260	100.0

Table 43-3. Bombardment for Outside Investigators

Investigator	Hours
Oregon State University	53
University of Oregon	34
Western Washington State College	20
Total	107

44. Nuclear Physics Laboratory Personnel

Faculty

John S. Blair, Professor
David Bodansky, Professor
John G. Cramer, Assistant Professor
Arthur W. Fairhall, Professor
George W. Farwell, Professor
James B. Gerhart, Professor
I. Halpern, Professor
Ksenofont Ilakovac, Visiting Associate Professor[1]
Fred H. Schmidt, Professor
Robert Vandenbosch, Associate Professor

Nuclear Physics Laboratory Research Staff

Jonas Alster, Research Assistant Professor
Charles D. Kavaloski, Research Assistant Professor
John S. Lilley, Research Assistant Professor
Ted J. Morgan, Research Associate Professor;
Supervisor, Nuclear Physics Laboratory
Nelson Stein, Research Assistant Professor
William G. Weitkamp, Research Assistant Professor
Claude F. Williamson, Research Assistant Professor

Predoctoral Research Associates

Chemistry

Walter Loveland

Physics

Joseph S. Heagney
David L. Hendrie[2]
Wojciech Kolasinski
Paul Mizera
E. Roland Parkinson[3]
Barry J. Shepherd
Gurnam S. Sidhu
Frederick W. Slee

Research Assistants

Chemistry

Charles J. Bishop
Dennis G. Perry
Charles T. Ratcliffe

Physics

Wilfred J. Braithwaite
Nelson Cue
Steve M. Ferguson
Thomas D. Hayward
Roger A. Hinrichs
R. Jerome Peterson
Ekkehard Preikschat
David C. Shreve
Derek W. Storm
Leslie J. Tomley

Full-Time Technical Staff

Machine Shop

Harvey E. Bennett, Foreman
Norman E. Gilbertson
Charles E. Hart
Floyd E. Helton[4]
Gustav E. Johnson
Edwin P. McArthur
Bernard Miller, Assistant Foreman
Byron A. Scott
Anthony J. Virant
Allen L. Willman

Electronic and Electrical

Laverne H. Dunning
Robert B. Elliott
Harold Fauska, Senior Physicist, Research Electronics Supervisor
George C. Monge
John W. Orth, Assistant Supervisor, Nuclear Physics Laboratory
Norman G. Ward

Technicians

Carl E. Linder
Georgia Jo Rohrbaugh
George E. Saling

Design and Drafting

Robert G. Clarke
Peggy Douglass
David W. Gough
Dolores Lenhart
Peter Momcilovich, Engineer
Lewis E. Page

Accelerator Operators

Barbara J. Barrett[5]
Jacque M. Beechel
Richard Clay[6]

Others

Tylaine C. Hansen, Office Assistant
Kyum Ha Lee, Laboratory Technician
Joanne M. Sauer, Radiochemist
Helene Turner, Secretary

Part-Time Technical Staff

Student Helpers

Marc W. Hansen
Bonnie C. Murray
Charles J. Peterson
John T. Thaxton
Harry V. Winsor
Akiko Yamanouchi[5]

Others

Mary A. Beard, Storekeeper

---

1 Now at Institut "R. Boskovic, Zagreb, Yugoslavia.
2 Now at Lawrence Radiation Laboratory, University of California, Berkeley.
3 Now at University of Pittsburgh, Pittsburgh, Pennsylvania.
4 Retired.
5 Terminated.
6 On military leave.

---

45. Advanced Degrees Granted, Academic Year 1964-1965

D. L. Hendrie: Ph.D. "A Study of Coincidences Between Inelastically Scattered 42-MeV Alpha Particles and De-Excitation Gamma Rays."

E. R. Parkinson: Ph.D. "An Experimental Study of Sub-Barrier Proton Emission in Compound Nuclear Reactions."

46. List of Publications

"Inelastic Scattering of 42 MeV α-Particles from Pb^{207}, Pb^{208}, and Bi^{209}" J. Alster, Proceedings of the Congres International de Physique Nucleaire II; Editions du Centre National de la Recherche Scientifique, Paris 1964.

"Inelastic Scattering of 42 MeV α-Particles from Sr^{88} and Y^{89}" J. Alster and D. C. Shreve, Bull. Am. Phys. Soc. 10, 130 (1965).

"Elastic Scattering of C^{12} Ions from Fe, Ni, Ag^{107}, In and Ta" J. Alster and H. E. Conzett, Phys. Rev. 136, B1023 (1964).

"$O^{16}(\alpha,Be^{8})C^{12}$ Reaction" R. E. Brown, J. S. Blair, D. Bodansky, N. Cue and C. D. Kavaloski, Bull. Am. Phys. Soc. 9, 549 (1964).

"(d,Li^{6}) Reactions on Light and Intermediate Weight Nuclei" F. W. Slee, Bull. Am. Phys. Soc. 10, 461 (1965).

"Single-Particle States in Bi^{209} and Po^{210} Excited by (α,t) Reactions" N. Stein and J. S. Lilley, Bull. Am. Phys. Soc. 10, 497 (1965).

"Angular and Energy Distributions of Prompt γ-Rays Produced by 42 MeV α-Particle Bombardment" C. F. Williamson and B. J. Shepherd, Bull. Am. Phys. Soc. 10, 428 (1965).

"(α,Li^{6}) Reaction on C^{12}, N^{14}, Al^{27}, and Ni at 42 MeV" C. D. Zafiratos, Phys. Rev. 136, B1279 (1964).